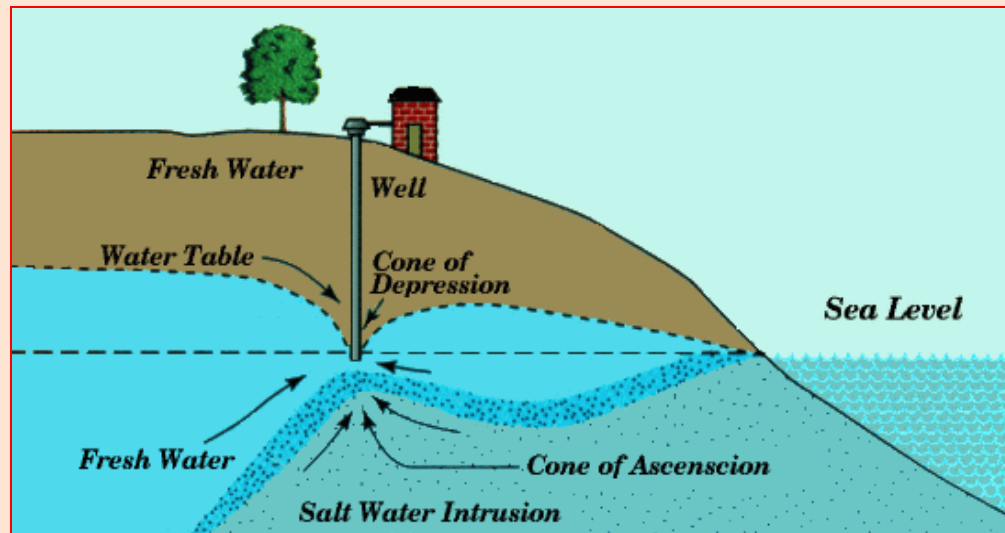


Final Report

Study of salt water intrusion in the Upper Aquifer in Azraq Basin



Prepared by

Prof. Dr. Ali El-Naqa

Professor of Hydrogeology & Water Resources Management

e-mail: elnaga@yahoo.com

6 October, 2010

Table of Content

List of Figures	4
List of Tables	6
Executive summary	7
CHAPTER 1 INTRODUCTION	12
1.0 Introduction	12
1.1 Scope of work.....	13
1.2 Methodology.....	14
1.2.1 Office Work.....	15
1.2.2 Field Work.....	15
1.2.3 Laboratory Work.....	15
1.4 Background Information	16
1.5 Physiography.....	20
1.5.1 Geographical Setting	20
1.5.2 Topography and Drainage	20
1.5.3 Land Use	20
1.5.4 Climate.....	22
1.6 Current Azraq water dilemma	24
1.7 Salt water intrusion in Azraq.....	26
CHAPTER 2 GEOLOGY OF AZRAQ BASIN	29
2.1 Geological framework.....	29
2.2 Geological Structure	30
2.2.1 Siwaqa Fault Zone.....	33
2.2.2 Ramtha-Wadi Sirhan Fault Zone.....	33
2.2.3 Fuluk Fault	33
2.2.4 Qaa' Abu Husain Fault	33
CHAPTER 3 HYDROGEOLOGY OF AZRAQ BASIN.....	35
3.0 Hydrogeology and Aquifer Systems.....	35
3.1 Aquifer Systems	35
3.2 Hydrogeology of the Upper Aquifer System.....	36
3.2.1 Quaternary Deposits.....	37
3.2.2 Basalt Aquifer	39
3.2.3 Wadi Shallala Aquifer	39
3.2.4 Rijam Aquifer (B4).....	39
3.3 Saturated Thickness	39
3.4 Aquifers Characteristics	40
3.5 Well Characteristics	41
3.6 Ground Water Level Fluctuations	41
3.7 Ground Water Movement	43
3.8 Recharge and Groundwater Flow Pattern	46
3.9 Farm Wells	48
CHAPTER 4 GEOELECTRICAL SURVEYS (VES & TDEM) AT QA' AL AZRAQ.....	50
4.0 Geoelectrical methods and hydrogeological problems.....	50

4.1 Electrical Resistivity Sounding (VES)	51
4.2 Theoretical background	52
4.3 Field survey and Data acquisition	52
4.4 Use of Geoelectrical and Electromagnetic methods in studying salt fresh water intrusion ..	53
4.4.1 TDEM Method.....	54
4.4.2 TDEM Field Survey.....	58
4.4.3 Data Preparation in GIS Platform	58
4.5 Geophysical Data Acquisition and Processing	60
4.5.1 TDEM Geophysical Data	60
4.5.2 DC-VES Geophysical Data	63
4.6 Combined (TEM & VES) Interpretation Results	64
4.7 Two Dimensional (2D) VES Interpretation.....	66
4.8 Two Dimensional (2D) TEM Interpretation.....	66
4.9 3D Image: Saltwater interface at Depth Slice (5m-40m).....	73
CHAPTER 5 HYDROCHEMISTRY AND WATER QUALITY OF UPPER AQUIFER	76
5.1 Background	76
5.2 Sampling and Analysis.....	76
5.3 Results and Discussion	79
5.4 Water Types	79
CHAPTER 6 CONCLUSIONS AND RECOMMENDATIONS.....	87
6.1 Conclusions	87
6.2 Recommendations	87
Acknowledgements	88
References	88

List of Figures

Figure (1.1): Location map of Azraq area	17
Figure (1.2): Location map of Azraq Wetland Reserve and Azraq Basin	18
Figure (1.3): Google earth satellite image of Qa' Al Azraq	19
Figure (1.4): Topographic map of the Azraq Basin showing the study area and distribution of groundwater wells penetrating the Shallow Aquifer	21
Figure (1.5): The mudflat of Qaa' Azraq in winter period 2010.....	22
Figure (1.6) : Land use map of the Azraq basin	23
Figure (1.7): Spring discharge against AWSA well field abstraction	25
Figure (1.8): The situation in Azraq a few years ago	27
Figure (1.9): The current situation in Azraq.....	27
Figure (1.10): Schematic diagram of salt fresh water interface developed in Azraq area	28
Figure (2.1): Generalized geological map of the study area (After Sahawneh, 1996).	32
Figure (2.2): Major Structural element and subsurface direction of groundwater -movement within AL Azraq Basin (After Sahawneh, 1996).	34
Figure (3.1): Simplified Hydrogeological cross section running SW – NE (<i>after</i> Dotteridge, 1998)	38
Figure (3.2): Fluctuation of groundwater level in observation well F1043	42
Figure (3.3): Fluctuation of groundwater level in observation well F1280	43
Figure (3.4): Groundwater contour map of the upper aquifer unit in steady state condition	45
Figure (3.5): Water uses in Azraq Basin	47
Figure (3.6): Hydrogeological cross section in the Azraq Basin	47
Figure (3.7) : Farm well in Azraq area	48
Figure (3.8) : Shallow hand-dug well in the farm area	49
Figure (3.9): Schematic hydrogeological cross section of the well F1014.....	49
(Worzyk and Huster, 1987).	49
Fig (4.1): Schlumberger array utilized in the site selection	53
Figure (4.2): Induced eddy currents at progressively later times after turnoff.	56
Figure (4.3): TDEM waveforms at three different stages of measurements.....	57
Figure (4.4): TDEM field configuration showing (a) Induced eddy currents at progressively later times after turnoff and (b) loop configuration.	59
Figure (4.5): The TDEM apparatus model.....	60
Fig. (4.6): Location map of TDEM, DC-VES geophysical measurements, boreholes and wells	61
Figure (4.7): Resistivity ranges for different substances see the three green arrows that describing clay, fresh water and saline water resistivities.	62
Fig. (4.8): Resistivity model obtained from the inversion of the TEM23 (using the TEMRES program) and its correlation with the Geological-log obtained from the borehole AZ 9.	63
Figure (4.9): Resistivity model obtained from the inversion of the VES 1 (using the IPI2WIN program) and its correlation with the geological-log obtained from the borehole AZ 13.....	64
Figure (4.10): Interpreted TEM and VES geophysical cross sections at depth ranges from 5m to 40 m, resistivity scale below 1 ohm.m (light to dark blue colors) is used to show the possible area of saltwater locations.	65

Figure (4.11): Interpreted VES profile along VES's 4,3,5 and 6; A) Apparent resistivity pseudosection , B) Inverted resistivity cross section, C) VES2 model curve, D) Resistivity interpretation into true resistivities and their corresponding thicknesses, E) Geoelectrical cross section model showing geological layers and their true resistivity..... 67

Figure (4.12): Interpreted VES profile along VES's 2,1,5 and 7; A) Apparent resistivity pseudosection , B) Inverted resistivity cross section, C) VES2 model curve, D) Resistivity interpretation into true resistivities and their corresponding thicknesses, E) Geoelectrical cross section model showing geological layers and their true resistivity..... 68

Figure (4.13):Two-dimensional representation of the TDEM resistivity distribution of section 1 with geological and hydrogeological design..... 69

Figure (4.14): Two-dimensional representation of the TDEM resistivity distribution of section 2 with geological and hydrogeological design..... 69

Figure (4.15): Two-dimensional representation of the TDEM resistivity distribution of of section 3 with geological and hydrogeological design..... 70

Fig.(4.16):Two-dimensional representation of TDEM resistivity distribution of section 4 with geological and hydrogeological design..... 70

Figure (4.17):Two-dimensional representation of TDEM resistivity distribution of section 5 with geological and hydrogeological design..... 71

Figure (4.18): Two-dimensional representation of TDEM resistivity distribution of section 6 with geological and hydrogeological design..... 71

Figure (4.19): Two-dimensional representation of TDEM resistivity distribution of section 7 with geological and hydrogeological design..... 72

Figure (4.20):Two-dimensional representation of TDEM resistivity distribution of section 8 with geological and hydrogeological design..... 72

Figure (4.21):Two-dimensional representation of TDEM resistivity distribution of section 9 with geological and hydrogeological design..... 73

Figure (4.22):Two-dimensional representation of TDEM resistivity distribution of section 10 with geological and hydrogeological design..... 73

Figure (4.23): Spatial extension of saltwater interface produced by combined interpretation of the collected TEM and VES data with the acquired hydrogeology and geology themes at depth slice from 5m to 40 m. 75

Figure (5.1): water sampling from a farm well in Azraq area 78

Figure (5.2): Water type of selected farm wells 81

Figure (5.3): Plotting of Water samples on expanded Durov diagram 82

Figure (5.4): Expanded Durov Diagram, for water from various environments..... 83

Figure (5.5): Groundwater contour map of the shallow aquifer in the study area 84

Figure (5.6): Groundwater conductivity map in microsiemens/cm for sampled wells..... 85

Figure (5.7) : Variation of Chemistry with depth of unsaturated zone in Azraq farms 86

List of Tables

Table (1.1): Analytical procedures used in measuring the physic-chemical parameters.....	16
Table (2.1): Geological and Hydrogeological Classification of the Rock units Unit in Jordan (Rimawi 1985)	31
Table (3.1): Major Units of the Shallow Aquifer in the Azraq Basin Area.....	35
Table (3.2): Groundwater balance of the main basins in Jordan (MWI,2006)	46
Table (4.1): Promising Coordinated sites to install underground saltwater sensors.	74
Table (5.1): List of Farm wells used in this study in Qa Azraq area	77
Table (5.2) Chemical analyses of selected farm wells	80

ملخص

يشكل حوض الأزرق الجزء الشمالي الشرقي من المملكة الأردنية الهاشمية حيث يقع بين إحدائيات فلسطين 230-250 شمال وتبلغ مساحة الحوض 12710 كم² يقع 94% منها داخل الأراضي الأردنية وأكثر من 5% ضمن الأراضي السورية واقل من 1% ضمن الأراضي السعودية يبلغ أعلى ارتفاع حوالي 1576م عن سطح البحر من الجزء السوري وحوالي 1234م في منطقة تل الرماح في الأردن . ويقع منخفض الأزرق نفسه على ارتفاع 500م عن سطح البحر أما معدل الارتفاعات فهو 750م عن سطح البحر كانت واحات الأزرق قبل جفافها في بداية التسعينات ظاهرة سياحية رائعة إضافة إلى إنها كانت تجلب الطيور المهاجرة من أوروبا.

يعتبر حوض الأزرق من أهم الأحواض في الأردن والذي يزود المدن الرئيسية بمياه الشرب. هناك ثلاث طبقات حاملة للمياه الجوفية في الحوض ، الخزان الجوفي العلوي والذي يعتبر أهم الخزانات الجوفية ، وذلك بسبب انخفاض تكلفة الحفر ووجود نوعية جيدة من المياه الجوفية. بدأ حوض الأزرق الجوفي يعاني من نزوب مستويات المياه الجوفية وذلك نتيجة زيادة الطلب على مياه الشرب والتي بلغت 65 مليون متر مكعب في السنة بالإضافة إلى ضخ المياه من الآبار الزراعية (مرخصة أو غير مرخصة) والتي تشكل أكثر من 70% من المياه المضخوخة من الخزان الجوفي العلوي ونتيجة لذلك فقد جفت واحة الأزرق تماما. أدى زيادة الضخ الجائر من الآبار المحفورة في الحوض سواء الآبار الزراعية أو التي تستخدم لأغراض الشرب والتي تشكل لحد الاحتياجات المتزايدة للمدن الثلاث الرئيسية (عمان ، اربد والزرقاء) إضافة إلى منطقة الأزرق نفسها إلى انخفاض مستويات المياه الجوفية وزيادة نسبة الملوحة في الحوض مما اخذ يهدد بخطر انتشار الملوحة في الخزان العلوي الضحل والمكون من البازلت والحجر الجيري الصواني وزيادة نسبة الملوحة في الحوض، ان زيادة ضخ المياه الجوفية يسرع من حركة المياه إلى أعلى ويؤدي إلى انخفاض في حركتها باتجاه الأسفل.

أظهرت التحريات الهيدروجيولوجية والهيدروجيوكيميائية وجود ثلاث خزانات مائية جوفية (العلوي ، الأوسط والسفلي) : يتكون الخزان المائي العلوي من البازلت ، الرسوبيات الحديثة وتكاوين الشلالة والرجام حيث يسمى "خزان البازلت- رجام" ، في منطقة شمال الأزرق في حين يتشكل من تكاوين الشلالة والرجام في الجزء الجنوبي من الحوض ويسمى " خزان الرجام" . وتعود أهمية هذا الخزان إلى نوعية المياه الممتازة وقلة تكاليف الحفر فيه خصوصاً في الجزء الشمالي . ويبلغ العمق إلى هذا الخزان ما بين عدة أمتار في من خفض الأزرق إلى أكثر من 200 م في المناطق الشمالية والجنوبية من الحوض.

ان المياه المالحة موجودة في قاع الأزرق على أعماق ضحلة في حين تم العثور على المياه العذبة في الجزء الشمالي والغربي من الحوض ، وقد أدى ذلك إلى تطوير فاصل بين مناطق المياه المالحة والعذبة. وهناك احتمالية كبيرة لهذا الفاصل ان يتجه نحو المياه العذبة في حقل الآبار بسبب الضخ الجائر (أبار AWSA) المستخدمة لأغراض الشرب ، تضخ إلى عمان لأغراض الشرب حوالي 17 مليون متر مكعب. لذلك ، فإنه من الضروري تحديد موقع هذا الفاصل والذي يؤدي لتداخل المياه المالحة مع المياه العذبة والتي بدأت ويتوقع أن تتسارع في المستقبل القريب.

فقد تم استخدام طرق المقاومة الكهربائية الجيوفيزيائية العمودية والحث الكهرومغناطيسي الوقي جنباً إلى جنب مع الطرق الهيدروجيوكيميائية التي تستخدم لتحليل حجم وسلوك تسرب المياه المالحة إلى المياه العذبة في الجزء الأوسط من حوض الأزرق الجوفي وتحديدًا في منطقة قاع الأزرق لدراسة التغيرات في سماكة

الجزء العلوي من الخزان الجوفي الضحل وتوزيع المقاومة الكهربائية فيه لتحديد الفاصل بين مناطق المياه المالحة والعذبة. المشكلة الرئيسية في دراسة عمليات تسرب المياه المالحة هو الرصد الزماني والمكاني لحركة الفاصل (Interface) بين المياه العذبة والمياه المالحة. لقد استخدمت الطرق الجيوفيزيائية في الماضي لدراسة اتجاه التداخل بين المياه العذبة والمياه المالحة. لقد أثبتت طريقة الحث الكهرومغناطيسي (TDEM) انها من اكثر الطرق فاعلية وتعطي نتائج أفضل من التقنيات الجيوفيزيائية التقليدية، في الواقع، الميزة الرئيسية لهذا الطريقة هو أن السير العميق للطبقات يمكن ان يتم في وقت قصير نسبياً. بالإضافة الى ان هذه الطريقة تكون مفيدة بشكل خاص للتمييز بين الطبقات ذات المقاومة المنخفضة، وبالتالي سهولة رصد تسرب وانتشار المياه المالحة وتداخلها مع المياه العذبة.

وأظهرت الدراسة أن تسرب المياه المالحة الى المياه الجوفية العذبة كان محصوراً في الجزء العلوي من الرواسب الرباعية في منطقة قاع الأزرق والذي يحده الحواجز الأفقية والعمودية. ان وجود الفاصل بين المياه المالحة والمياه العذبة يكون بشكل انتقالي ويؤدي الى تشكيل منطقة خلط (Mixing zone). ان حركة المياه المالحة تكون أفقية في البداية حتى تجتاز الصدع الرأسي ثم تتحرك بشكل رأسي تحت تأثير الكثافة. لقد كان امتداد حركة المياه المالحة بشكل رأسي وتتحرك في الوقت الحاضر بشكل أفقي في اتجاه منطقة حقل ابار مياه التابع لسلطة المياه . ان الآبار المجاورة لقاع الأزرق تظهر زيادة مستمرة في الملوحة حيث ان مستوى المياه الجوفية قريب جداً الى السطح بحيث لا يتجاوز بضعة امتار.

لقد تم تنفيذ سبعة وثلاثون (37) مقطعاً بطريقة الحث الكهرومغناطيسي الوقتي بالإضافة الى سبعة (7) مقاطع سبر كهربائي عامودي في المنطقة القريبة من قاع الأزرق خلال فترة اسبوع من 8 الى 15 تموز 2010 ، وقد تم تحليل المعلومات التي تم الحصول عليها من خلال توزيع قيم المقاومة الكهربائية مع العمق والذي يبين طبيعة نوعية المياه الجوفية في طبقات الخزان الجوفي العلوي الضحل، وهناك علاقة عكسية بين مقاومة المياه وتركيز الأملاح المنحلة أو المذابة ويتعكس ذلك على الصخر الذي يحوي المياه ، ولذلك فان الصخر المشبع بمياه عذبة تصل مقاومته الكهربائية الى 30 اوم.متر بينما نفس الصخر المشبع بمياه مالحة لا تتعدى مقاومته 0.1 الى 5 اوم.متر. فقد امكن تمييز الطبقات التي تحوي مياه عذبة عن تلك المالحة من خلال قيم المقاومة الكهربائية وقد كانت تتدنى قيم المقاومة الكهربائية في المياه المالحة الى ما دون 0.1 اوم.متر وقد تم تحديد النطاقات التي تحتوي على مياه مالحة جداً في الخزان الجوفي العلوي وكذلك تم معرفة عمق الفاصل بين المياه العذبة والمياه المالحة والذي كان يتراوح بين عمق 5 الى 40 متر من سطح الأرض.

وتشير النتائج إلى أن معدلات الاستخراج الحالية من ابار المياه ما زالت تفوق حد الاستخراج الآمن (اي حوالي 65 مليون متر مكعب / سنة) ، ولذلك يخشى ان تواصل المياه المالحة التحرك باتجاه حقل الآبار (AWSA). اما الوقت المتوقع لوصول هذه المياه المالحة الى حقل AWSA هو بين 500 - 2000 عام. وهناك احتمالية كبيرة ان تقدم المياه المالحة باتجاه المياه العذبة يكون ضعيفاً لوجود تراكيب جيولوجية مثل الصدوع والبنى الخفية التي تعمل كحواجز لمنع تسرب المياه المالحة الى مصادر المياه العذبة كما ظهر في خرائط توزيع الملوحة الموجودة في متن هذا التقرير.

أن زيادة استخراج المياه من حوض الأزرق سواء من ابار حقل AWSA أو من ابار المزارع المنتشرة في حوض الأزرق بشكل يفوق حدود الأسخراج الآمن (Safe Yield) سوف يؤدي الى هبوط في مستويات المياه الجوفية وجفاف العديد من الآبار والينابيع في اتجاه شرق والأزرق. اما السيناريوهات الأكثر تفاؤلاً

هو ان كمية الاستخراج يجب ان تكون في حدود 16 حتي 18 مليون متر مكعب / سنة ، وهو حد الأستخراج الآمن المناسب للخران الجوفي العلوي. وبناء على ما سبق فان الطرق الجيوفيزيائية مع الدراسات الجيولوجية والهيدروجيولوجية تشكل أداة مفيدة لتحديد الحد الفاصل بين تداخل المياه المالحة مع المياه العذبة في طبقة المياه الجوفية الضحلة وقد تم تأكيد وجود علاقة من خلال التوزيع المكاني لقيم المقاومة الكهربائية مع الخطوط التكتونية الرئيسية في المنطقة القريبة من المناطق الملوثة بسبب تسرب المياه المالحة. وهذه الشقوق والفواصل تعمل بمثابة حاجز لنقل المياه العذبة إلى المياه المالحة ، والعكس بالعكس.

وبناء على نتائج المسح الكهربائي والكهرو مغناطيسي في تحديد الحد الفاصل بين المياه المالحة والمياه العذبة فقد تم اقتراح خمسة مواقع (5) لتثبيت أجهزة استشعار (Sensors) تحت الأرض على عمق محدد يتراوح بين 5-40 متر لرصد ومراقبة حركة المياه المالحة باتجاه المياه الجوفية العذبة.

وأخيرا يمكن القول ان تسرب المياه المالحة الى المياه العذبة يشكل خطرا على موارد المياه العذبة. علما بان استراتيجيات التخفيف التي يتم تصميمها لإبطاء أو وقف معدل تسرب المياه المالحة يمكن أن تكون مكلفة ولكنها ضرورية لحماية الموارد المائية من المزيد من الضرر.

وأخيرا نوصي وزارة المياه والري بوضع خطة عمل لمساعدة السكان المحليين من منطقة الأزرق لاستخراج المياه عالية الملوحة والتي تزيد في بعض الأحيان عن 200.000 ملغم/لتر لإنتاج الأملاح وللحد من الضخ من الآبار التي تستخدم لأغراض الري والزراعة لتعزيز منع تسرب المياه المالحة نحو ابار حقل AWSA في المستقبل القريب كجزء من حل شامل ومتكامل ضمن إطار وسياسة وطنية.

Executive summary

Azraq basin supplies Amman with excellent water for drinking water purposes, but due to over-pumping from the Amman Water and Sewage Authority (AWSA) well-field as well as from the farm wells used for irrigation, the water level dropped dramatically and signs of salinization and depletion are starting to occur. The severe drawdown in the AWSA well-field caused a reverse in the hydraulic gradient and consequently, the saltwater in the center of the basin (Qa-Azraq) started to move in the direction of the well-field. In this study a geophysical survey combined with hydrogeochemical investigation were used to analyze the size and behavior of the fresh saltwater intrusion.

One of the main problems in studying saltwater intrusion processes is the temporal and spatial monitoring of the fresh-saltwater interface. In the past geophysical methods have been used to study its evolutionary trend. Time Domain Electromagnetic (TDEM) methods have proven to be most efficacious, producing better results than the traditional galvanic techniques. In fact, the major advantage of this method is that deep soundings can be performed in a relatively short time. TDEM sounding appears to be particularly useful for discriminating between layers having low resistivity and consequently for monitoring salt water intrusion and diffusion, as well as artificial recharge procedures.

The study showed that the saltwater was initially confined to the top of the Quaternary sediments in Qa-Azraq as it is bounded by horizontal and vertical barriers. The interface between freshwater/saltwater is transitional forming a mixing zone. The induced movement caused the saltwater to move horizontally in the beginning until it passed the vertical boundary fault and then tended to move vertically under the influence of its density. The saltwater completely extended vertically and tends at present time to flow horizontally in the direction of the well-field. The wells that are adjacent to the Qa-Azraq are showing a continuous increase in salinity. The geophysical model using results indicate that if present abstraction rates continues (1998: 66 MCM/yr), the saltwater will continue moving. Expected arrival time to the AWSA well-field ranges between 500 - 2000 year. Pessimistic prediction scenarios showed that any increase in abstraction from the AWSA well-field or in the area north of the well-field, will cause severe drawdown and dryness of several wells in the springs area to the east and Azraq center. Optimistic scenarios showed that an abstraction quantity of 16 - 18 MCM/yr, is the appropriate safe yield of the Upper Aquifers System. The water injection simulations showed promising results and showed that it could be used as a replenishments method for the springs and the wetland. It could be also used as vertical boundary to prevent saltwater intrusion. Finally, any remedy measures in Azraq basin should be addressed as a part of larger comprehensive and integrated national policy framework.

CHAPTER 1 INTRODUCTION

1.0 Introduction

Saltwater intrusion is the movement of saline water into freshwater aquifers. Most often, it is caused by ground-water pumping from coastal wells,^[1] or from construction of navigation channels or oil field canals. When fresh water is withdrawn at a faster rate than it can be replenished, the water table is drawn down as a result.

Seawater intrusion is a principal cause of fresh groundwater salinization in many regions of the world (Bear et al., 1999). Fresh groundwater in arid and semi-arid regions, like the Mediterranean basin, is even more threatened by this type of contamination. In deed, such regions are characterised by a constant increase of water demand, especially for agricultural purposes, contrasting with the limited possibility of natural recharge and the high rates of evapotranspiration. Geochemical, geophysical, hydrodynamic and modelling tools have been used to study seawater/freshwater interaction along the transition zone. In this work we are applying geochemical methods to identify processes accompanying seawater/freshwater mixing in the Qa' Al Azraq area, northeast of Jordan. These hydrochemical processes can be considered as indicators of the evolution of seawater intrusion (Custodio and Bruggeman, 1987).

Azraq basin is one of the most important groundwater basins in Jordan. It is located in the Northeastern part of Jordan. It extends northwards into Syria and southwards into Saudi Arabia. The Azraq Oasis (called locally Sabkhah or Qa'a Azraq) which is located in the central part of the basin is at a distance of about 120 km northeast of Amman. Qa'a Azraq is a relative large mudflat located in the central part of the basin. Two villages are located on the western side of the Qa'a Azraq, these are: Azraq Shishan and Azraq Drouz. A well field called AWSA was established north of Azraq Drouz Springs (northern springs) where about 15-20 million m³ per year (MCM/a) of water is pumped to the capital Amman for drinking purposes since 1982. Farmers in the area are using around 45 MCM/a. Therefore, the total abstraction from the basin is about 65 MCM/a (El-Naqa et al., 2007).

Two groups of springs exist at the border of the Azraq Sabkhah; The Drouze springs and Shishan springs. The discharge of these springs was about 15 MCM/a before 1981. This quantity of water was in equilibrium with the water balance of the basin representing the steady state condition. The over-exploitation of groundwater aquifers in the basin was dramatically affected the discharge of these springs. Drouze springs dried completely in 1986 and the Shishan springs discharge was reduced by about 80%. The consequences of over-expolitation affected the ecosystem in the area and many of the rare birds and plants disappeared totally. Rising concern among Non-Governmental Organization (NGO's) for protecting the environment, they pose more pressure on the local farmers and the water authorities to alleviate the total abstraction

of groundwater to allow natural rehabilitation of the aquifer. Water Authority of Jordan (WAJ) brought the abstraction rate down from approximately 20 MCM in 2001 to about 15 MCM in 2002 and 2003.

The central area forms a real threat to the whole basin, like the effect of the salt water intrusion on the fresh ground water puff, either as back flow from the Sabkha area or through the upward leakage from the deeper saline bodies.

There are three aquifers in the basin, the upper one is the most important, due to its low drilling cost and good quality of ground-water (El-Naqa et al., 2007). Due to an increase in demand for drinking water (65 MCM), the basin started to suffer from a depletion of ground-water levels. As a result, the Azraq oasis is now completely dry. Increasing ground-water pumping accelerates the upward movement and causes a decrease in the downward leakage. The major exploited aquifers are the alluvial deposits, the fractured basalt rocks mainly in the northern part of the basin, and the chert limestone of the Rijam aquifer. These groups of aquifers are known as Shallow Aquifer system. A saline water is exist in the mud flat area (Qa') at shallow depths while the fresh water is found in the northern and western part of the basin, this has led to a development of an interface between fresh and saltwater zones. Since there is a possibility of this interface moving towards the fresh water well field (i.e AWSA well field) as a cause of extensive pumping. The AWSA well field used for drinking purposes, of which 17 million cubic meter pumped to Amman to use for drinking. Therefore, it is necessary to determine the location of this interface, since saline water intrusion has started and is predicted to accelerate in the near future.

1.1 Scope of work

The main objectives of the current study is the following:

1. To investigate the location and extend of the fresh-salt water interface in the upper unconfined aquifer (Basalt and B4);
2. To determine the location and extend of the fresh-salt water interface and to assess the influence of the salty water in the sabkha area on the surrounding fresh water in an escalating manner using geophysical techniques: the Vertical Electrical Sounding (VES) and Time Domain Electromagnetic (TDEM) combined with the available hydrogeochemical data of the existing farm wells.
3. To assess the influence of the salty water in the sabkha area on the surrounding fresh water in an escalating manner and the possible causes and mechanisms of salinity of the upper aquifer system
4. To help in installing a series of sensors to monitor continuously the movement of saline water into the shallow fresh water in Qa' area.
5. Evaluate various techniques for mitigating saltwater intrusion (eg. Optimizing pumping rates, freshwater injection, etc.).

6. To investigate local geochemical processes (dissolution) in wells that were subject to salinization.
7. To investigate the effect of over pumping of the private wells and the agricultural sector which is exceeding the upper aquifer safe yield.

1.2 Methodology

The methodology of the study can be summarized as the following:

a. Literature review and data collection: collecting all data available related to hydrogeological, and geochemical data and other related data documented in the available technical reports.

b. Collection of necessary data during this work in order to confirm the data collected and to compile the missing data. These data contains, pumping rates, static and dynamic water levels, and pumping test analysis.

c. Construction of groundwater flow map from the static water levels data from the groundwater wells in the vicinity of the central part of Azraq Basin.

d. Collection of water samples to determine the chemistry and quality of groundwater from the target aquifer. The samples will be collected from the existing wells. The sample will be analyzed for Physico-chemical parameters; include total dissolved solids (TDS), temperature, electrical conductivity (EC), pH, Ca, Mg, Na, K, HCO₃, CO₃, SO₄, NO₃, Cl, DO (dissolved oxygen), Mn, Fe, Eh, total and ferric iron, pH, turbidity. The analyses of water samples will be checked and the accuracy of the analysis will not exceeds 5%.

c. Data evaluation: The pumping analysis will be evaluated for the target aquifer systems in order to calculate the aquifer characteristics (transmissivity, permeability and storage coefficient). These evaluations will be done using commercial computer software.

e. Conduction Vertical Electrical Sounding (VES) and Time Domain Electromagnetic (TDEM) in in the central part of the Azraq Basin to delineate the interface between the fresh and salt waters. In fact, there is highly saline water in the mud flat area at shallow depths while to the north and the west freshwater exists in the basalt and chert limestone aquifers, has led to the development of an interface between fresh and saline water zones. Since there is a possibility of the interface moving towards the freshwater wellfield as a cause of extensive pumping.

The methodology that has been adopted in the current study can be summarized briefly in the next sections.

1.2.1 Office Work

During the execution of the present study data related to existing boreholes, geology, springs, hydrology, hydrogeology, water levels, hydrochemistry and the essential maps (Geologic, topographic, land use etc..) required were compiled from different sources: the Ministry of Water and Irrigation (MWI), Royal Geographic Center and from various published reports, journals, and researches. In addition to reviewing the national and international literature related to the subject.

1.2.2 Field Work

The field work has been completed during the period 12 July and 15 August, 2010 with the following accomplishments:

- Thirty five (35) Time Domain Electromagnetic (TDEM) survey and ten Vertical Electrical Sounding (VES) were carried out in the Qa' area to detect and to delineate the salt fresh water interface have been carried out in the central part of Azraq Basin (i.e. Qa' Al Azraq area). The VES survey was completed with 29 schlumberger electrical sounding configuration with a maximum current electrode spacing (AB) ranging from 800 m to 2000 m (El Waheidi, 1992). The position of the transect lines were determined using a hand – held GPS system.
- Water Sampling was carried out from private irrigation wells. In the case of private wells which were not pumping when visited the static water level was measured, then were allowed to pump for 15 minutes only before sampling. Pumping was not possible for a longer time because the farmers were keen not to loose water.
-
- Field visits to collect 16 representative water samples from farm wells in the Qa' Al Azraq to be analyzed in the Central Laboratories of the Ministry of Water and Irrigation for their chemical and physical constituents. These samples were collected from specific points along some of the survey lines in order to carry out geochemical analyses to ground truth the geophysical data.

1.2.3 Laboratory Work

- The Chemical and the physical analyses of the collected water samples were carried out in the Central Laboratories of the Ministry of Water and Irrigation. The water samples was collected for the determination of the following parameters:
- Major cations Ca^{+2} , Mg^{+2} , Na^+ , K^+
- Major anions (HCO_3^- , Cl^- , CO_3^{-2} , SO_4^{-2} , NO_3^- , PO_4^{-3})
- The pH- value, electrical conductivity (EC) and temperature were measured at site.

The analytical methods used for the analyses of the different parameters are listed in Table (1.1). These analytical techniques were performed according to the procedures mentioned in the Standard Methods for Examination of Water and Wastewater (1998).

Table (1.1): Analytical procedures used in measuring the physico-chemical parameters

Parameter	Analytical Methods
Electrical Conductivity (EC, $\mu\text{s}/\text{cm}$ at 25C°)	Field EC-meter
pH-Value	Field pH-meter
Temperature(C°)	Field thermometer of 0.1 C° accuracy
Total Hardness (T.H)	Titration with 0.02N EDTA using Eriochrom. Black T as indicator
Sodium, Potassium, (Na^+ , K^+)	Flame photometer
Calcium(Ca^{+2})	Titration with 0.02N EDTA using Murexide as indicator
Magnesium(Mg^{+2})	By calculation
Bicarbonate (HCO_3^-)	Titration with 0.02N H_2SO_4
Chloride (Cl^-)	Titration with 0.01 AgNO_3 using Potassium Chromate(K_2CrO_4) indicator
Sulfate(SO_4^{-2})	Ultra violet visible spectrophotometer wave length 492 nm
Nitrate (NO_3^-)	Ultra violet visible spectrophotometer- wave length 206 nm
Phosphate(PO_4^{-2})	Ultra violet visible spectrophotometer- wave length 690 nm
Ammonium (NH_4^+)	Ultra violet visible spectrophotometer- wave length 425 nm

1.4 Background Information

Azraq (Arabic: الأزرق) is a small town in the province of Zarqa Governorate in central-eastern Jordan, 100 km east of Amman (Figure 1.1). The population of Azraq was 9021 persons in 2004. Azraq has long been an important settlement in a remote and now-arid desert area of Jordan. The strategic value of the town and its castle (Qasr Azraq) is that it lies in the middle of the Azraq oasis, the only permanent source of fresh water in approximately 12,000 square kilometers of desert. According to the Jordan National Census of 2004, the population of Azraq was 9,021 persons, of whom 7,625 (84.5%) were Jordanian citizens. 4,988 (55.3%) were males, and 4033 (44.7%) females. The next census is scheduled on 2014.

The Azraq Basin, about $12,750\text{ km}^2$ in size, is located in the northeastern Badia region; the Badia forms 85% of Jordan's land surface. The drainage pattern of the main basin has been delineated as shown in Figure (1.2). Climatic changes have occurred in the region since the Neolithic age

(8,500-3,750 BC); the climate is hot and dry. Evidence exists that a large lake totaling 4,500 km² covered the Azraq depression in the Pleistocene age (Bender, 1974). Qa Al Azraq covers some 75 km², and is fed by surface run-off from an extensive network of wadies. The Qa is partly or wholly flooded in most winters, creating a temporary fresh to brackish lake with a maximum depth of 1.25 m and broad muddy margins. The Qa when flooded is considered to be the most important site as a stopover and wintering site for migratory wildfowl in Jordan (Bird Census Report, RSCN, 2003). Figure (1.3) shows the satellite google image to Azraq town and Qa' Al Azraq.

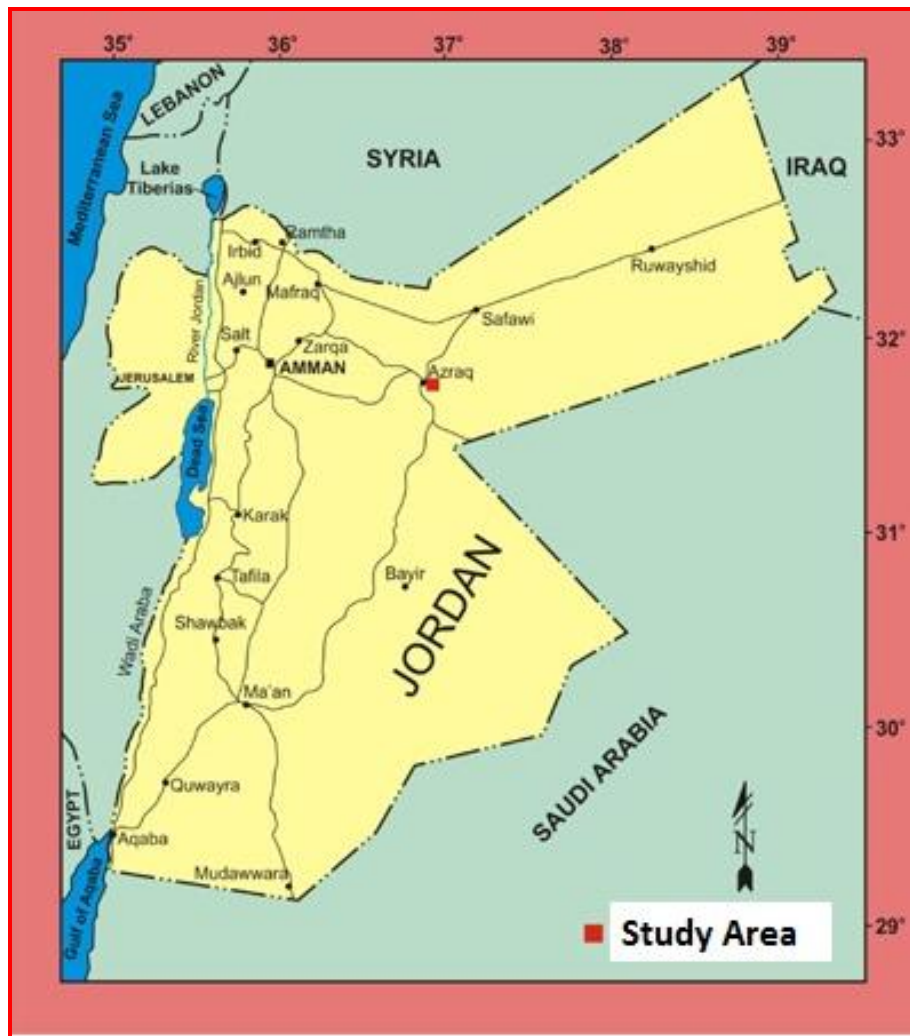


Figure (1.1): Location map of Azraq area

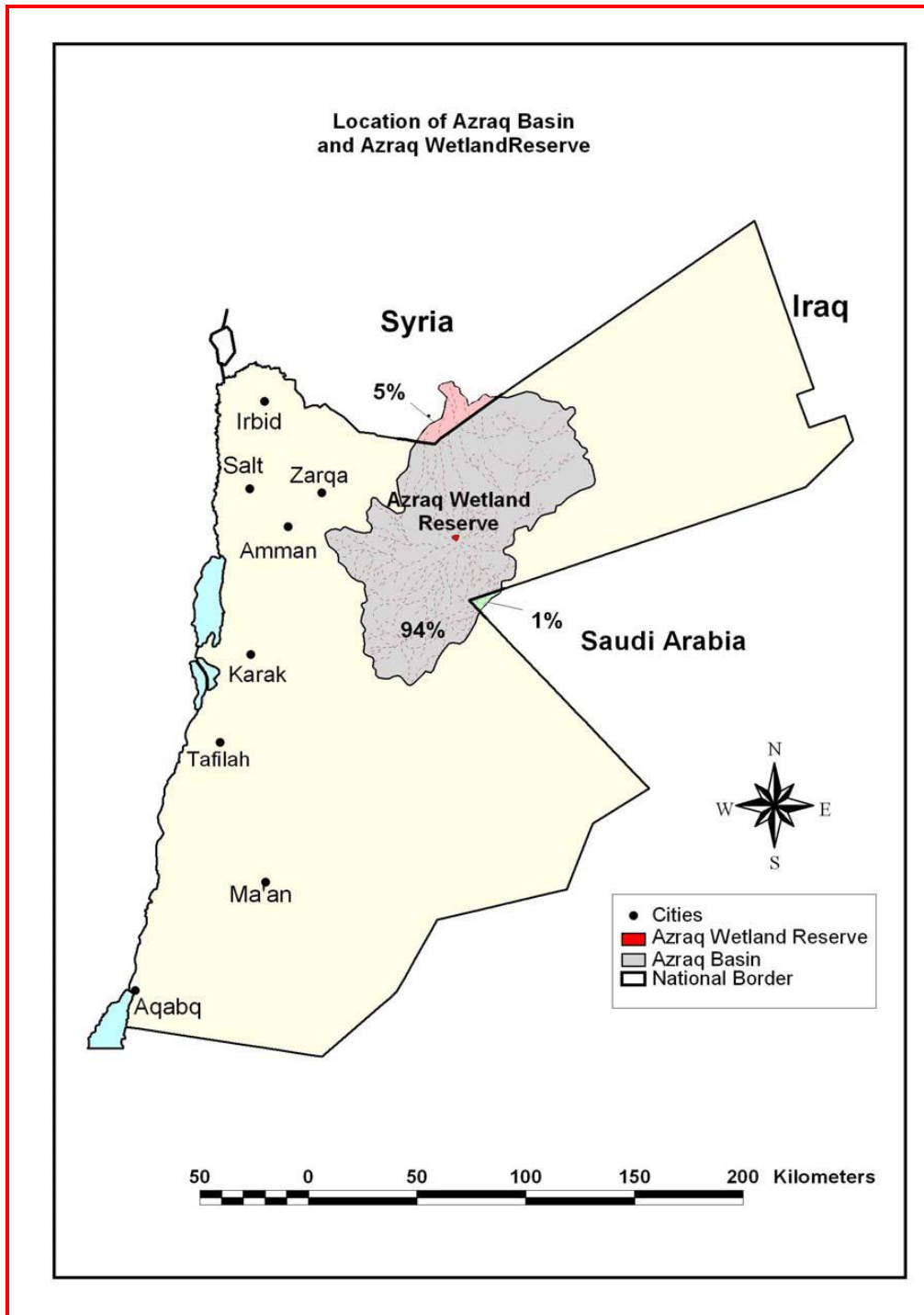


Figure (1.2): Location map of Azraq Wetland Reserve and Azraq Basin

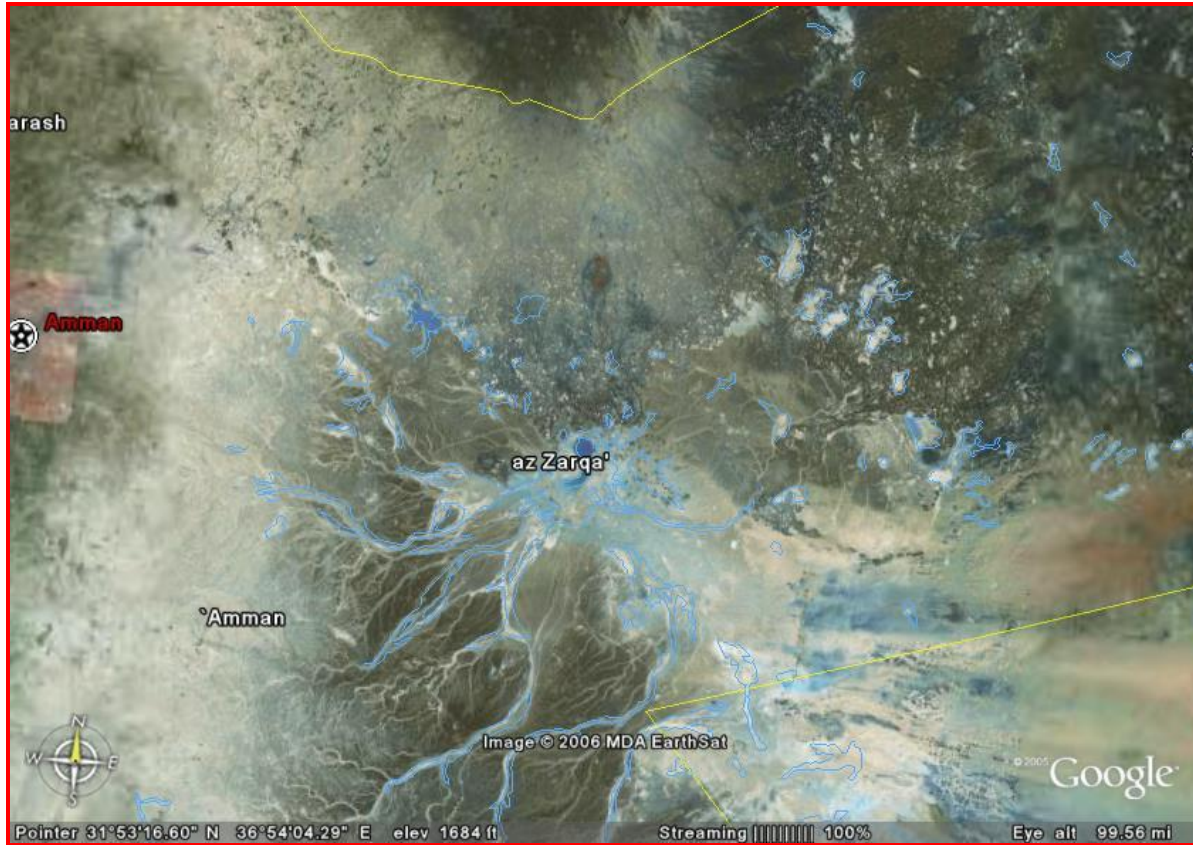


Figure (1.3): Google earth satellite image of Qa' Al Azraq

The Azraq basin forms the largest resource of good-quality ground and surface water in northeastern Jordan. The water quality, resources and borehole yields in other Jordanian aquifers, such as in the Sirhan and Hammad basins, are all inferior to those in the Azraq basin.

Azraq basin consists of three aquifer systems: the upper shallow fresh water basalt aquifer (the target aquifer of extraction) is currently under the threat of salinization due to overexploitation, the middle limestone brackish water aquifer (600 to 15,000 mg/l) of ages more than 30,000 years and the deep sandstone aquifer which has low yields and poor quality water. The pattern of water-flow indicates that the velocity of groundwater flow from the recharge area to the springs in Azraq Oasis is very slow. Recent studies have shown that the groundwater in the well field about 3 km north of the oasis is between 4,000 and 20,000 years old.

The Azraq Oasis, or Azraq Wetlands Reserve, is a unique ecosystem in a fragile environment, lying at the heart of the Azraq Basin and recognized as a RAMSAR Site. Oasis is the fertile tract of land that occurs in a desert wherever a perennial supply of fresh water is available. Oases vary in size, ranging from about 1 hectare (2.5 acres) around small springs to vast areas of naturally watered or irrigated land. Underground water sources account for most oases; their springs and wells, some of them artesian, are supplied from sandstone aquifers whose intake

areas may be more than 800 km (500 miles) away. The Azraq area contains a wealth of biodiversity and habitats, and the richest habitat of all exists in its wetlands. Despite its desert location the oasis contains a variety of habitats and micro-habitats that are found only in wetland environments, which are extremely rare in the region.

1.5 Physiography

1.5.1 Geographical Setting

Azraq Basin is one of the large desert basins in Jordan that comprises an area of about 12710 km², of which about 6% extends into Syria in the north and Saudi Arabia in the southeast of the basin. According to Palestine Grids, the area lies between 250 to 400 E and 055 to 230 N. It is bordered by the Syrian Druze Mountains to the north and Hammad Basin and Sirhan Basin to the southeast and Mujib Basin from south, (Figure 1.1). The town of Azraq and its oasis are located in the center of the basin, 100 km east of Amman. Safawi (H5), is 45 km northeast of Azraq town and 110 km west of Ruweished town.

1.5.2 Topography and Drainage

The Azraq Basin is a depression surrounded by hilly relief and consequently all water courses drain in a mudflat of Qaa' Azraq, at an average elevation of about 500 m a. m. s. l. Slopes in the basin are gently with an average slope of 1% except in the north where the gradient increases to 3% in the vicinity of Syrian border. The surface water divide rises to 900 m a. m. s. l. in the south, east and west. In the north, the elevation of the ground rises more steeply to about 1550 m a. m. s. l. in the Syrian Jebel Druze area, adjacent to Tillin town. Topography is shown in (Figure 1.4). The drainage network are controlled by different factors such as type of soil, type of rock and structures. The main wadis in the study area are Wadi Butum, Wadi Rajil and Wadi Shomari draining in the western and southwestern parts and Wadi Rajil draining in the eastern and northeastern parts. The wadis discharging into the mudflat of Qaa' Azraq are characterized by wide shallow flow-beds with relatively low slopes. Intermittent flow in the wadis occurs in winter and drains into Qaa' Azraq, where it evaporates within few months (Figure 1.5). There are ten major wadis draining into the Azraq depression, of which wadi Rajil is the longest

1.5.3 Land Use

There are two nature reserves in the study area; these are being the Azraq Oasis and the Shoumary wildlife reserve (Figure 1.6). The Azraq Oasis is currently neglected, but there are plans to rehabilitate it with the use of pumped ground water. The Shoumary wildlife reserve in the southwest of the basin attract visits from schools and tourists, The rest of the rural area is populated by Bedouin, of whom 5% are still nomadic (HCST, 1993). Rangeland is grazed by sheep and goats. Overgrazing is apparent at Shoumary, where prolific shrubbery and barren land.

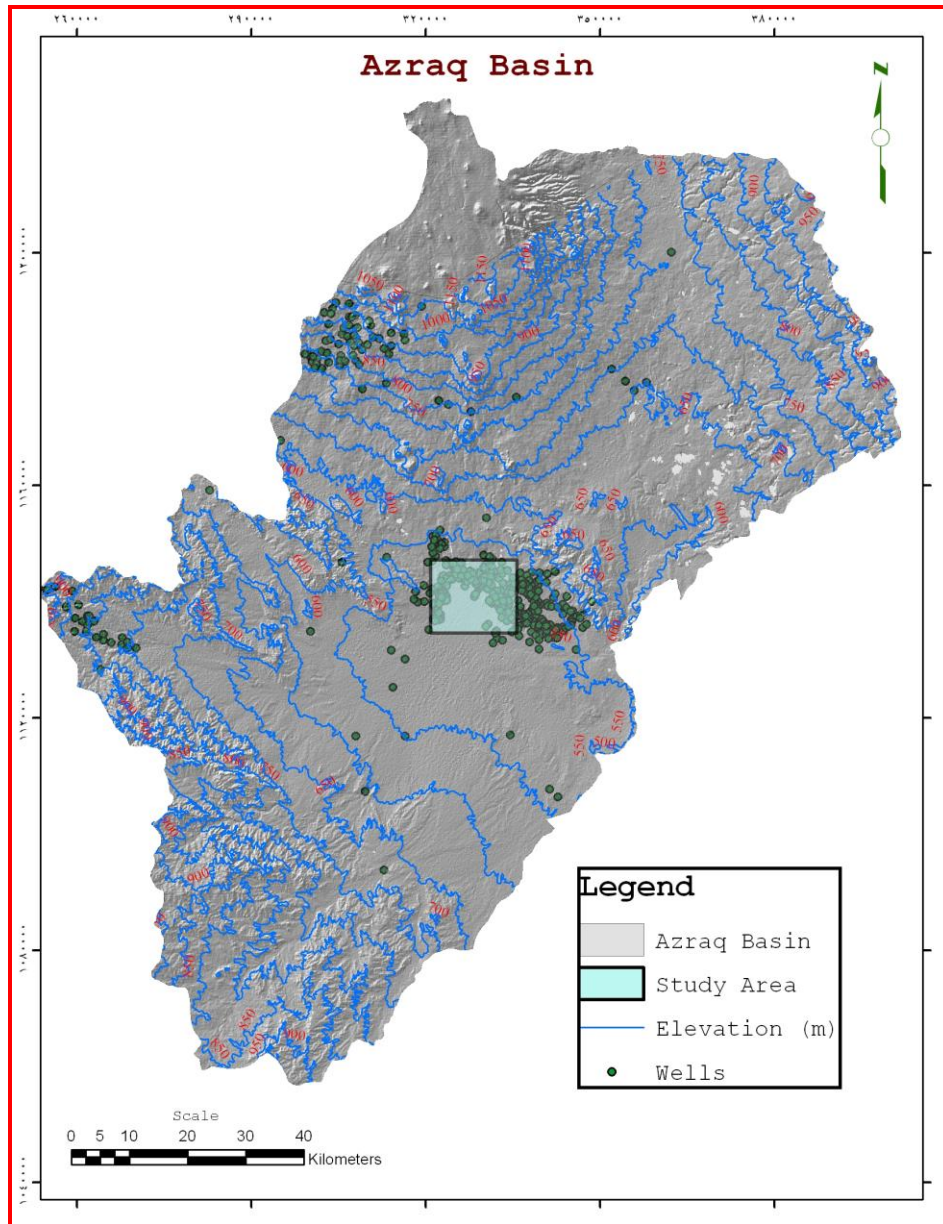


Figure (1.4): Topographic map of the Azraq Basin showing the study area and distribution of groundwater wells penetrating the Shallow Aquifer



Figure (1.5): The mudflat of Qaa' Azraq in winter period 2010

1.5.4 Climate

The climate of the Azraq Basin is characterized by two well-defined seasons, hot and dry summer, relatively wet and cold winter. Most of the study area is arid and small portion can be considered as semi arid (Ayed, 1986). Ayed, (1996) conducted a comprehensive study on the climatological and hydrological variables of the Azraq Basin. The record length extends from 1967 to 1995. According to his study, the average relative humidity varied from 49.9 to 61% in summer and from 56 to 82% in winter. The average annual minimum and maximum temperatures are 11.6 °C and 26.6 °C respectively. The coldest month of the year is January while the hottest months are July and August. The recorded maximum temperature is in July 1978, while the absolute minimum -9 °C is observed in January of 1993.

The Azraq drainage basin is irregular in shape and forms a relatively shallow depression with a central playa (Qa'a Azraq), surrounded by mud flats and salt pans. The area is typical for arid to semi arid zone. The precipitation ranges from 50 mm/a in Azraq Oasis to 500 mm/a in Jabal Arab. The average precipitation for the entire basin is 87 mm/a, most of which occur as storms between January to March.

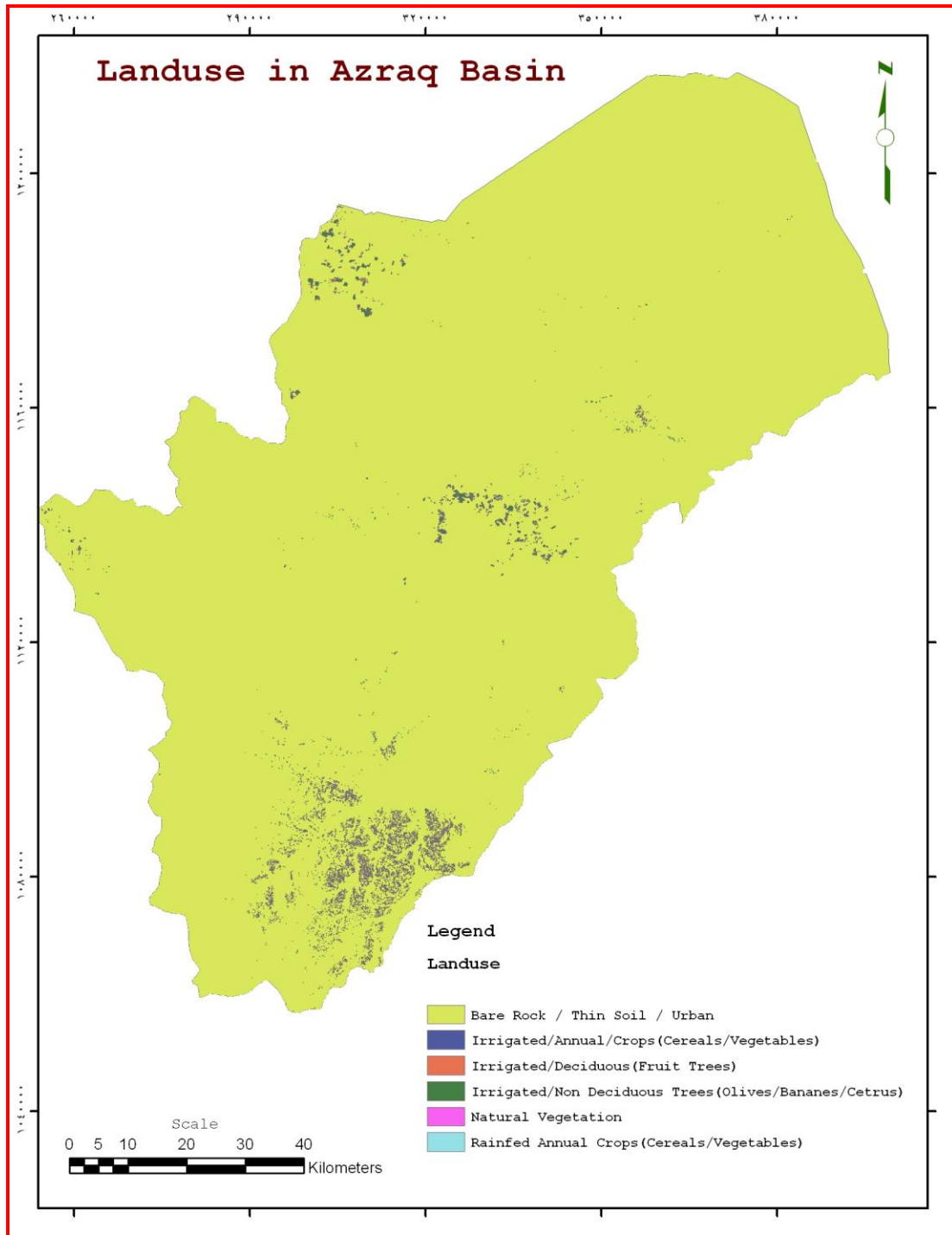


Figure (1.6) : Land use map of the Azraq basin

During the year, sunshine duration changes with the season. A minimum of about 8 hours/day is recorded in December and January, while the maximum sunshine duration occurs in June, with absolute value 13.3 hours/day (hrs/d) is observed in 1987. In general, sunshine duration in the Azraq Basin ranges between 8 to 8.3 hrs/d in winter and between 8.7 to 11.9 hrs/d in summer.

The daily average evaporation observed from class A pan is 10.4 mm, and varies from 5 to 19 mm/d in summer and from 3 to 12 mm/d in winter. The annual average wind speed is 11.6 km/hr, which ranges between 10 to 18 km/hr in summer, and between 7 to 12 km/hr in winter. Comparatively strong northwesterly winds in summer, shifting to the southeast in the winter season. During rainy season easterly and southwesterly winds also occur. They are cold dry in winter, but hot, scorching and consequently harmful to the vegetation in summer.

The area in general is lightly vegetated although in the farm areas a wide range of vegetables, fruits and olive trees is grown under irrigation.

1.6 Current Azraq water dilemma

Major changes have occurred to the wetlands of Azraq Oasis in the last twenty years. The two springs at Druze dried out completely in 1987; one of the large springs at Shishan ceased to overflow in 1990, and the other finally stopped discharging in August 1992 (Scott, 1995). The cessation of springs flow has occurred as a direct result of the overexploitation of groundwater from the Azraq aquifers for water supply to Amman and the irrigation of agricultural land around the oasis. As the water table has been lowered, the natural discharge of the springs has fallen from an estimated 14-16 million cubic meters (MCM) in the 1960s, before the extraction of groundwater commenced, to 10.5 MCM in 1981, 0.3-0.4 MCM in 1991, and zero by the end of 1992. Figure (1.7) illustrates groundwater abstraction of AWSA well field versus the reduction in the discharge of the springs since 1980.

Abstraction of water from the Azraq Basin by the government and farmers increased dramatically from the early 1980s. Currently, 904 wells abstract about 60 MCM/yr (over three times of the annual safe yield). About 20 MCM of water is abstracted by the government in order to supply Amman and Zarqa governorates, while the rest amount of pumped water is extracted by the farmers.

The intensive pumping carried out through the last 20 years has caused a lowering of the basin's water table, which in turn incited the increased salinity of water and soils. Over-extraction also led to the drying up of the springs in 1993, and increasing dry environment. The lowering water table of the basin, in turn, has encouraged deeper excavation of wells that once provided large outputs of water for irrigation, which contribute to lowering and degrading the water table even further. The decrease in water table in the wellfield area cause the salt water intrusion from Qa Azraq toward the wellfield.

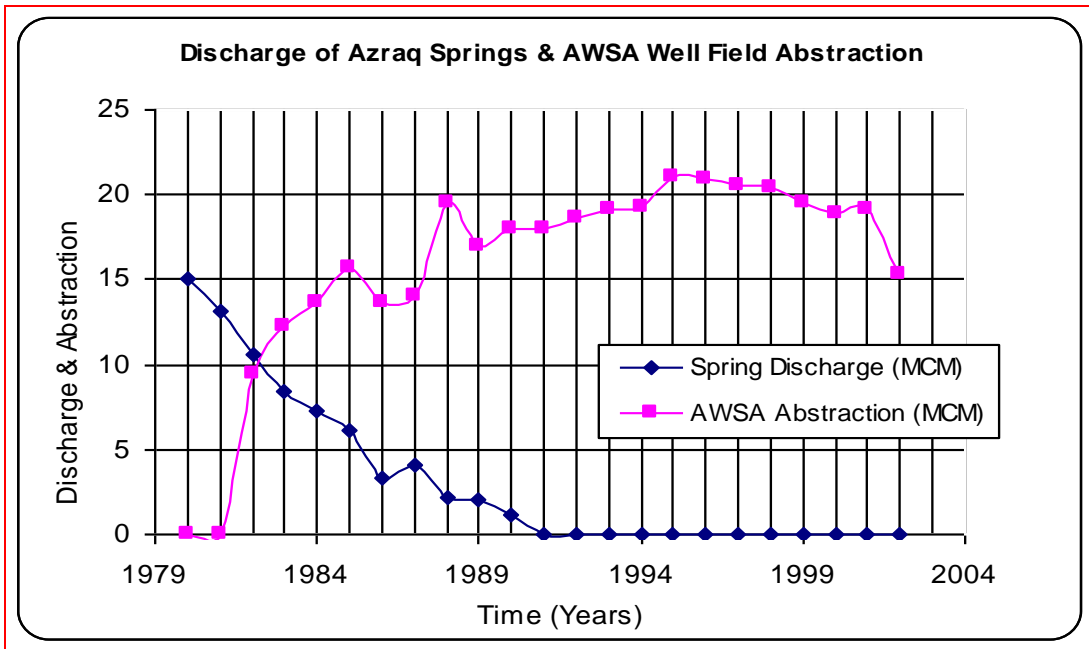


Figure (1.7): Spring discharge against AWSA well field abstraction

Deterioration in the Azraq Oasis was considerable as water resources were over extracted of groundwater through illegal wells and increasing demand by Amman City for drinking purposes, eventually leading to lowering in the water table as well as increasing the salinity.

All were affected in the area, the environment and the population, especially farmers and livestock owners. Women were also affected not only in their household needs but also in those water-reliant simple projects through which they were generating a much-needed additional income such as small home gardens with yields sold in the neighborhood. In addition, as municipality water is supplied to the houses only three days a week working housewives also suffer for not being able to benefit from the limited pumping durations while being at work. Figure (1.8 and 1.9) show the situation in Azraq few years ago and the current situation respectively.

The area lies in semi-arid region which characterized by high rate of evaporation, so using plants that is not adapted to semi-arid region will increase the evapo-transpiration rate and about 80% of water will be lost by evaporation during summer time. All agriculture in Azraq depends on introduced plants which consume large amount of water. Using such plants has the following problems:

- The plants consume very high amount of water to be able to survive especially during summer when temperature exceeds 40° C.

- The farmers start to use very high amount of fertilizers and pesticides which infiltrate through the soil to contaminate the main water resource.
- Water that was used for irrigation leach salts from the surface of soil back to the basin which increases the salinity of water.

1.7 Salt water intrusion in Azraq

The Saltwater intrusion and salinization are characterized by the increase of ion concentrations in freshwater aquifers. This occurs predominantly along coastlines, though there are instances of inland salinization. Saltwater intrusion can have several causes, some of which are natural and some are induced by human activities. Once saltwater intrusion has occurred, it is almost impossible to reverse, making this a significant threat to freshwater resources. Mitigation strategies that are designed to slow or halt the rate of saltwater intrusion can be expensive but are necessary to protect the water resources from more damage.

The salinization in the shallow aquifer (basalt/B5/B4) in the azraq basin is believed to be the return flow from Sabkha to AWSA well field resulting from low hydraulic gradient of the aquifer water table and increased drawdown in the AWSA well field that would cause the natural flow direction of the ground water to be reversed (Figure 1.10). Movement of the fresh-salt water interface depends mainly on the distance as well as on the amount of withdrawal and on the hydrogeological situation in the area. Well logs indicated that the B3 Aquitard including the marl and marly limestone content has some crystals of gypsum and halite (Reference) which was also recorded during the drilling of AWSA wells especially in AWSA-15, AWSA-1, AWSA-12. Salt bodies in the B3 Formations do exist. One evidence are salt deposits noticed downstream in the Wadis, which have erosion parts of B3 formation in the catchment basin (these salts might also be the main cause of the salt body, which is located in the middle of the Azraq basin where those sediments drain). Another evidence is salinity behavior of the deep middle aquifer wells during pump tests. The high salinity of the these wells decreased during the pumping tests where the logs showed a resistivity change from 0.5ohms to 18 ohms in Azraq deep well drilled in 1980 (Reference). The type of water is absolutely different than the B2/A7 Water as it contains high evaporites such as Anhydrite, Gypsum and Halite. This saline water is likely to be withdrawn from the B3 formation bearing the saline connate water.

One of the most dramatic forms of saltwater intrusion occurs in Azraq area that are dependent upon groundwater for drinking water and irrigation needs. The most common scenario involves the overpumping of the freshwater aquifer from the upper aquifer in AWSA wellfield . This reduces the head difference at the saltwater-freshwater interface and induces the flow of saltwater from the Qa' area towards the freshwater system in AWSA wellfield. This is often exacerbated by insufficient recharge to the freshwater aquifer, which can occur in times of drought.



Figure (1.8): The situation in Azraq a few years ago



Figure (1.9): The current situation in Azraq

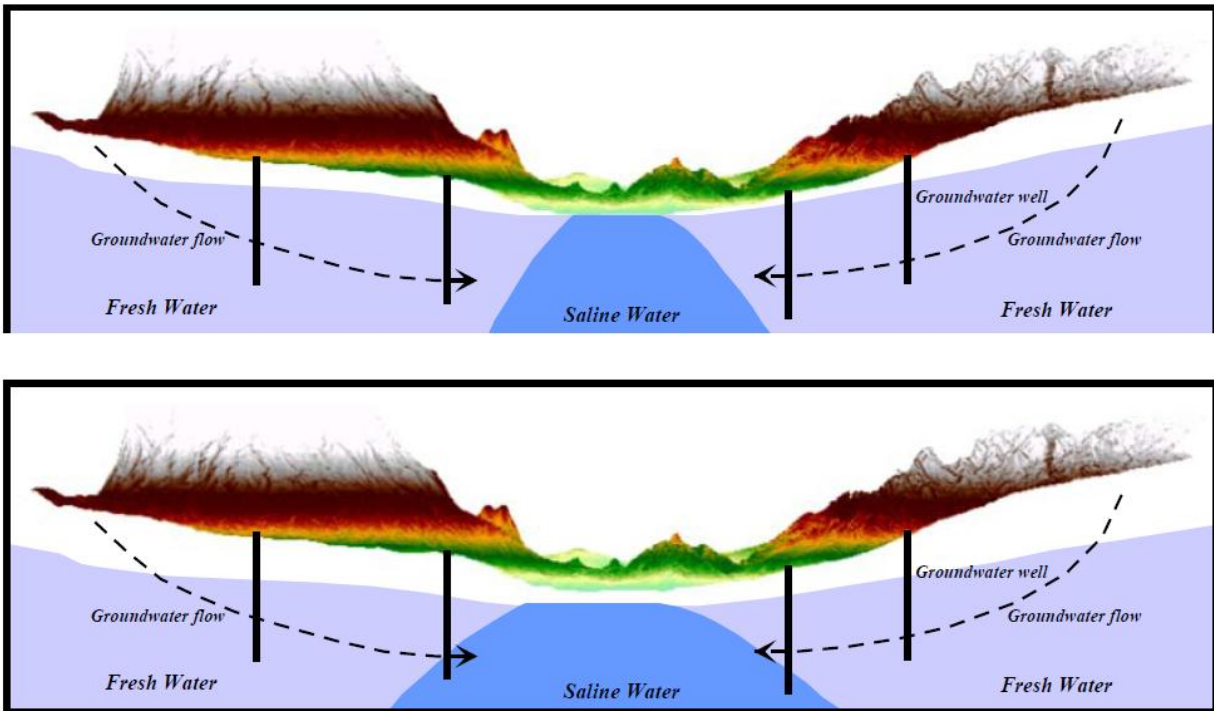


Figure (1.10): Schematic diagram of salt fresh water interface developed in Azraq area

In areas that are experiencing saltwater intrusion due to overpumping of the overlying freshwater aquifers such as in Azraq area, the mitigation solution involves cooperation at multiple levels. The main problem of pumping groundwater at a rate that is not sustainable must be addressed. Conversely, the impact of the saltwater intrusion must be quantified. This could be done by delineation of salt fresh water interface using geoelectrical survey in order to monitor the movement of this interface and what the projection is for future impacts given current pumping rates.

With potential of climate change and global warming, saltwater intrusion and salinization will continue to be an important water resource issue. Advances in technology and innovations in how we use our water resources will be key in the mitigation of saltwater intrusion.

CHAPTER 2 GEOLOGY OF AZRAQ BASIN

2.1 Geological framework

The Azraq basin is part of limestone plateau in eastern Jordan. The northeastern part of this plateau and tuff (Bender, 1968). The northeastern half of the basin is dominated by basaltic lava originating from Miocene/Oligocene volcanic activity. During the Neogene, the first lava flows occurred as a result of volcanic eruptions where this activity continued until the Holocene. The basalt reaches a thickness of more than 1500 m in the area of Mount Arab in Syria, and becomes progressively thinner towards the south. Table (2.1) illustrates the stratigraphy of Jordan and the sequence of geological layers in the study area.

The basin incorporates exposures of sedimentary rocks and basalt, ranging in age from Cretaceous to Quaternary (Figure 2.1). In the southern part of the basin and on the surface, the Quaternary deposits and recent sediments cover the underlying Tertiary deposits. The latter are intermittently exposed at the surface in the south, southwest, and southeast. Eocene and top Tertiary sediments lie on the top of the sequence beyond the "Fuluk" fault to the south and southeast at Wadi Hazim and the Jebel El-Fuluk. The sedimentary sequence includes limestone, chert, marl, chalk, sandstone, clay, and evaporites. These rocks are frequently covered with a variably thick sequence of superficial deposits including alluvium, mud-silt flats, chert pavement, Pleistocene gravels, and sand and evaporate incrustations. To the north and northeast, basalt eruptions of different age appear on the surface and extend northwards to cover a wide area known as the "Basalt Plateau." This basalt area is related to the North Arabian Volcanic Province, which extends from Syria across Jordan into Saudi Arabia, covering in Jordan an area of 1,1000 km².

In the Azraq playa (wetland reserve) the basalt is missing. Upper Tertiary sediments (B5) (Wadi Shallala) are located in the structural depression zones. The (B5) Formation consists of Marly-Clayey layers in the area of AWSA well field and acts here as an aquitard between the B4 (Rijam) and the Basalt aquifer. Towards the southeast, the B5 Formation contains more sandy layers and it is classified as an aquifer in this area. South of the basalt areas the landscape is dominated by Paleocene and Eocene Marly limestones, chalks, and chalky limestones with chert layers of the B4 formation.

The B4 formation is underlain by the Maastrichtian B3 (Muwaqqar) formation. B3 formation reaches a thickness of about 300 m and consists of marl and marly limestone with some gypsum and evaporite. The underlying Campanian to Turonian B2/A7 formations (Amman/Wadi Sir) is mainly formed by chert and limestone.

The upper Cretaceous and Tertiary Limestones and Marls overlie the Kurnub sandstone formation which belong to lower Cretaceous age, this formation is very deep in Azraq depression.

The entire Azraq basin is dissected by an extensive network of wadis, especially in the limestone areas. During Quaternary times the wadis carried large amounts of superficial deposits Alluvium

and top soil into the central depression. The fluvial gravels and sand dunes as well as clayey Calcareous and sandy sediments of mud pans are the youngest deposits

A Graben trending NW-SE is the dominant structure. The Jabal Fuluk Fault which stretches from the Basalt is the main Fault in the northern part of this Graben. Some Faults are extending NW-SE parallel to the Graben, and others have a NWW-SSE strike.

The Azraq Basin represents a thick stratigraphic section. The area has been subject to extensive oil exploration activities, which added a lot of information regarding the stratigraphic sequence and sedimentary section. In the subsurface, a thick sedimentary section that is changing in thickness and varying in the lithostratigraphic and formation units represents the basin. These sediments range in age from early Paleozoic to Pleistocene, and are primarily composed of carbonates, sandstones and shales. The major thickness reduction in the sequence appears towards the south and southwest directions, while a remarkable increase in thickness is observed east of Azraq town towards the Fuluq fault.

The Cretaceous-Tertiary deposits in the basin comprise a thick sedimentary section measuring more than 3,500 m of mostly marine deposits. The lower Cretaceous boundary, identified by a recognizable sandstone unit of the Nubian type known as the "Kurnub Sands tone," is identified in several wells, as the sandstone formation underlying the carbonate facies of the Cenomanian age. This sandstone unit varies in thickness and depth, and marks the transition zone on the major unconformity between the Jurassic and the early Cretaceous.

2.2 Geological Structure

The basin is characterized by the presence of distinctive structures including the Sirhan-Fuluq Siwaqa, Zarqa Main, and Baqal- Wisad fault systems (Figure 2.2). Structurally, the area is tectonically active and dominated with NW-SE, E-W, NESW and N-S faults and lineaments; the NW-SE and the EW

fault systems are the main ones believed to have controlled the development of the Azraq depression and Azraq Lake. The regional dip is towards northeast. Folds are relatively small with gentle dip and mainly associated with some NE faults and lineaments.

The geology of the Azraq Basin is controlled by the relative northeastern movement of the Arabian Plate with respect to the African Plate. The sediment record the closure of the Tethys Ocean, followed by crustal down warping, attenuation and finally volcanism. The basin is asymmetric in shape trending northeast to northwest. It is separated from the Sirhan depression by Jebel Waqf Es-suwan swell. The western margin is defined by the rapid shallowing of the sediments which ultimately outcrop in the vicinity of Amman. There are two major fault systems in the Azraq Basin one trending E-W and a second, NW-SE.

Table (2.1): Geological and Hydrogeological Classification of the Rock units Unit in Jordan (Rimawi 1985)

Epoch	Age	Group	Formation	Symbol	Rock type	Thickness (m)	Aquifer Potentiality	Permeability (m/s)
Upper Cretaceous	Holocene	Balqa	Wadi Fill	All	Soil, Sand and Gravel	10-40	Good	2.4×10^{-7}
	Pleistocene		Basalt	V	Basalt. Clay	0-50	Good	-
			Wadi Shallala	B5	Chalk, marly limestone with gluconite	0-555	Good	
	Maestrichtain		Umm Rijam	B4	Chert and limestones	0-311	Good	
			Muwaqqar	B3	Chalk, marl and Chalky limestone	60-70	Poor	-
	Campanian		Amman	B2	Chert, limestone with phosphate	80-120	Excellent	$10^{-5} - 3 \times 10^{-4}$
	Santonian		Ghudran	B1	Chalk, Marl and Marly limestone	15-20	Poor	-
	Turonian		Wadi Sir	A7	Hard Crystalline Limestone. Dolomitic and Some Chert	90-110	Excellent	$1 \times 10^{-7} - 1 \times 10^{-4}$
	Cenomanian		Shueib	A5-6	Light Grey limestone interbedded with Marls and Marly Limestone	75-100	Fair to poor	$6.3 \times 10^{-5} - 7.2 \times 10^{-4}$
			Hummar	A4	Hard dense limestone and Dolomitic Limestone	40-60	Good	$8.1 \times 10^{-7} - 7.6 \times 10^{-4}$
			Fuheis	A3	Gary and Olive Green soft Marl. Marly limestone and limestone	60-80	Poor	$5.3 \times 10^{-7} - 1.7 \times 10^{-5}$
			Na'ur	A1-2	Limestone interbedded with a thick sequence of Marl and Marly Limestone	150-220	Poor	$2 \times 10^{-8} - 3.1 \times 10^{-5}$
			Kurnub	K	Massive White and Varicolored Sandstone with layers of Reddish Silt and Shale	300	Good	$6.9 \times 10^{-3} - 5.2 \times 10^{-2}$
Lower Cretaceous	Albian – Aptian	Ajlun						

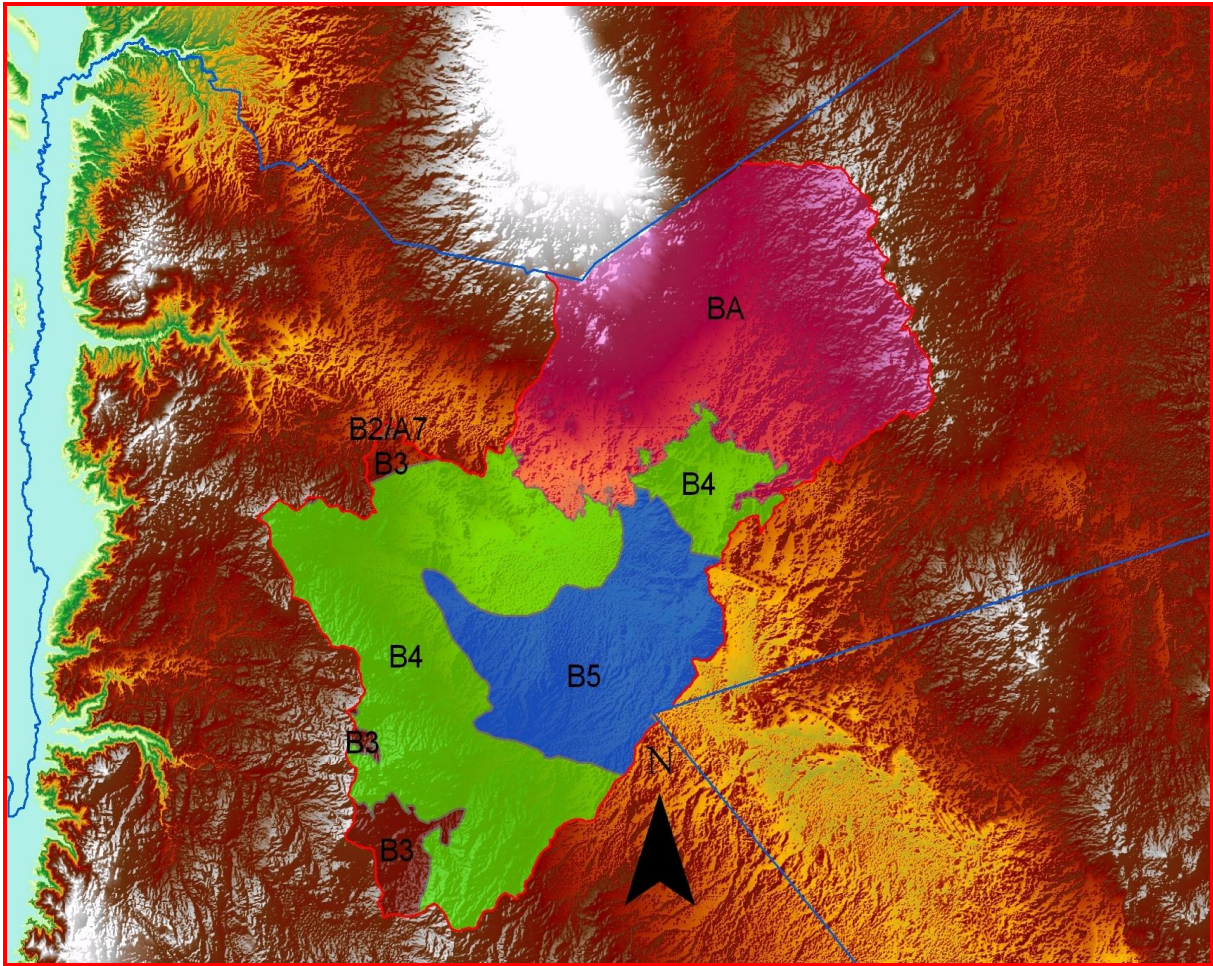


Figure (2.1): Generalized geological map of the study area (After Sahawneh, 1996).

2.2.1 Siwaqa Fault Zone

The Siwaqa Fault Zone has a length of approximately 200 km and crosses the Jordan Platform from the Dead Sea Graben in the west to Saudi Arabia in the east. It downthrows to the north at 100 to 200 m although locally the throw of the main fault may be nil. The deformation associated with the fault zone comprises small drag folds in the Cretaceous-Tertiary.

2.2.2 Ramtha-Wadi Sirhan Fault Zone

This zone is considered as the most important fault system in the Azraq Basin. It comprises a complex series of faults downthrowing to the NW and extending for some 325 km from Ramtha in the NW and Saudi Arabia in the SE. The fault zone is responsible for the Hamza and Azraq grabens and the Sirhan Basin in Saudi Arabia. The synsedimentary role of the fault gave to the thick Cretaceous and Tertiary sediments in Azraq, Hamza and Sirhan.

2.2.3 Fuluk Fault

The Fuluk Fault forms the eastern flank of the Hamza Graben and the associated structural depression south and southeast of Azraq town. This fault extends for some 100 km from Azraq into Saudi Arabia. The extent of the Fuluk Fault beneath the basalt to the north of Azraq is not known. East of the Fuluk Fault thicknesses are normal. The vertical displacement along the Fuluk Fault reaches more than 3000 m, (Beicip, 1981).

2.2.4 Qaa' Abu Husain Fault

This fault is located in the basalt Plateau (Al Harra) in the northeast of the Azraq Basin. In Jordan it has a length approximately 140 km, but extends northwestwards into Syria and the southeast in Saudi Arabia. Due to its tensional character, it is associated with many volcanic dykes.

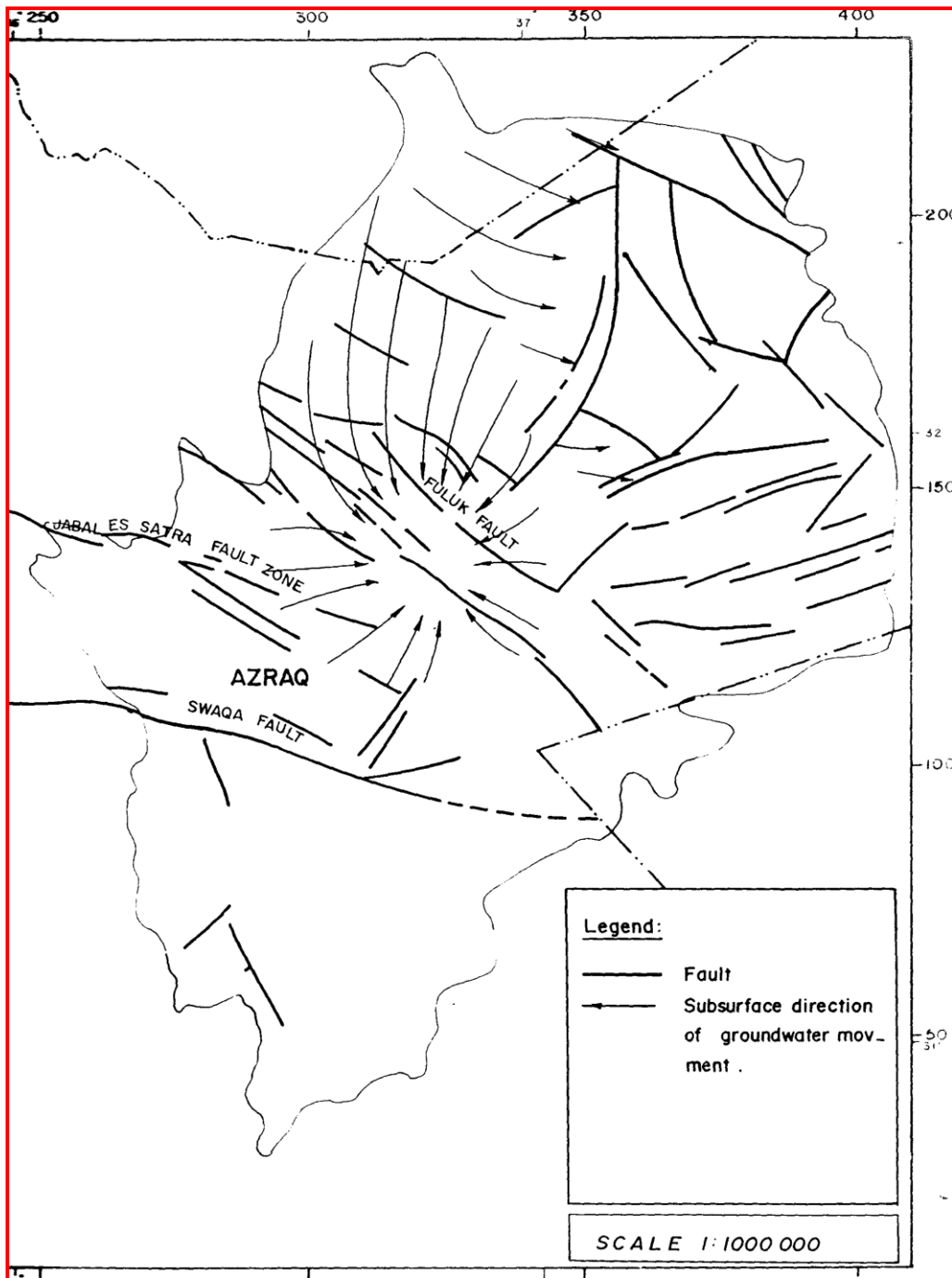


Figure (2.2): Major Structural element and subsurface direction of groundwater -movement within AL Azraq Basin (After Sahawneh, 1996).

CHAPTER 3 HYDROGEOLOGY OF AZRAQ BASIN

3.0 Hydrogeology and Aquifer Systems

3.1 Aquifer Systems

Ground water aquifers in Jordan was divided into three main hydraulic complexes (Agrar and Hydrotechnick, 1977). These main aquifer complexes are, the Shallow Aquifer System (Upper Aquifer) comprising Quaternary and Tertiary Formations (Basalt, Rijam and Sirhan); the Upper Cretaceous (Middle Aquifer System) Amman Wadi Sir Hydraulic Complex; and the Deep Sandstone (Lower Aquifer System), Kurnub and Disi Hydraulic Complex. The main aquifer systems of the Azraq Basin are shown in Table (3.1).

Table (3.1): Major Units of the Shallow Aquifer in the Azraq Basin Area

Age	Formation	Lithology	Thickness (m)	Hydraulic Character
Recent	Alluvium	Sands and gravel	0-20	Aquifer
Quaternary				
L. Tertiary	Basalt	Basalt	0-400	Aquifer
L. Eocene	Um Qirma (B5)	Weathered limestone	0--15	Aquifer
L. Eocene	Wadi el Shall ala (B5)	Marl and Chalk	160-430	Aquiclude
Mid-Eocene	Urn Rijam (B4)	Argillaceous silicified limestone	170-300	Aquifer
E. Eocene	Muwaqar (B3)	Marly limestone	>100	Aquiclude

The Upper (Shallow) Aquifer and the Middle Aquifer Systems are separated by the Muwaqar (aquiclude) Formation (B3). The Upper Aquifer System is an unconfined aquifer and forms the major aquifer of the Azraq Basin. The aquifer consists essentially of four different members partly separated from each other by low permeability layers, partly directly connected. These are Quaternary sediments, Basalt, Shallala (B5) and Rijam (B4). Two major groups of springs were existed in the central part of the Azraq Basin comprising the main discharge outlets of the Shallow (Upper) Phreatic Aquifer.

The basalt extends from the center of the basin to the north and ends up in the highlands of Syria (Bajjali and Hadidi, 2005). The basalt is hydraulically connected to the underlying calcareous rocks of the B4 (Rijam) Formation. The groundwater flow is from north towards south and the groundwater moves from all directions towards the Azraq depression (NJWRIP,

1989). The upper aquifer system, is under water table condition. The depth to the ground water table is from few meters in the center of the oasis to 400 m in the northern catchment area.

The Middle Aquifer System, locally known as Amman-Wadi Sir (B2/A7) Aquifer System. This aquifer is a confined aquifer due to aquiclude bituminous marl of the (B3) formation . This aquifer system underlies the Upper Aquifer System and outcrop in the western part of the basin. The Amman Formation (B2-Aquifer) is composed of chert, chalk and limestone.

The (A7) Formation of the second aquifer forms one composite aquifer system with the (B2) Formation. More than 15 water wells penetrating the B2/A7 Aquifer System were drilled in the Azraq Basin. The (B2/A7) composed of karstic limestone and chert formations overlain by the B3 aquitard (confining) formation. The potentiometric heads of the middle and upper aquifers in the AWSA well field area were 520 and 510 m above sea level (ASL) respectively in steady state becoming 520 and 495 masl in transient conditions; increasing the driving force of upward flow; WAJ 2002). Figure 3 illustrates potentiometric head in the upper aquifers in steady state condition (BGR and WAJ, 1994). The aquifer is considered confined throughout the basin, and it is recharged mainly from the Jebel (mountain) Druze recharge area in the north (BGR and WAJ, 1994).

The Middle and Lower Aquifer Systems are separated by marls and marly limestones of the low permeability Ajlun Group (A1/6). The aquiclude Khreim Shales separate the Early Cretaceous (Kurnub Group) from the deeper Paleozoic Disi Sandstone.

The deeper aquifer unit known as the Kurnub Sandstone Aquifer. The geological formations between B2/A7 and Kurnub Sandstone aquifer are mostly marly limestone and limestones and marl. All together act as semi-permeable layer. The pressure in the Kurnub Sandstone aquifer is lower than that of the middle aquifer (Kharabsheh, 1991).

The upper shallow fresh water basalt aquifer (i.e. the target aquifer of this study) is currently under the threat of salinization due to overexploitation, the middle limestone brackish water aquifer (600 to 15,000 mg/l) of ages more than 30,000 years and the deep sandstone aquifer which has low yields and a poor quality water.

3.2 Hydrogeology of the Upper Aquifer System

The Upper Aquifer System of the Azraq Basin form an essentially closed composite system. Before the Amman Water and Sewerage Authority (AWSA) well-field abstraction began in 1982 to Amman, this aquifer was discharging as springs and seeps near Azraq Shishan and Azraq Druze and as evaporation from the shallow water table in the vicinity of the Qaa' Azraq. The lower boundary surface of the Upper Aquifer System is formed by low permeability sediments. The lateral boundary to the west is defined by the limit of saturation. The eastern and northwestern boundaries were ground water divides between the Sirhan and Dhuleil Aquifer System respectively. The northern part of the system extends northwards into the major aquifer system formed by the Basalt Plateau which radiate from the Jebel Druze in Syria.

The ground water of the Upper Aquifer System in unconfined aquifer except at the Qaa' Azraq. The Qaa' Azraq deposits form a lens up to 15 meters thick overlying the aquifer and give rise to leaky artesian conditions. This aquifer system is composed of the following formations (Figure 3.1):

- A. Quaternary Deposits.
- B. Basalt.
- C. Wadi Shallal Formation (B5).
- D. Rijam Formation (B4).

3.2.1 Quaternary Deposits

The Quaternary Deposits are mostly exposed in the central part of the basin. These sediments consist of strewn plain, comprising angular, poorly sorted largely black chert clasts, in a silty to sandy matrix. At the periphery of Qaa' Azraq, these sediments 1.5 to 6 m thick consist of silt particles cemented by evaporites. Alluvial fans are developed at the mouths of some wadis. Most of the hand-dug wells were drilled in the Quaternary sediments are used for irrigation. These sediments in the Qaa' area can be divided into three parts: On top, the formation consists of permeable to semipermeable layers 10 to 30 m thick. The underlying layer of clay and marl has a lower permeability and is 20 to 40 m thick. This is underlain by permeable to semipermeable sediments. Exposures in the hand-dug wells in the farms area show that, the

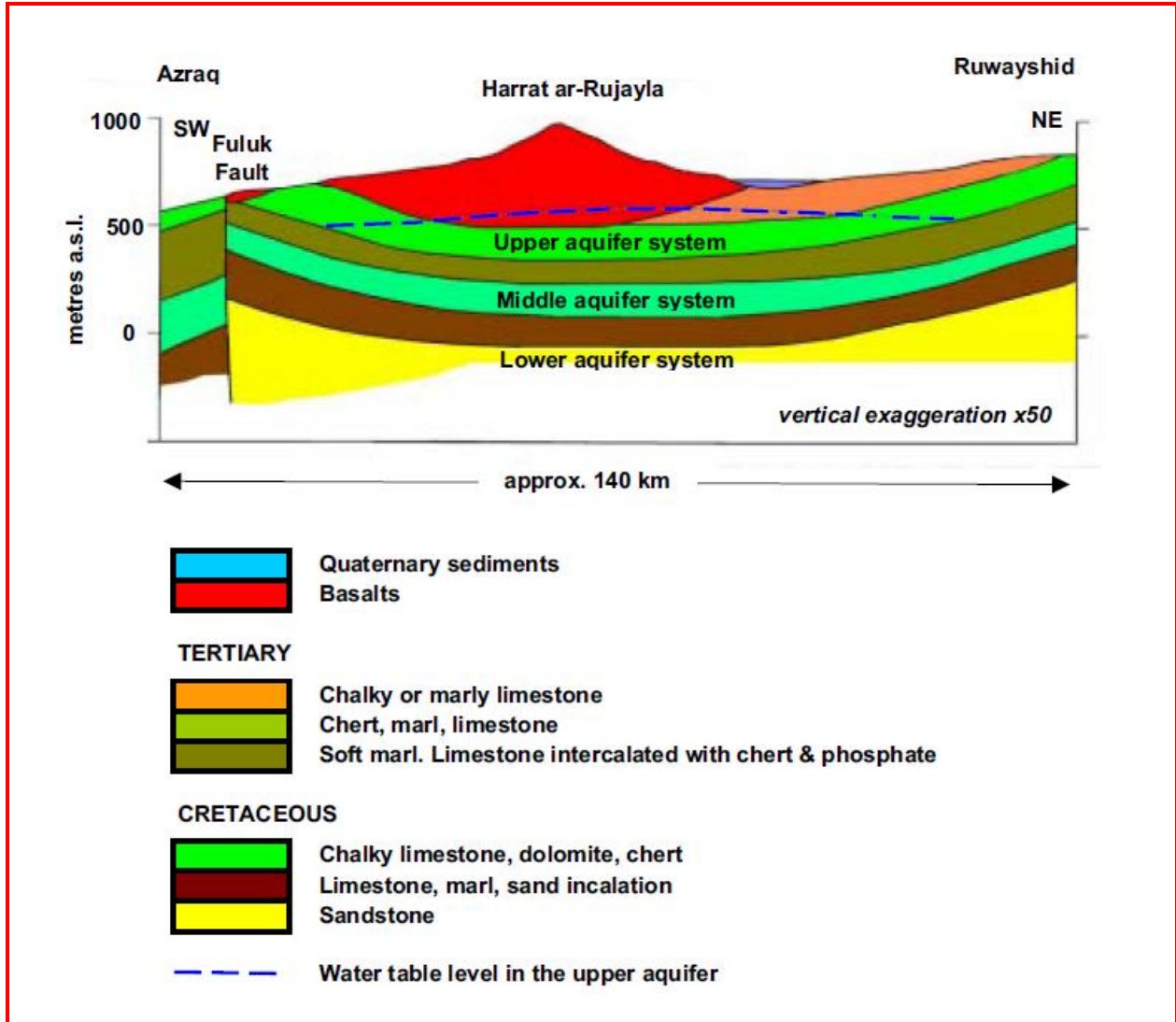


Figure (3.1): Simplified Hydrogeological cross section running SW – NE (after Dotteridge, 1998)

**Dotteridge, Jane (1998) "Water Resources Quality, Sustainability & Development" in Dutton RW et al: Arid Land Resources & Their Manangement. Keegan Paul International (Jane Dotteridge*)*

Upper Quaternary Formation consists of marly and chert layers (fluvial detritus) intercalated with lacustrine sediments and clay (Worzyk, and Huster, 1987). This aquifer occur in hydraulic continuity with the underlying Shallala Limestones, and its water levels are shallow and unconfined.

3.2.2 Basalt Aquifer

This aquifer covers the northern part of the Azraq Basin, extending from Jebel Druze mountains in Syria to Azraq. The basalt aquifer consists of alkali olivine lava flows intercalated by the layers of red clay. This lava flows of Tertiary to Quaternary overly unconformably the sedimentary successions of the Belqa Group (B4/B5). Five lava flows have been identified by (Al-Dmour, 1992) in the Azraq Basin. The basalts are hydraulically connected with the underlying Shallala (B5) Aquifer, and the Rijam (B4) Aquifer. These basalts in the Azraq Basin tend to be productive and good aquifer due to, high fracturing of the basalts. The thickness of the basalt increases from the center of Azraq to the north reaching a maximum thickness in Jebel Druze upto 1500 m.

3.2.3 Wadi Shallala Aquifer

Shallala Formation which underlies the basalt in the AWSA well-field consists of marl, clay and marly limestone and acts as an aquifer between the two good aquifers, the B4 and the Basalt Aquifer.

The thickness of the B5 in the well-field area reaches about 70 m. Southeast of the well-field, the B5 contains more sandy layers and in this area can be classified as an aquifer. The B5, is unconfined aquifer and hydraulically connected with the underlying B4 Aquifer. Thicknesses increase eastward towards the Fuluk Fault from 160 to 428m, (Gibbs, 1993).

3.2.4 Rijam Aquifer (B4)

This aquifer underlies the Shallala Formation, but at Qaa' Azraq is probably replaced by the Sirhan sandstone and marl. It consists of white limestone, chalky limestone, and nodules of brown to black chert. The Rijam Formation outcrops in the central, southern and western part of the basin. The average thickness of the B4 Formation is about 60 m. From the general hydrogeology of the Azraq Basin, it appears that, the B4 Aquifer is hydraulically connected with the Basalt Aquifer via Shallala (B5) or through the Sirhan Sandstone.

The base of the Upper (Shallow) Aquifer drops from elevation of about 800 m a.s.l in the west of the basin to minus 200 or less in the Hamza Graben and Wadi Sirhan. The base of B4/B5 Aquifer System also drops from elevations of about 500 m in the AWSA well-field (northwest of the Druze Springs) to less than minus 200 m in the Hamza Graben area. It rises again towards northeast of the Fuluk Fault (Taa'ni, 1998).

3.3 Saturated Thickness

The saturated thickness of the Upper Aquifer Systems in the Azraq Basin varies from place to another, regarding the variations in the hydraulic properties of the different layers. The Basalt Aquifer has an average saturation thickness of about 90 m, and constitutes the main north of Azraq. Water in the aquifer is stored under water table conditions with depth to water varying from 5 to 40 m in the Azraq well-field and more than 300 m at the north of the basin.

Wadi Shallala, which underlines the basalt in the well-field area, acts as an aquifer separating the Rijam (B4) Aquifer from the Basalt Aquifer. In the Basalt Plateau, where the overlying basalts are saturated, the Shallala limestones appear to be also saturated. Where the Shallala (B5) outcrops in the Azraq Basin, the aquifer is partially saturated. The saturation thickness varies from few meters to about 70 m.

Generally, the ground water of the B4 Aquifer is stored under water table conditions, and therefore, the aquifer is unconfined. In the Hamza Graben at the western part of the basin, the aquifer is confined beneath a thick cover of sediments including the B5 marls and the younger strata. The saturation thickness of the B4 Aquifer varies from 35 to 75 m. The maximum saturated thickness of about 200 m is calculated in the well-field area NW of the Druze springs and also in the east of the field area. The saturation thickness decreases in all directions from the center of the basin.

3.4 Aquifers Characteristics

The upper aquifer complex is an unconfined aquifer and forms the major aquifer of the Azraq basin. This aquifer consists of four different members which makes large differences in the chemical and physical characteristics of the groundwater (Karanth, 1989). The water of this aquifer differs in depth, quantity and quality from one place to another. Depth to water ranges between few meters to more than 200 m. Regional drawdown in the groundwater ranges between 8 and 12 m (German Water Engineering GMBH, 1991). The average transmissivity is approximately 11000 m²/d with values ranging between 16 and 26352 m²/d. The permeability shows values of less than 0.5 m/d to more than 115 m/d and decreases towards the north and east from the well field area (Kharbsheh, 2000).

The hydraulic properties of the Basalt Aquifer, are only known in detail in the wellfield area, where all production wells had been pump tested. The average transmissivity is about 11000 m³/d/m, and ranges between 54 m³/d/m and 65664 m³/d/m (Humphreys, 1982). Areal, transmissivity seems to be less in the northern part of the well-field, on average 4500 m³/d/m.

The permeability also ranges between 1.6 m/d, and 365 m/d in the wellfield area. The transmissivities and permeabilities of Shallala Aquifer are dependent on the degree of fracturing and the presence of marls and therefore, variable. It ranges between a few m³/d/m to about 250 m³/d/m, corresponding permeabilities are less than 0.5 m/d to about 5.0 m/d. The transmissivity of the Rijam Aquifer (B4) in the well-field area, and north of Azraq smaller than that of the overlying basalt. It ranges between 23 m³/d/m and 660 m³/d/m. Figure (5.3 and 5.4) show the areal distribution of the transmissivity and permeability for the entire Shallow Aquifer System in the Azraq Basin. The relatively high transmissivity in the well-field area, probably related to fracturing in the vicinity of the Fuluk Fault.

The hydraulic gradient is relatively high in the northern part of the basin and it ranges between 1.7×10^{-3} and 1.2×10^{-3} . A storativity value can't be obtained from draw-down data in a pumped well, but in the study of the Water Resources in the Azraq Basin (WAJ, 1989),

storativity values were estimated from the ground water model carried out in the study. Also storativity estimates made for a model by (Barber and Carr, 1973) are, 7.5% for scoriaceous basalts and 3% for other basalts and Rijam Formation (B4).

3.5 Well Characteristics

Three types of boreholes were constructed and penetrated the Upper Aquifer System in the Azraq Basin. These are, productive, exploratory and observation wells. More than 600 water wells were drilled in the basin and most of them are located north and east of the Azraq Oasis. Of which 43 governmental wells (26 productive and 18 exploratory), and the rest are private wells. Twenty four of the governmental wells are used for domestic and the other two wells are used for irrigation. All the private wells are used for irrigation except two wells are used for industrial purposes. Presently, about 300 wells of the 600 wells are in operation. The total depth of these wells range between few meters in the center of the basin to more than 400 m at north and northeast of the basin.

The yields of the water wells are variable and range between 7 m³/h to 107 m³/h in the B4/B5, between 13 and 200 m³/h in the Basalt and between 14 and 304 m³/h in the Basalt/Rijam (B4) Aquifer. The specific capacities have a range between 12.1 and 337.4 m³/h/m in the Basalt, between 0.4 and 584.6 m³/h/m in the Basalt/B4 and between 0.2 and 70.5 m³/h/m in the B5/B4.

Generally, the depth of water table varies from few meters in the center of the basin to more than 300 m in the north and northeast of the basin at the Basalt Plateau. The elevation of the water level ranges from 475 m a. m. s. l. east and 564 m a. m. s. l. in the north. Table (5.1), represents, the hydrogeological data, and the hydraulic parameters of the significant boreholes in the study area.

3.6 Ground Water Level Fluctuations

The ground water of the Upper Aquifer System, generally occurs under unconfined conditions in the Azraq Basin. Therefore, the water table is not stable and fluctuates according to wet and dry seasons and also according to withdrawal of ground water. Until now, ground water in the study area is only abstracted from Shallow Aquifer (Alluvium, Basalt, B5 and B4). Four observation wells (F1022, F1043, F1060 and F1280), are used to monitor the water level fluctuations of the Upper Aquifer. These observation wells are equipped with Stevens Automatic Recorders and operated for monthly readings. These wells have total depths of 88, 255, 116 and 195 m respectively. F1060 borehole terminates in the basalt, the others penetrate both basalt and B4 limestone.

The observation wells' temporal static water level (SWL) variations are compared as depths to water in Figures (5.7, 5.8, 5.9 and 5.10). These graphs show, the declining of the water levels with time and are described below.

F1022 (AZ-11), this well is located about 6 km south of the AWSA well-field's southern end. AZ-11, is furthest from immediate discharge area. Its average SWL was almost constant from 1984

to 1989 and thenceforth declined at a rate of 0.2 m/year (m/y). The well seems to be relatively uninfluenced by nearby pumping.

F1043 (AZ-12), is located in the center of the AWSA well-field, north Azraq Druze. This well has the greatest rate of water decline of 0.6 m/y. This is consistent with its location in the center of AWSA well-field. The hydrograph clearly shows, the regional ground water depletion due to pumping in the AWSA well-field.

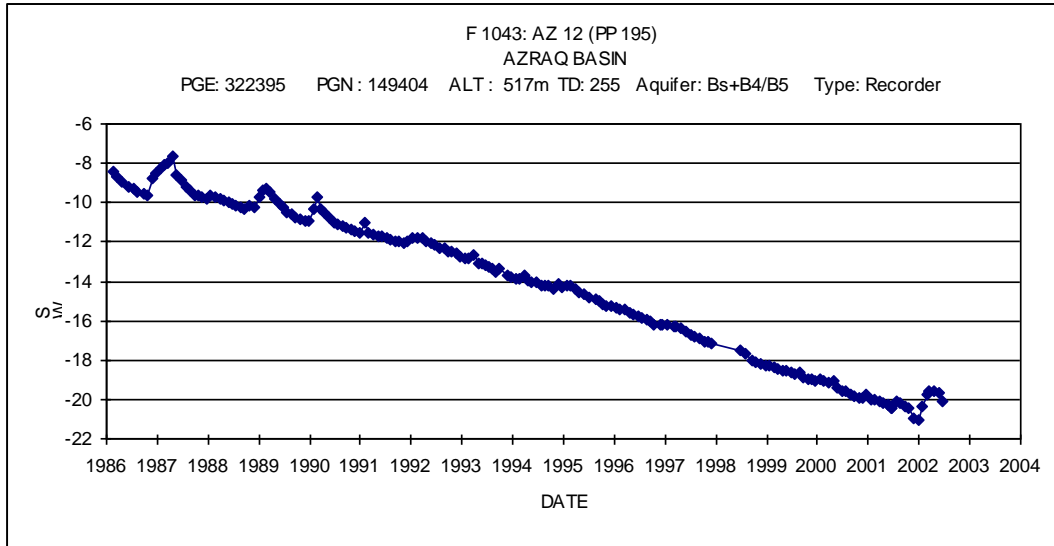


Figure (3.2): Fluctuation of groundwater level in observation well F1043

F1280 (AZ-2), is located about 2 km southeast of the AWSA well-field's southern end. This is the second closest observation well to the AWSA well-field and correspondingly has the second largest rate of water level decline. Between 1985 and 1992, the depletion rates were in the range of 0.4 m/y.

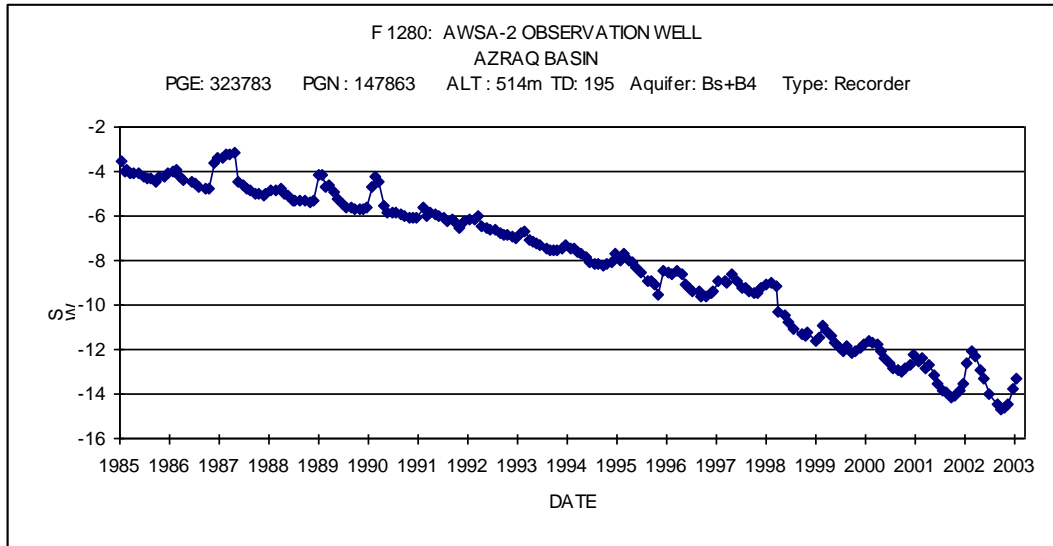


Figure (3.3): Fluctuation of groundwater level in observation well F1280

F1060 (AZ-10), is located in the farming area, about 10 km east of Qaa' Azraq and 15 km SSE of the AWSA well-field. The nearest production well is only about 100 m away from the monitoring well and the graph reflects the influence of the pumping pattern. Average water levels have declined at about 0.3 m/y since 1987. Water levels almost were constant between the year 1986 and 1988.

The distance between the production well is sometimes less than 300 m. Differences in amplitudes and rates between the wells are attributed mainly to proximity and abstraction sites. More observation wells are needed in the basin particularly east of Qaa' Azraq, where agriculture is extensive. A general draw-down trend of water levels in the range of 0.2 to 0.6 m/y can be seen in the observation wells.

3.7 Ground Water Movement

Ground water movement generally, depends on the hydraulic conductivity and the hydraulic gradient. Ground water moves from areas of high potential to lower potential areas. The shape of the piezometric surface is illustrated in Figure (3.4). This shows that, the flow lines in the Upper Aquifer System converge towards the Qaa' Azraq.

The groundwater contour map of the upper aquifer complex shows the major recharge from the north, northeast, and northwest, with minor recharge from the west. Groundwater flows from Jebel El Arab to reach the graben structure, where the well field is located. This relates to the high permeability of the rocks (TODD, 1980). The amount of infiltration was calculated to be about 35.3 MCM and the amount of natural recharge was estimated to be about 20 MCM. About 1 MCM infiltrates through the Sirhan structure to adjacent areas. About 14 MCM of the infiltrate are lost equally to evapotranspiration from the upper aquifer complex and the long

term discharge of the springs (Al- kharabsheh, 1991). The Fuluk fault acts as a barrier to the groundwater, because of different hydraulic characteristics of the groundwater flows north and south of the barrier (Fig. 3.4)). The hydraulic velocity of water moving from Jabel El Arab to the well field area is very slow. The age of the groundwater was determined to be about 5000 to 20000 years (Rimawi, 1985). Measurements made by Frohlich et al.(1987) showed that, because of withdrawal from the well field area, the groundwater is becoming younger in age as a result of the increase of the hydraulic gradient towards the cone of depression.

Ground water elevations are highest in the northeast of the basin, decreasing from 564 m asl to about 500 m asl towards the center of the basin. The northeastern ground water flow forms about 85 percent or more of the ground water flows in the basin. This indicates that, the general flow direction in the basalt is from NE to SW towards the centre of the basin and the outcropping B4 Aquifer in Wadi Rattam. In the northern part of the AWSA well-field, flow appears to be in a northerly direction. In addition to the horizontal flow component, ground water from the basalt appears to flow vertically downward into the Rijam Formation. Ground water flow in the outcropping B4 Formation is from west and northeast towards Qaa' Azraq. A small amount of ground water flows from southeastern part of the basin to Qaa' Azraq.

The over-pumping from a large number of wells existing in the basin that causes a dramatic drawdown of the local water table and consequently affect the groundwater resources in the area (Rimawi and Udluft, 1985). The increase in groundwater abstraction by the beginning of 1980s can be considered as the major factor affecting the steady state conditions and lead to the current transient state. The degradation of groundwater quality and salinization were taken place of some wells in the AWSA wellfield, Azraq farms and Azraq depression (Qa'a Azraq or Sabkha. The amount of pumping exceeds the amount of recharge estimated by various authors (Agrar et. al, 1977, Al-Momani, 1991). Therefore, the water table in AWSA well field decline ranged from 11 to 16 meters since 1982. The decline of the water table has a general trend in Azraq basin. The aquifer has the tendency to recover with lower abstraction rates as the water table was raised by one meter when the abstraction was lowered from 15 to 12 MCM/a during the first half of year 2002. Due long- term exploitation of the Upper Aquifer, the water table in AWSA well field decline ranged from 11 to 16 meters since 1982 (Al-Momani et al., 2003). The decline of the water table has a general trend in Azraq basin. The aquifer has the tendency to recover with lower abstraction rates as the water table was raised by one meter when the abstraction was lowered from 15 to 12 MCM/a during the first half of year 2002 (Figure 4). Furthermore, the over pumping of both the government and private wells caused gradual reduction of the springs discharges and finally drying the whole total spring flow (Figure 5).

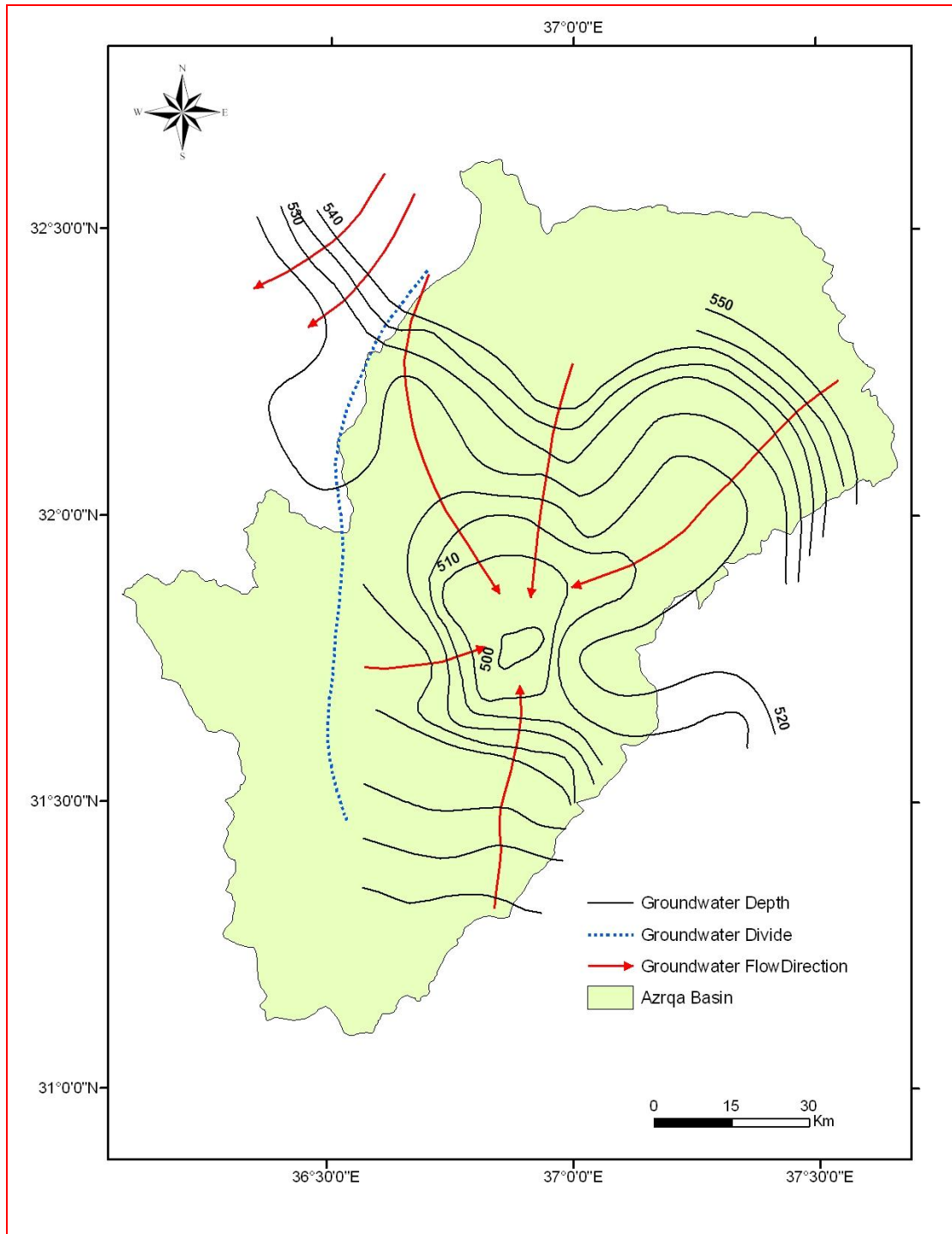


Figure (3.4): Groundwater contour map of the upper aquifer unit in steady state condition

3.8 Recharge and Groundwater Flow Pattern

The main recharge of the upper aquifer originates from infiltration through the basalt from the high rainfall areas at Jabal Arab in southern Syria. Intensive thunderstorms and flash floods in the Azraq Basin also contribute to minor ground water recharge (Humphreys, 1982). The estimated total recharge is about 34 MCM/Yr (Bajjali, 1990). The residence time of the groundwater from recharge area in Jebal Arab to Azraq Oasis is long enough and the age of the groundwater is ranging between 4000 to 20000 years (BGR and WAJ, 1994).

Most of the water in the Azraq Basin is concentrated in the upper aquifer that is the main source of water in this region. During the 1980's, numerous wells were drilled there, and water that was pumped fulfilled the water needs of the farmers in the area and those of greater Amman (Figure 3.5). Increasing demands on this aquifer, however, have caused the water table to decline by several meters. The Azraq basin is the second most pumped aquifer in the country. As a result, the aquifer's safe yield is exceeded by 260% (Table 3.2). To safeguard future supplies of fresh water, it is necessary to consider the impact of these abstraction rates and their sustainability.

As a result, some of the Azraq springs became saline, some dried up, and the Azraq Nature Reserve was severely damaged. The water authorities are implementing a plan to reduce pumping by 2 million m³ per year.

The water in the upper aquifers flows eastward along the slope of the layers. It percolates through cracks and along the rift plane to the lower sandstone layers and continues westward, bursting out as hot springs in the Dead Sea area (Figure 3.6).

Table (3.2): Groundwater balance of the main basins in Jordan (MWI,2006)

Basins	Yield	Safe Yield	Unsustainable over-extraction	Percent excess of Sustainable Yield
Amman-Zarqa	138.16	88	-50.16	157%
Yarmouk	59	40	-19	147.5%
Azraq	62.5	24	-38.5	260.4%

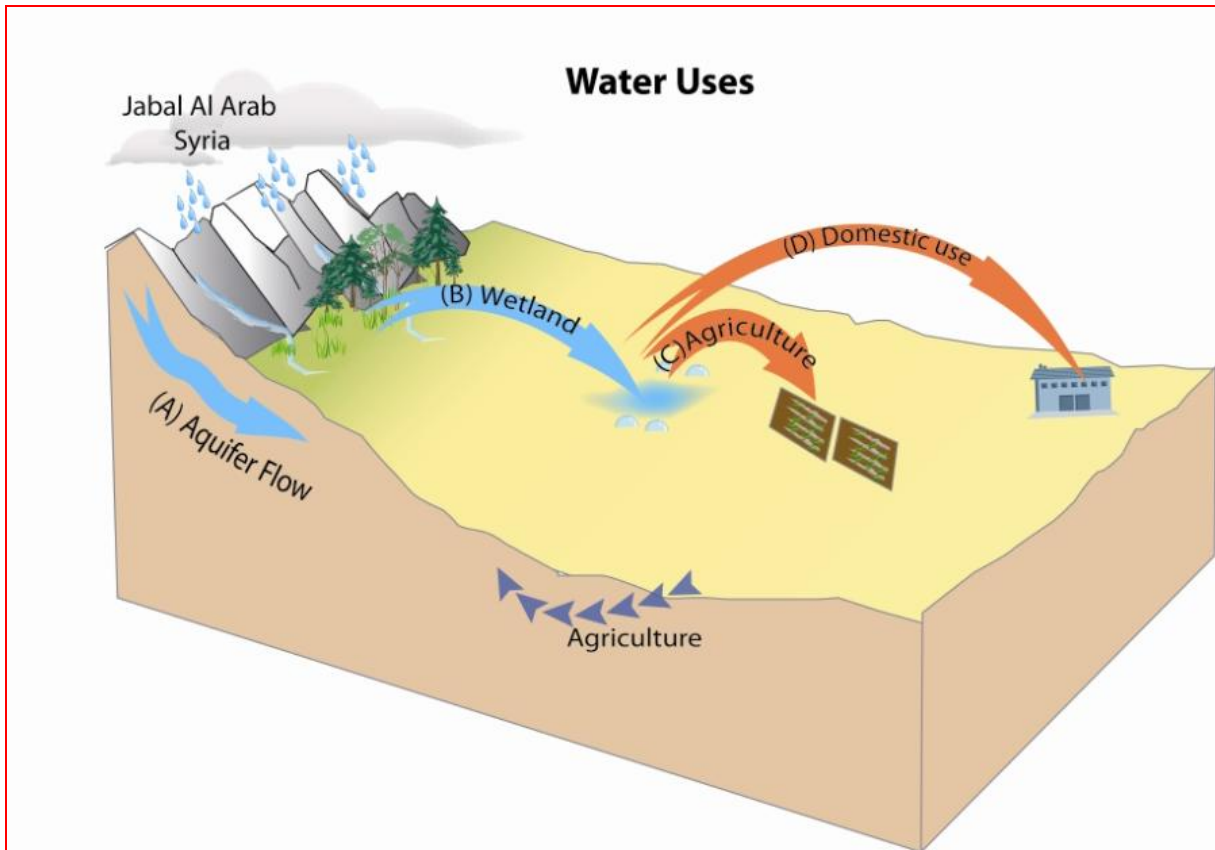


Figure (3.5): Water uses in Azraq Basin

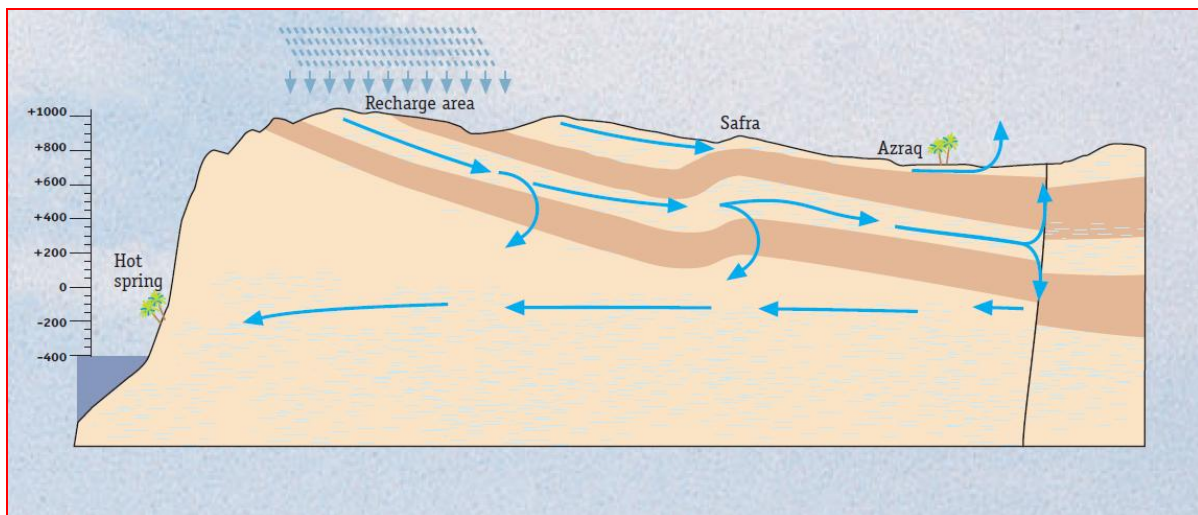


Figure (3.6): Hydrogeological cross section in the Azraq Basin

3.9 Farm Wells

Azraq farms grow a wide variety of vegetables, fruits and olive trees (Figure 3.7). Most of unlicensed wells were drilled in late 80's and beginning of 90's. Total abstraction by farmers is around 46 MCM/year.

The upper aquifer in Qa' Al Azraq area is very shallow, and the water table can be found at only few meters below the ground surface and hand dug wells are commonly found (Figure 3.8) . All the hand dug wells are located in the farm areas northeast of Azraq Drouz and east of the wellfield area. They were excavated within the first ten meters of the alluvial deposits to obtain water for irrigation purposes. The hand-dug and other shallow wells in the farm area show that the upper Quaternary Formation consists of Marl and Chert layers, intercalated with Lacustrine sediments and clay, accordingly the transmissivities are low. The alluvial deposits in the Qa' is subdivided into three parts: (1) the upper part includes permeable sediment layers with thickness ranging between 10-30 m; (2) the middle part includes a low permeable clay and marl layer with a thickness between 20 – 40 m and (3) the lower part includes permeable and semi-permeable Quaternary age sediments of Shallala formation.



Figure (3.7) : Farm well in Azraq area

The geoelectrical survey which were conducted by Worzky and Huster (1987) have shown local water bodies at depths 50 to 80 m. Changes from salt to fresh water in greater depths can be explained by an existing aquitard layer between the two aquifers as shown in Figure (3.8).



Figure (3.8) : Shallow hand-dug well in the farm area

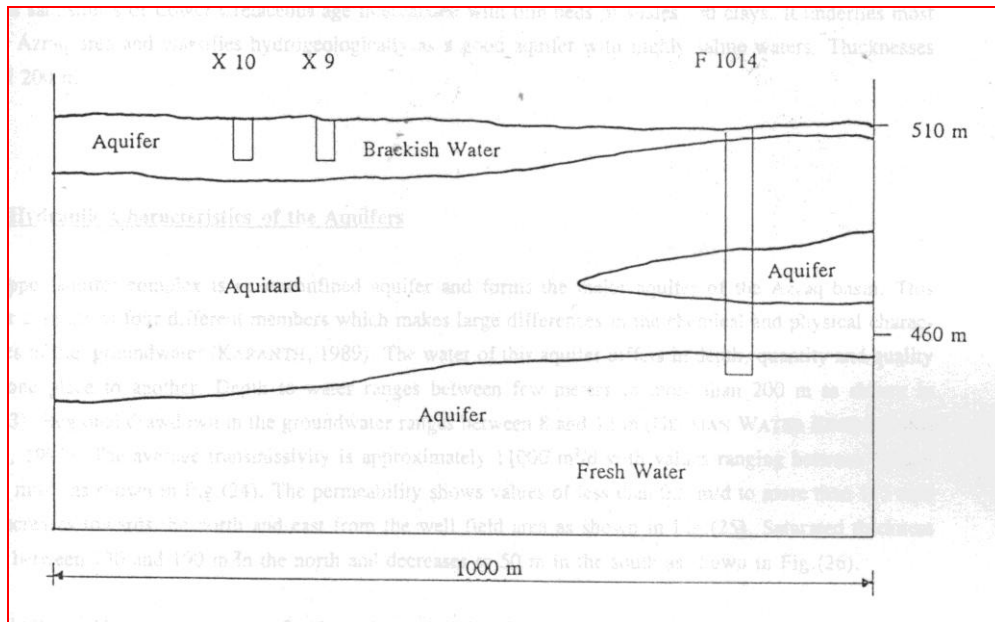


Figure (3.9): Schematic hydrogeological cross section of the well F1014 (Worzyk and Huster, 1987).

CHAPTER 4 GEOELECTRICAL SURVEYS (VES & TDEM) AT QA' AL AZRAQ

4.0 Geoelectrical methods and hydrogeological problems

Managing groundwater resources in aquifers affected by saltwater intrusion zone are very crucial. The existing hydrogeological conditions in this case are particularly dynamic and complex due to tectonic features of aquifers, human activities and other geological factors. A great amount of information regarding the geometrical and hydraulic properties of the aquifer is necessary. Most of this information is provided by observation and pumping wells; however, due to their scarcity and inevitably very local character of the information they provide, the supplementary cost-effective, non-invasive geophysical methods can provide continuous subsurface structural information to help mapping fresh–saline groundwater interface.

The geophysical techniques offer a suitable method for determining the geometrical characteristics of an aquifer, since costs are reduced and results are good compared to the construction of wells, Among all geophysical techniques (gravity, GPR, magnetic, seismic refraction, etc.), electromagnetic and resistivity methods are undoubtedly the leading ones in the exploration and management of groundwater. The most successful applications of the methods reported in the literature focus mainly on the studies of geometrical features of different geohydrological targets such as the configuration of groundwater depth, the thickness and type of an aquifer, alluvial fill and gravel lenses over bedrock, the thickness and depth of sand and gravel lenses in till, etc.

The direct current (DC) or resistivity method is probably the most popular in groundwater studies due to the simplicity of the technique, easy interpretation of the data and rugged nature of the associated instrumentation. The technique is widely used in soft and hard rock areas. The transient electromagnetic (TEM or TDEM) method has been used worldwide for hydrogeological surveys since several theoretical studies on the applicability of the method for groundwater investigation were undertaken. It is well known that DC soundings are quite sensitive to resistive layers and structures imbedded in section and sensitive to conductive layers. The TEM shows a complementary behavior because it is very sensitive to conductive layers and insensitive to resistive ones. The TEM method is a fast and cost-effective method for exploring the subsurface. In the last decade, many scientists used the TEM method to solve hydrogeological and environmental problems, since the method was fully updated. Specifically, recent advances in digital technology have led to more innovative TEM instrumentations (e.g., TEM-Fast 48, DIALOG, Geonics PROTEM47, Sirotem Mk3, ARTEMIS, Zonge NanoTEM) with improved capabilities for reconstructing the subsurface (from 10 m till 200 m beneath the surface) at areas where it was not always possible to deploy other geophysical methods such as DC resistivity. Moreover, the development of novel schemes for processing of the acquired TEM data can provide geologically (realistic interpretive model) two-and three-dimensional resistivity models without much reliance on the availability of a priori subsurface information.

This research describes a recent evaluation study of the applicability of TEM and DC- VES geophysical investigation and other hydrogeological systems to determine the fresh –saline groundwater interface in azraq “Qa” area. A total of 30 TDEM soundings and 7 VES were acquired at different locations with different acquisition parameters for deeper penetration and better resolution. Prior to the geophysical work. Detailed geological and tectonic mapping was accomplished and all the available information was used to construct a GIS platform. The available prior information from boreholes in the study area was useful for calibrating our results.

Relationships between aquifer characteristics and electrical parameters of the geoelectrical layers have been studied and reviewed by many authors such as (Mazac et al., 1985; Huntley, 1986). Some researchers assume that the geology and groundwater quality remains fairly constant within the area of interest and the relationships between aquifer and geophysical parameters are deduced, based on this assumption. the correlation between aquifer and geoelectrical parameters in saturated and unsaturated zones of the aquifers is robust and very helpful to draw the variation in aquifer characteristics.

Geophysical methods can now contribute substantially towards this initiative and can greatly reduce the number of necessary pumping tests, which are both, expensive and time consuming. These methods includes vertical electrical sounding (VES) combined with Electromagnetic (EM). These methods allow calculating the so called “apparent resistivity”. This parameter integrates the thickness and electrical resistivity of the layers constituting the soil and rocks. Then, the “real” resistivity is determined by solving the inverse problem, i.e., by proposing a model of the geoelectrical layer which would result in theoretical values as close as possible to those measured.

The main objectives of conducting the geoelectrical surveys is: (a) to create preliminary hydrogeological/geophysical expectation models for the study area, (b) to combine the geological, tectonic, hydrolithological, geophysical and other information to generate scenarios that could provide answers to the key hydrogeological questions developed for the area under investigation, (c), to upgrade and re-interpret the hydrogeological expectation model based on the final 2D geophysical models, and (d) to identify a saline-fresh groundwater target area based on available and interpreted information for the construction of suitable sites for the groundwater salinization sensors.

4.1 Electrical Resistivity Sounding (VES)

Site investigation for purpose of the construction of nuclear power plants can be well carried by the combination of three geophysical methods. These are the Seismic refraction, vertical electrical sounding and resistivity imaging methods.

Surface electrical resistivity surveying is based on the principle that the distribution of electrical potential in the ground around a current-carrying electrode depends on the electrical resistivities and distribution of the surrounding soils and rocks. The usual practice in the field is to apply an electrical direct current (DC) between two electrodes implanted in the ground and to measure the difference of potential between two additional electrodes that do not carry current. Usually, the potential electrodes are in line between the current electrodes, but in principle, they can be located anywhere.

Mineral grains comprised of soils and rocks are essentially nonconductive, except in some exotic materials such as metallic ores, so the resistivity of soils and rocks is governed primarily by the amount of pore water, its resistivity, and the arrangement of the pores. To the extent that differences of Lithology are accompanied by differences of resistivity.

Generally, since the resistivity of a soil or rock is controlled primarily by the pore water conditions, there are wide ranges in resistivity for any particular soil or rock type, and resistivity values cannot be directly interpreted in terms of soil type or Lithology. Commonly, however, zones of distinctive resistivity can be associated with specific soil or rock units on the basis of local field or drill hole information, and resistivity surveys can be used profitably to extend field investigations into areas with very limited or nonexistent data. Also, resistivity surveys may be used as a reconnaissance method, to detect anomalies that can be further investigated by complementary geophysical methods and/or drill holes.

4.2 Theoretical background

Data from resistivity surveys are customarily presented and interpreted in the form of values of apparent resistivity (ρ_a). Apparent resistivity is defined as the resistivity of an electrically homogeneous and isotropic half-space that would yield the measured relationship between the applied current and the potential difference for a particular arrangement and spacing of electrodes. An equation giving the apparent resistivity in terms of applied current, distribution of potential, and arrangement of electrodes can be arrived at through an examination of the potential distribution due to a single current electrode.

Consider a single point electrode, located on the boundary of a semi-infinite, electrically homogeneous medium, which represents a fictitious homogeneous earth. If the electrode carries a current I , measured in amperes (a), the potential at any point in the medium or on the boundary is given by:

$$U = \rho \frac{I}{2\pi r}, \quad (1)$$

where

- U = potential, in V,
- ρ = resistivity of the medium,
- r = distance from the electrode.

4.3 Field survey and Data acquisition

To investigate changes in resistivity with depth, the size of the electrode array is varies, AB are current electrodes and MN are potential electrodes (Figure 1). The apparent resistivity is affected by material at increasingly greater depths as the electrode spacing is increased.

Because of this effect, a plot of apparent resistivity against electrode spacing can be used to indicate vertical variations in resistivity. The using of schlumberger array is adapted in this kind of survey using the following AB/2 (m) distances: 10, 30, 50, 60, 80, 100,150, 200, 250, 300, 350, 400, 500, 600, and 700 m with variable MN distance from 5m to 50m. The Ves's sites can be conducted in the area using resistivitymeter for detecting vertical variations of resistivity of geological layers. The apparent resistivity calculations depend on the following equation:

$$\rho_a = \pi \left[\frac{s^2}{a} - \frac{a}{4} \right] \frac{V}{I} = \pi a \left[\left(\frac{s}{a} \right)^2 - \frac{1}{4} \right] \frac{V}{I}, \quad (2)$$

where

- ρ_a = apparent resistivity, ohm-m
- a = MN distance, m
- s = AB distance, m
- V = Voltage, volt
- I = current, amp

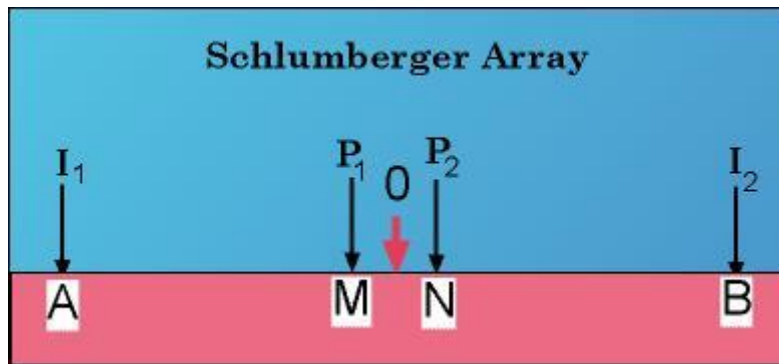


Fig (4.1): Schlumberger array utilized in the site selection

4.4 Use of Geoelectrical and Electromagnetic methods in studying salt fresh water intrusion

In many developed and developing countries there is not only a heavy reliance on ground water as a primary drinking supply but also as a supply of water for both agricultural and industrial use. Among these interesting areas in Jordan, is the Azraq Basin. The study area suffers extreme arid conditions with long, hot, rainless summers and mild winters. Geophysics, especially

geoelectric techniques have been successfully used to detect the fresh/salt-water interface in Qa' Al Azraq. These methods include the DC resistivity method (Yang, et al. 1999) and transient electromagnetic induction (TEM) method (Stewart and Gay, 1986). Resistivity surveys are often used to search for ground water in both porous and fissured media. These methods provide detailed information about the geometry, source and amount of contamination in the groundwater (Kelly, 1976). In areas where the ground water is significantly saline, the aquifer resistivity is reduced considerably and resistivity method can delineate the boundaries of the body of saline water. Griffith and Barker (1993) present the results of strong resistivity contrast, which can occur across the junction between fresh and saline water using the resistivity survey. Additionally, large differences between the resistivity of saltwater and freshwater saturated zones have been used by many investigators for determination of saltwater intrusion in many coastal areas (e.g. Frohlich et al., 1994). This work represents an attempt to delineate the seawater intrusion in the fresh shallow water aquifer in Azraq Basin.

The electrical resistivity is strongly dependent on parameters like granule geometry and content of conductive materials (water, clay, salt contents and metal minerals). Its measurement is thus a suitable tool for the study of layered structure and groundwater exploration. Surveys methods based on electrical (Resistivity Sounding VES and Time domain electromagnetic TDEM measurements) allow calculating the so called "apparent resistivity". This parameter integrates the thickness and electrical resistivity of the layers constituting the soil and rocks. Then, the "real" resistivity is determined by solving the inverse problem, i.e., by proposing a model of the geoelectrical layer which would result in theoretical values as close as possible to those measured.

4.4.1 TDEM Method

Developed in Russia in the early eighties for studying deep structures, since 1985 the TDEM has found wide application in geological, engineering and environmental spheres and today represents a potentially promising method for investigating electrical parameters of the subsoil. Much has been published on the TDEM, including applications in hydrogeological research (Sorensen K.I., 1996; Fittermann D.V. and Stewart M.T., 1986; Christensen N.B. and Sorensen K.I., 1994; Meju M.A., 1995), and for studying the specific problem of salt water intrusion (Yuhr L. and Benson R.C., 1995; Hoekstra P. and al. 1996; Richards R.T. and al. 1995; Goldmann M., 1996). Other workers (Nabighian M.N. and Mcnae J.C., 1991; Auken E., 1995; Sorensen K.I., 1998; Christensen N.B., 1997; Meju

M.A., 1994,1994) have studied various aspects of the application, processing and interpretation of TDEM soundings and its use in combination with other geophysical techniques.

A variety of geophysical methods has been adopted in saltwater intrusion investigations. Conventional DC resistivity techniques have long been used to characterise shallow aquifers, gravity and magnetic methods have been applied to reconstruct deep aquifers and the bedrock. Barbieri G. et al., 1986 applied the I.P. method to describe the temporal evolution of saltwater intrusion. Other applications have involved electromagnetic and seismic methods.

Based on the experience gained from using TDEM sounding in many different applications, some practical recommendations are summarised below:

- The maximum depth of investigation is determined by the maximal time t , in which it is possible to reliably register a signal $V(t)/I$ and not exceed the loop side by 3 times;
- the TDEM technique performs effectively in sections with high conductivity: the layers, for example, with $\rho = 1$ and $\rho = 1.5$ Ohm m are reliably stratified;
- it is practically impossible to distinguish layers with very high resistivity;
- super-small antennas (less than 10-15 meters) for stratifying layers at shallow depths can only be used for rocks with low resistivity; 5. at high levels of resistivity it is necessary to use large antennas;
- the most favourable range of specific resistivity for stratification of rock is $10 \text{ Ohm m} < \rho < 300 \text{ Ohm m}$;
- mean resolution is about 1/10 of the loop side.

Time-domain electromagnetic (TDEM) methods in groundwater exploration are useful as sounding techniques, as opposed to profiling techniques. Sounding techniques measure the depth to an interface, or interfaces. They can be used to measure the thickness of a gravel unit, depth and thickness of a clay aquitard, or depth to bedrock.

In the most common groundwater exploration configuration, TDEM soundings are made by laying out a loop of wire 20 to 200 meter on a side and pulsing it with a controlled current. Measurements are made, usually in the center of the loop, with an antenna coil about three feet across. All the equipment is easily portable; six to sixteen soundings can be made in a day, depending on field conditions. Time domain electromagnetic (TDEM) survey involves the transmission of a current through a rectangular loop, commonly laid on the ground (Figure 4.2).

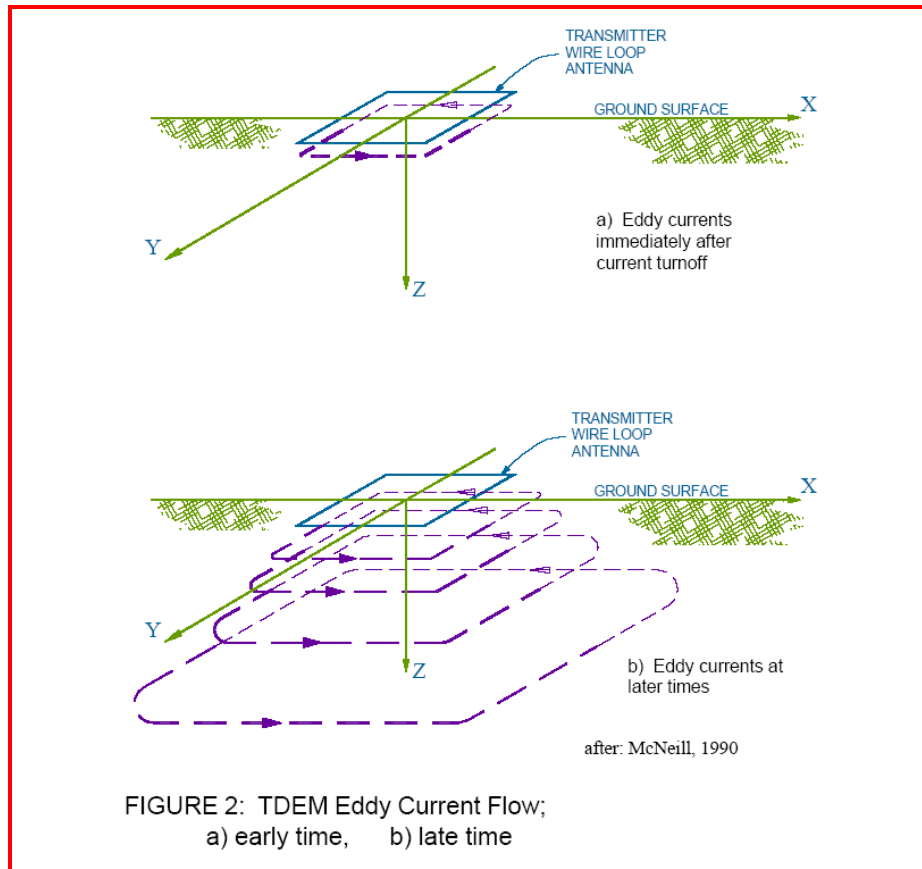


Figure (4.2): Induced eddy currents at progressively later times after turnoff.

The primary magnetic field spreads into the ground. By rapidly reducing the transmitter current to zero, the changing primary magnetic field will induce eddy currents in the subsurface which are dependent on the subsurface resistivity distributions. The eddy currents will generate a changing magnetic field that can be detected by a receiver coil at the surface. The voltage generated in the receiver coil, which is proportional to the change of the secondary magnetic field created by the eddy currents, is measured versus the time.

Secondary magnetic fields decay quickly in poor conductors and slowly in good conductors. By measuring the decay of the magnetic field, an estimate of subsurface resistivities can be achieved. The measured voltages can be transformed into apparent resistivity values to represent the properties of the subsurface.

The principles of TDEM resistivity sounding are relatively easily conducted. The process of abruptly reducing the transmitter current to zero induces, according to Faraday's law, a short duration voltage pulse in the ground, which causes a loop of current to flow in the immediate vicinity of the transmitter wire (Figure 4.3). In fact, immediately after the transmitter current is turned off, the current loop passes into the ground immediately below the transmitter and, on

account of the finite resistivity of the ground, the current amplitude immediately starts to decay. Similarly the decaying current induces a voltage pulse which causes more current to flow at a greater distance from the transmitter loop, and also at greater depth. The deeper current flow also decays due to finite resistivity of the ground, inducing even deeper current flow and so forth.

To determine the voltage produced by the decaying magnetic field at the receiver coil at successively later times, measurements are made of the current flow and thus also of the electrical resistivity of the earth at increasingly greater depths, and it is this process that forms the basis of resistivity. The decay characteristic of the voltage in the receiver is determined for a number of time gates (Figure 4.3), each measuring and recording the amplitude of decaying voltage. The time gating differs with time. In fact, to minimize measurement distortions, the early time gates, which are located where the transient changes rapidly with time, are very narrow, whereas the later gates, where the amplitude of the transient decay diminishes, are much broader to enhance the signal-to-noise ratio. Only the (two) transients that occur when the transmitter current has just been shut off are measured. Lastly, particularly for sounding at shallower depths, where it is not necessary to measure the transient characteristics out to very late time, the period is typically of the order of one millisecond or less, which means that in a total measurement time of a few seconds, measurements can be made and stacked on several thousand transient responses to improve signal-to-noise ratio. To increase depth the variations must be recorded at a later time (by some seconds). Apparent resistivity in TDEM soundings, the voltage response can be divided into an early stage (where the response is constant with time), an intermediate stage (response shape continually varying with time) and a late stage (response is a straight line on log-log plot).

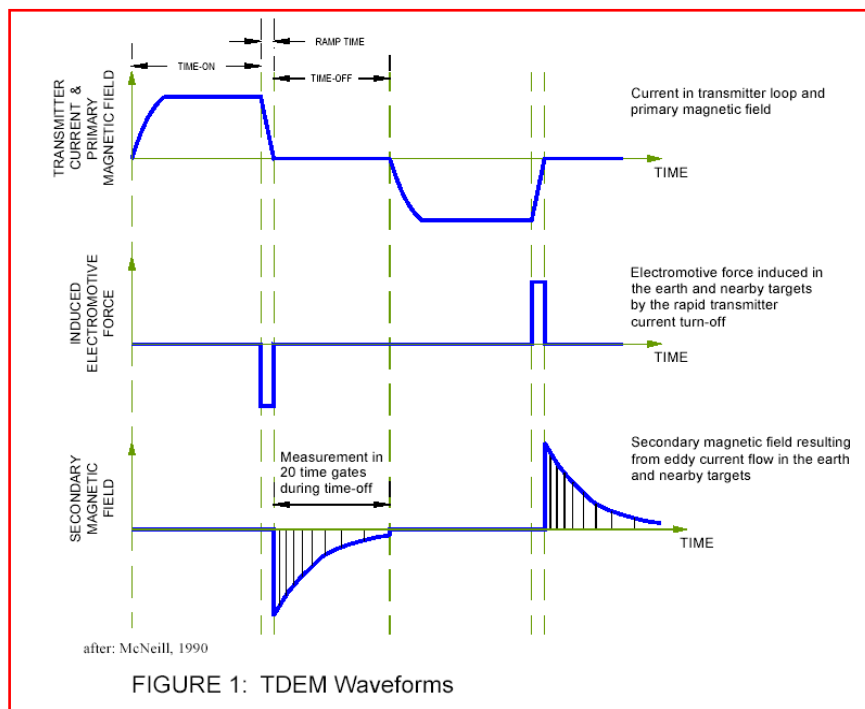


Figure (4.3): TDEM waveforms at three different stages of measurements.

4.4.2 TDEM Field Survey

The field configurations can follow central geometries (transmitter and receiver have the same centre), or with offset geometries (the receiver coil is placed outside the transmitter coil) (Figure 4.4). The investigation depth depends on the characteristics of the transmission and of the subsurface. The main advantages of this method are the good ratio of the penetration depth over the space required by the layout, and a high sensitivity to the well-conducting soil layers. The main disadvantages are a rather poor resolution obtained for the resistive layers as well as for the near surface layers.

The TDEM apparatus used for the survey is the TEM of (Aemr company) (Buselli and O'Neill, 2008), (Figure 4.5). This apparatus is recommended for the investigation of depths going from 2 to 500 m; the transmitting loops must be as close as possible to a square; the advised dimension of the transmitting loops for this apparatus varies in general from 1 *1 m for the smallest to 500 per 500 m for the biggest loop.

4.4.3 Data Preparation in GIS Platform

To create the appropriate information platform on which to proceed in a systematic way toward applying the groundwater models through the use of geological and geophysical data, all available data in the form of maps were used as the basis for the creation of GIS thematic layers.

The data pre-processing involved their implementation into a GIS environment. Several maps were geo-referenced to the local projection system of Jordan (Clarke_1880_Benoit: International_1924) so that they could all be tied to the same projection system (Palestine Grid), together with all future information that may become available. In the next pre-processing phase, digitization of all the relevant data maps, namely lithological, structural was carried out. The Digital Elevation Model (DEM) of the study area with continuous raster layer, in which data values represent elevation, was generated digitally from available resources. The lithology layer was derived through the digitization of the published geological maps, which display major rock groups and structural features.

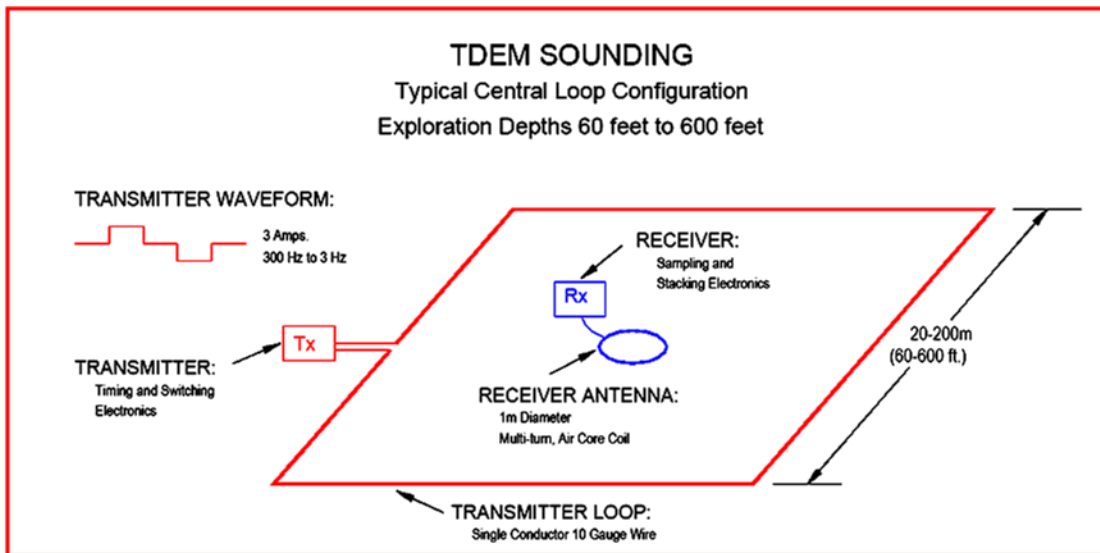
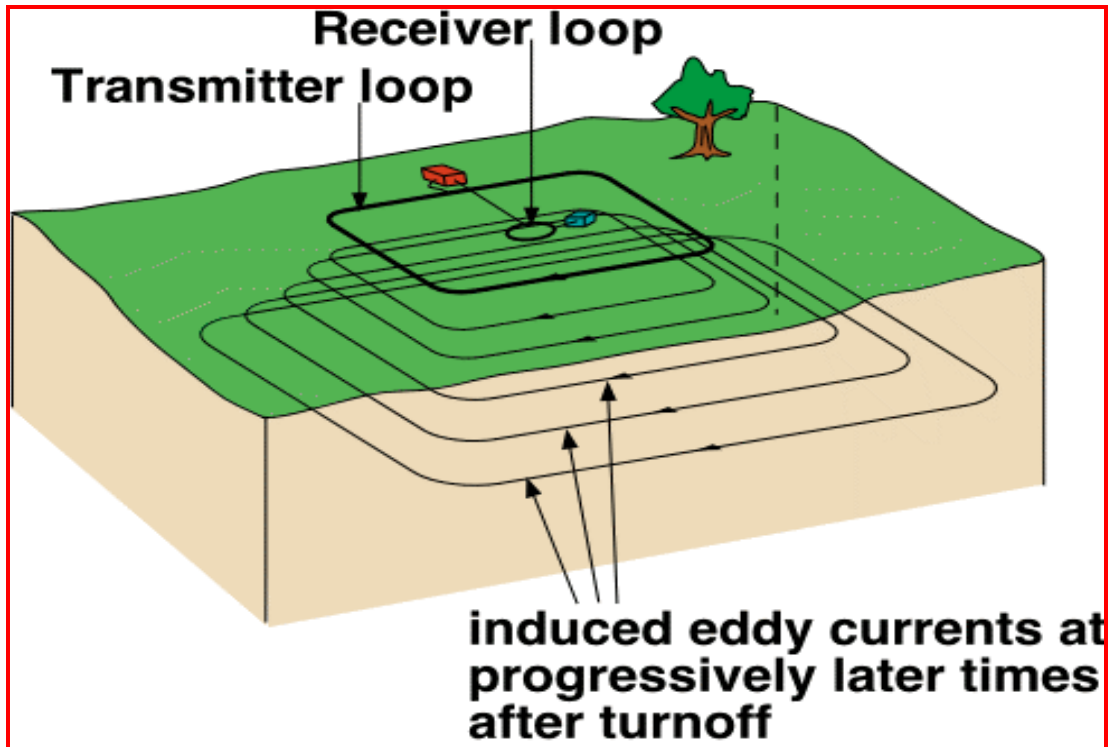


Figure (4.4): TDEM field configuration showing (a) Induced eddy currents at progressively later times after turnoff and (b) loop configuration.



Figure (4.5): The TDEM apparatus model.

4.5 Geophysical Data Acquisition and Processing

The geophysical measurements were carried out in a detailed survey location regarding to possible area of salt invasion (optimum site selection) and to the nearest location of wells to be able to detect the environmental conditions Fig. (4.6).

4.5.1 TDEM Geophysical Data

Thirty conducted sites of TEM geophysical survey in which single turn of 100 m * 100 m loop was used to gain sufficient penetration depth (~100m). The system was set to transmit current up to 4 A with 32 active time gates from 4 to 1,024 microseconds and a stacking time of about 5 min. To define and avoid aliasing effects (high-frequency (HF) noise from radio sources); the measurements were repeated several times at each sounding location. Based on the international bibliography and depending on the geological conditions of the study area, It is clear that resistivity zone below 1 ohm.m is good value to separate saline groundwater from fresh groundwater that may exceeds 4 ohm.m (Figure 4.7). The target zone is mainly imbedded in clay materials with other weathered igneous (basalt ash) and sedimentary (limestone, marl

and chalk) rocks, this assumption is valid for our case in which the inverted resistivity interval is lay between 0.1 and 30 ohm.m.

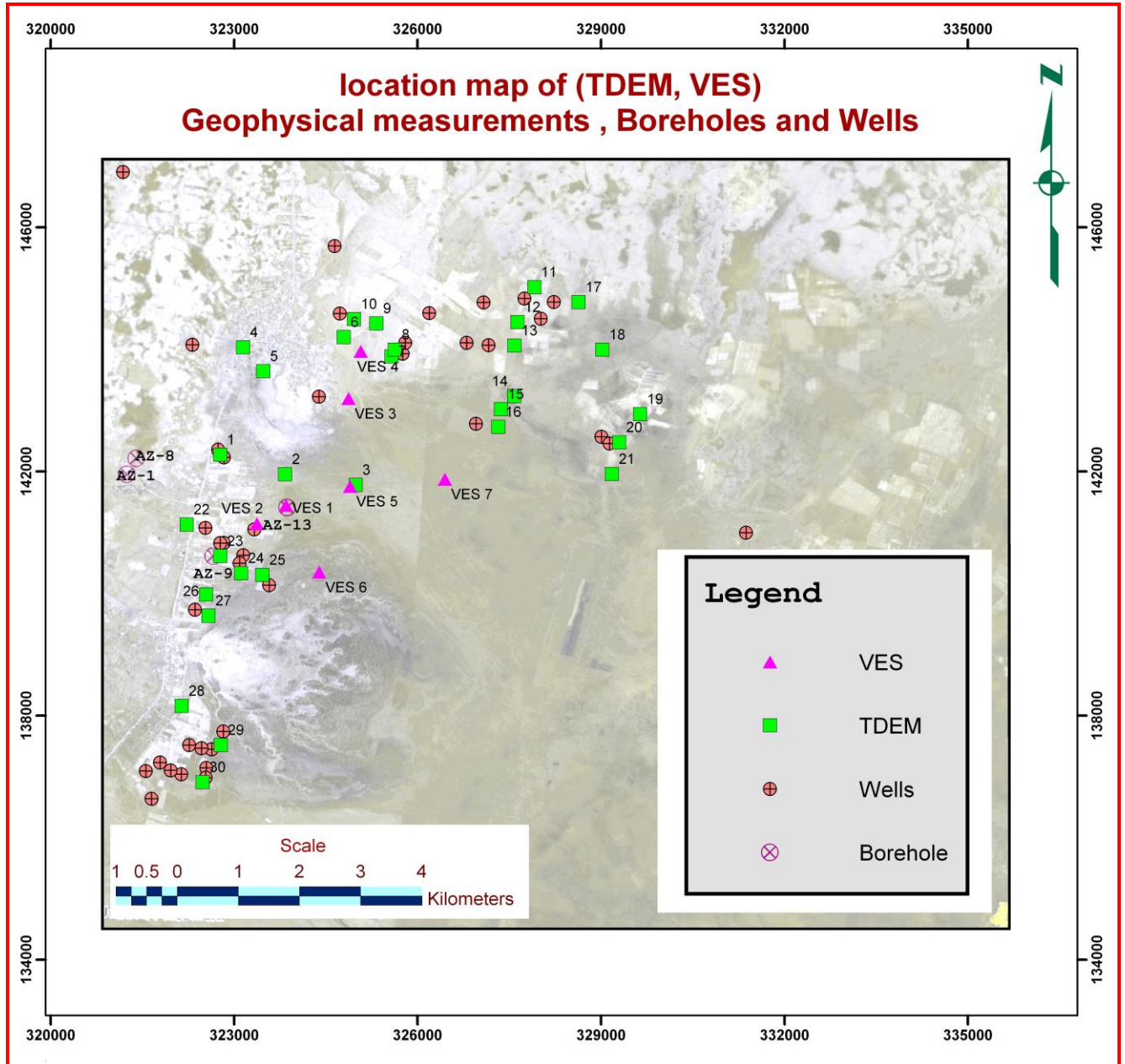


Fig. (4.6): Location map of TDEM, DC-VES geophysical measurements, boreholes and wells

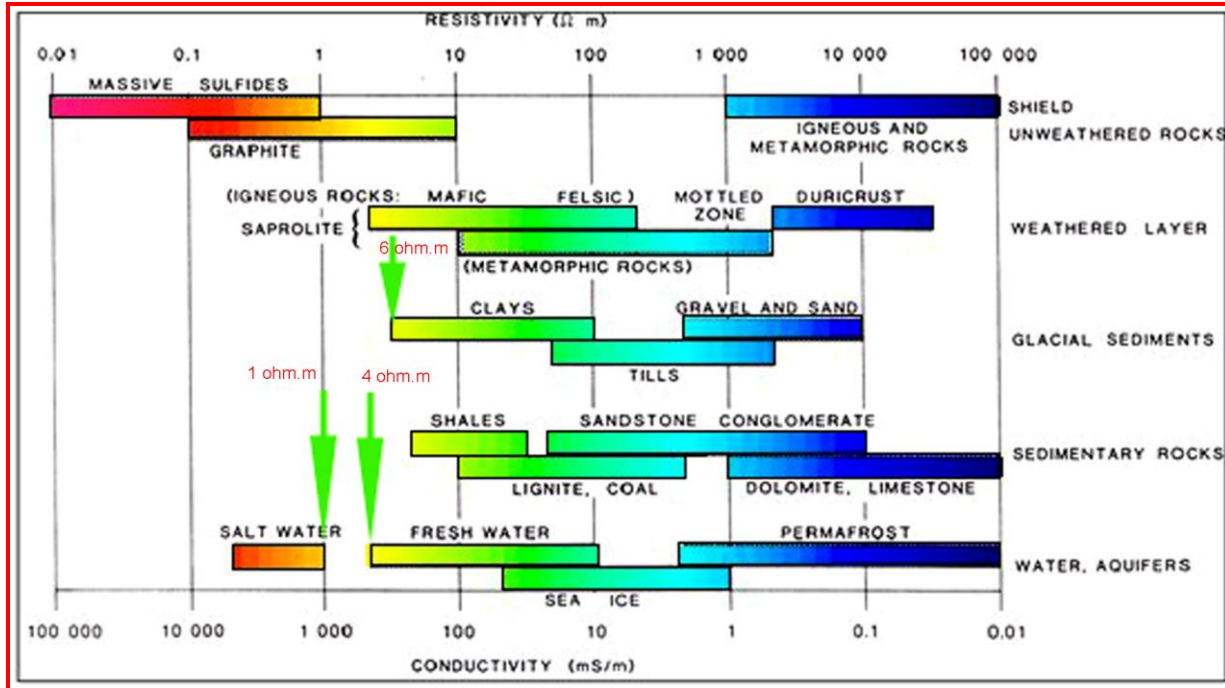


Figure (4.7): Resistivity ranges for different substances see the three green arrows that describing clay, fresh water and saline water resistivities.

The collected data were processed after the acquisition providing the one-dimensional (1D) distribution of resistivity with depth. The TEM-Software is a Windows-integrated interpretation system, was the tool for data processing of TEM data and inverse problem solution. The program is a user-friendly tool that is convenient for TEM data editing, smoothing, analysis and processing. Geoelectrical sections (2D pseudo-sections) and depth slices (resistivity and conductivity maps) are easy to be constructed in the class of gradient or layered structures.

Generally, the 1D inversion approach gives a satisfactory reconstruction of the true model. Of course, in case of high-resistivity geological contacts and/ or contrast and strong 3D features, the 1D approximation is strongly influenced by 3D effects. Statistically, the root mean square (RMS) error of the final data models was less than 3 % (between 0.15 and 3%) which is a good indicator of high quality data and subsurface hydrogeological response.

TEM 23 was conducted at Borehole AZ 9 to calibrate the resistivity ranges of sounding model to the earth geological layers (Figure 4.8). This model is good example to show how transient current has resolved the 1D earth class. The inverted model was achieved at 0.65 RMS error and returned electrical information to about 100m depth. Three different lithological layers has been identified, Clay and gravel, Chalky limestone and Marl. The GWL is recognized at 5 m depth of moderate groundwater quality .

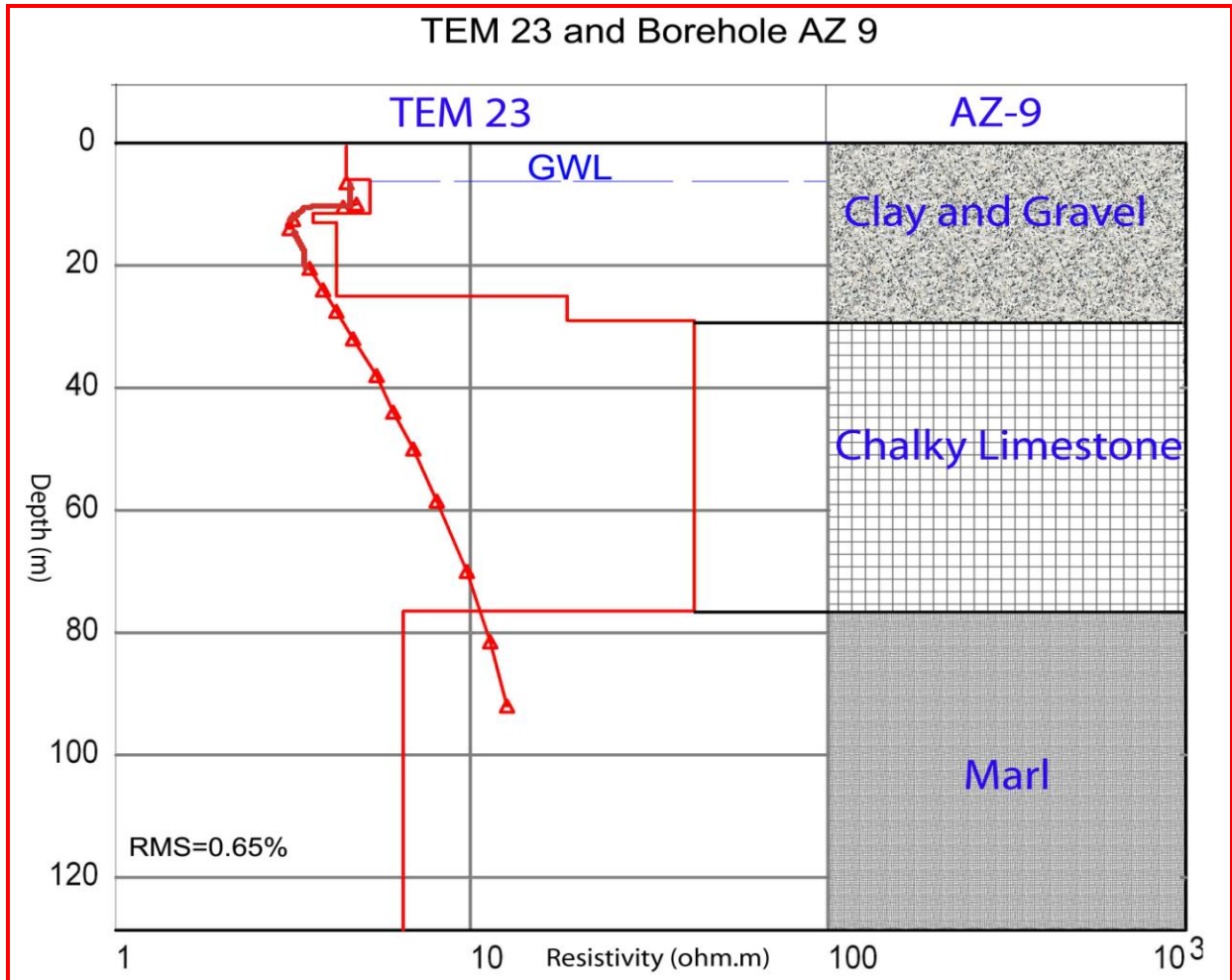


Fig. (4.8): Resistivity model obtained from the inversion of the TEM23 (using the TEMRES program) and its correlation with the Geological-log obtained from the borehole AZ 9.

4.5.2 DC-VES Geophysical Data

Seven VES's were undertaken with expanding current electrodes separation, i.e., Schlumberger configuration with AB/2 distance is varying from 3 to 200 m. The data were acquired using a SYSCAL resistivity meter. The apparent resistivity data acquired at each site was inverted using the IPI2win software (IPI2Win-1D). Figure (4.9) shows example of apparent resistivity curve of VES1 and its inversions compared to lithology of borehole AZ 13.

The calculated models exhibit in general four geoelectrical units representing the first 100 m depth section in the study area. These units correlate from the top to bottom with the deposits, Clay and Gravel, Clays, Clay and Basalt ash and Chalky limestone. The GWL is found at 7 m depth with high salinity of groundwater quality.

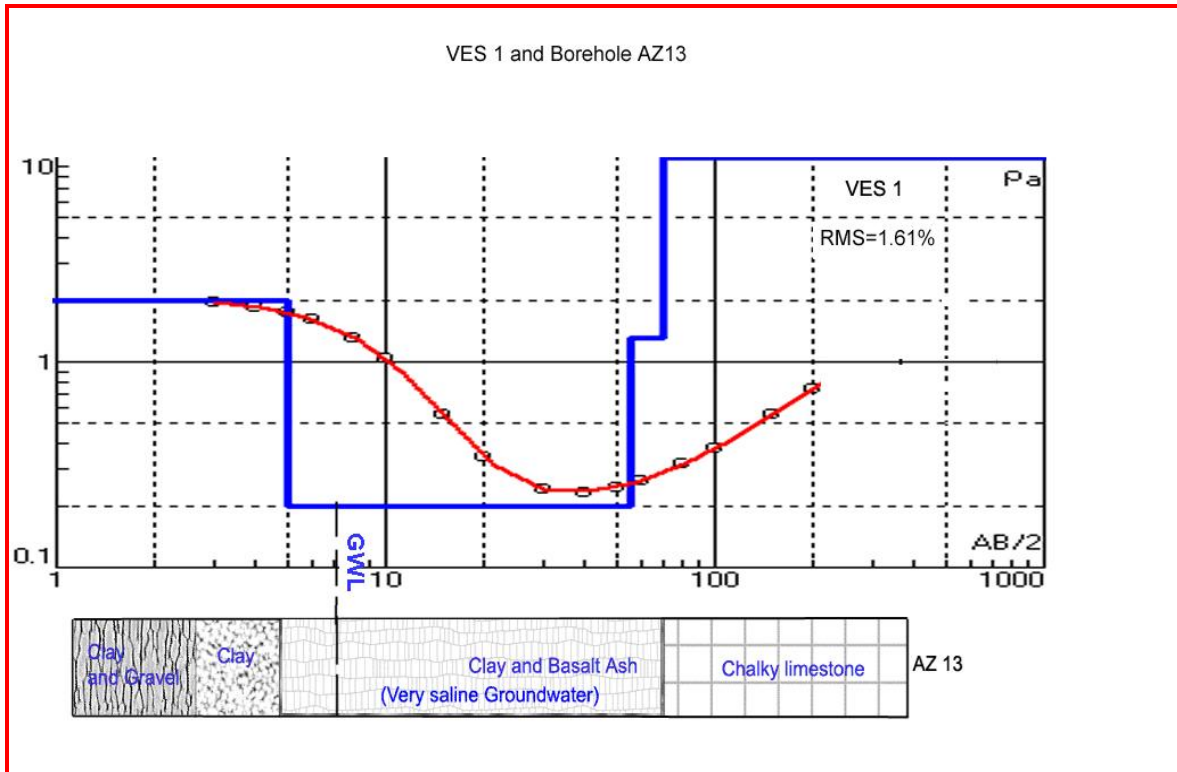


Figure (4.9): Resistivity model obtained from the inversion of the VES 1 (using the IPI2WIN program) and its correlation with the geological-log obtained from the borehole AZ 13.

4.6 Combined (TEM & VES) Interpretation Results

According to the previous indicated hydrogeological studies and tectonic/geological data, the following question should be answered prior to suggestion and construction of the main problem in the study. Is there any possibility to detect the contamination of groundwater using geophysical methods due to the proximity with the invasion of saltwater intrusion? The first interpretation of resistivity and electromagnetic methods has resolved this problem smoothly and with good data coupling at VES1 and TEM 23. The TEM and VES methods are capable of detecting of interface between fresh groundwater body and an underlying saline one through the expected sharp drop of resistivities. On the other hand, the type of groundwater salinity could be extracted directly from groundwater resistivity.

In many cases, the subsurface cannot be resolved into plane homogeneous layers, as required for VES or a TEM investigation, or into simple zones of lateral conductivity variation as required for depth section interpretation. As a result, a combination of the two techniques is usually applied. The Thirty (30) TEM and seven (7) VES measurements sites were conducted as indicated by field engineer who is helped to manage the geophysical location of most candidate area of saltwater contamination. Furthermore the location of VES's were coordinated to fill the gap among TEM locations. For that reason a good and complete pictures of the lateral variation

of groundwater salinity is possible through the spatial distribution of geophysical conducted sites. The data were processed and interpreted using all available information to model the true subsurface hydrogeological structures regarding to identify precisely where the interface between the fresh and saline groundwater is. Figure (4.10) shows the TEM-VES depth slice from 5 to 40 m depth where the interface is mostly located within it using groundwater elevation/quality and subsurface geological and structural data. This zone is considered as geometric characteristics of the groundwater and specifically the real elevation of the roof and bottom of the interface. We can safely assume any possible spatial changes in groundwater resistivity using modeled values as indicated by resistivity scale. For that reason different TEM and VES depth section were constructed to track resistivity zone below 1 ohm.m.

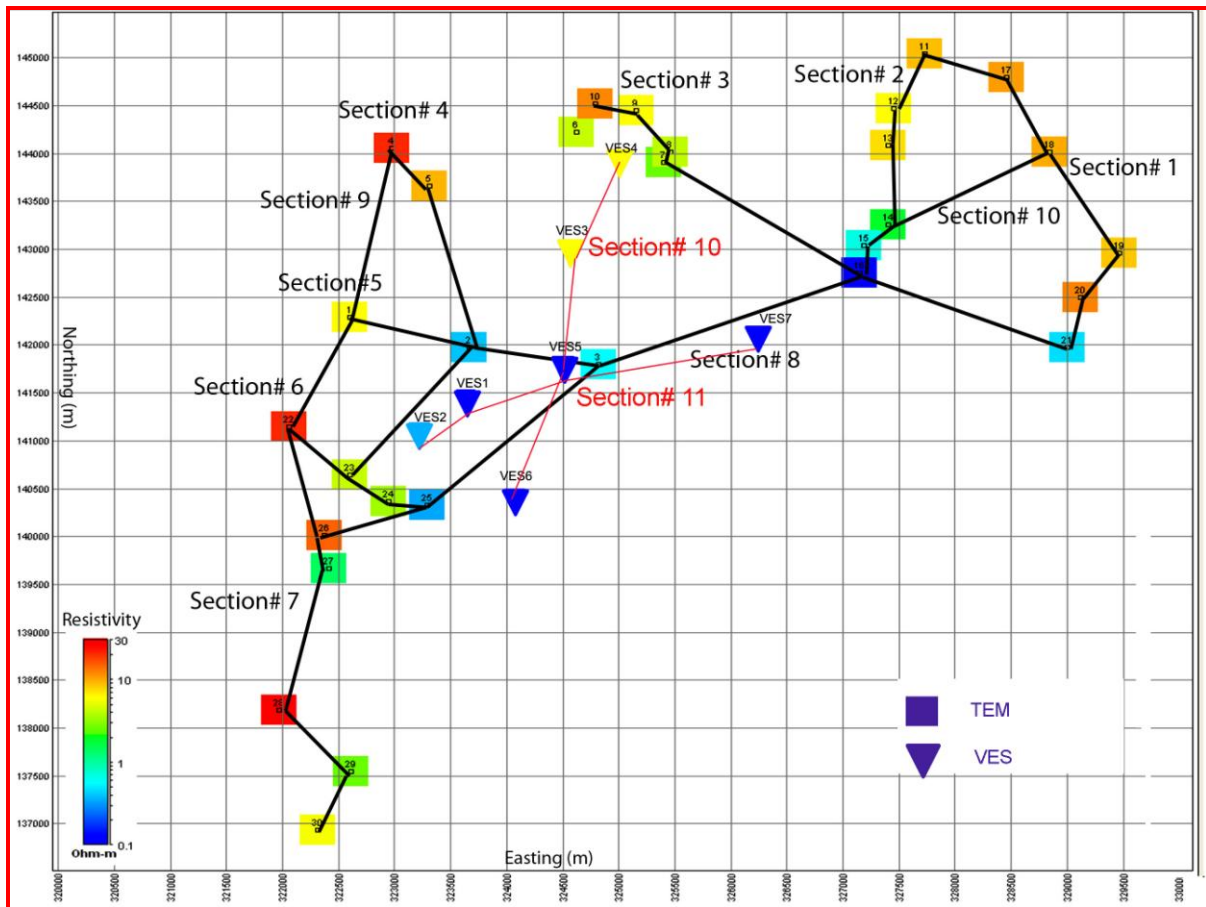


Figure (4.10): Interpreted TEM and VES geophysical cross sections at depth ranges from 5m to 40 m, resistivity scale below 1 ohm.m (light to dark blue colors) is used to show the possible area of saltwater locations.

4.7 Two Dimensional (2D) VES Interpretation

Two different VES cross sections were constructed to track the possible location of saltwater interface and to isolate it from any lithology electrical variations. Figures (4.11) and (4.12) depict different geoelectrical zones of different geological materials using VES modeled data. The resistivity cross section taking the north-south direction Figure (4.11) has resolved the saline water interface between clay and chalky limestone, it is found between VES3 and VES5. Whereas the east west cross section Figure (4.12) bound the roof and floor of this saline water. The area of saline water at this section appeared as a zone that extends through all VES's with length exceeds 2600m. This means that the strike of the interface is most likely take east west direction of the study area.

4.8 Two Dimensional (2D) TEM Interpretation

As mentioned above, TEM soundings are commonly used to define aquifer properties and other subsurface characteristics. Of course, those kinds of structures are multi-dimensional, but 1D inversion is used to determine geologic structure for groundwater models. Generally, they can be imaged without big errors.

The construction of a geoelectrical sections is based on transformation and inversion of decayed curve. Ten (10) cross sections were constructed using most of the TEM conducted sites to identify the location of saltwater interface see Figure (4.10) for section's location and to show the applicability of the TEM method for mapping the subsurface and for determining the hydrogeological regime of the study area. In all TEM cross section the hot (red) colors represent high-resistivity formations and the cold (blue) colors depict the low-resistivity units as well. The saltwater interface in all sections appears as blue line. From all cross sections, the sharp transition zone of groundwater resistivity to saline can be determined. The subsurface structures and groundwater level have been inserted using overlaid interpreted geo-database data.

Section's 1 to 6 locate the saltwater interface in lateral variation mode that striking near north-south direction, the Subsurface structures don't appear as control factor due to same sense of section direction (see Figures 4.13 to 4.19). Further more, sections from 7 to 10 bound the saltwater interface as a zone, that controlled by subsurface structures. Generally and as conclusion, it is important to draw the interface where the section is across the interface and parallel to geological structures (Figures 4.20 to 4.22).

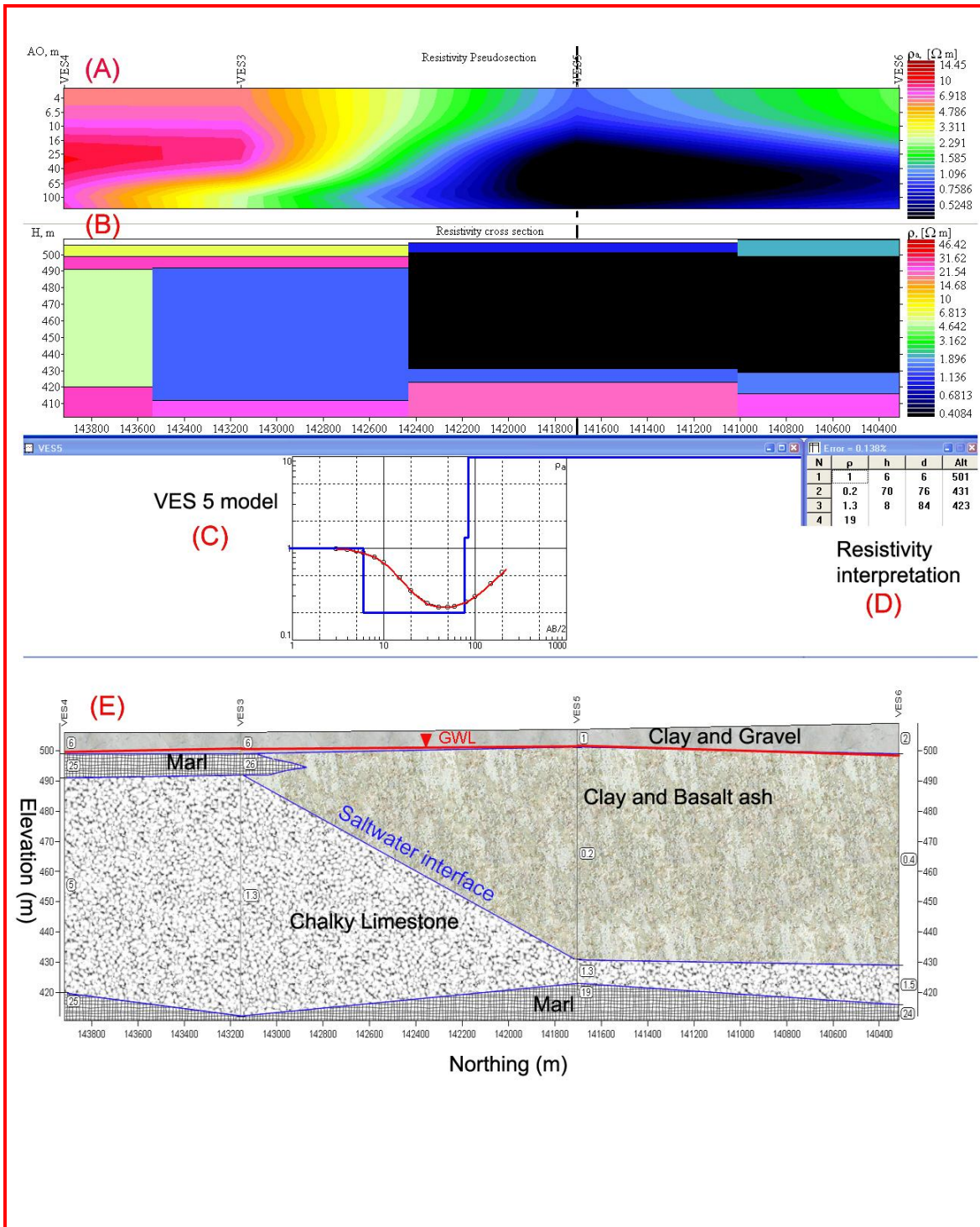


Figure (4.11): Interpreted VES profile along VES's 4,3,5 and 6; A) Apparent resistivity pseudosection , B) Inverted resistivity cross section, C) VES2 model curve, D) Resistivity interpretation into true resistivities and their corresponding thicknesses, E) Geoelectrical cross section model showing geological layers and their true resistivity.

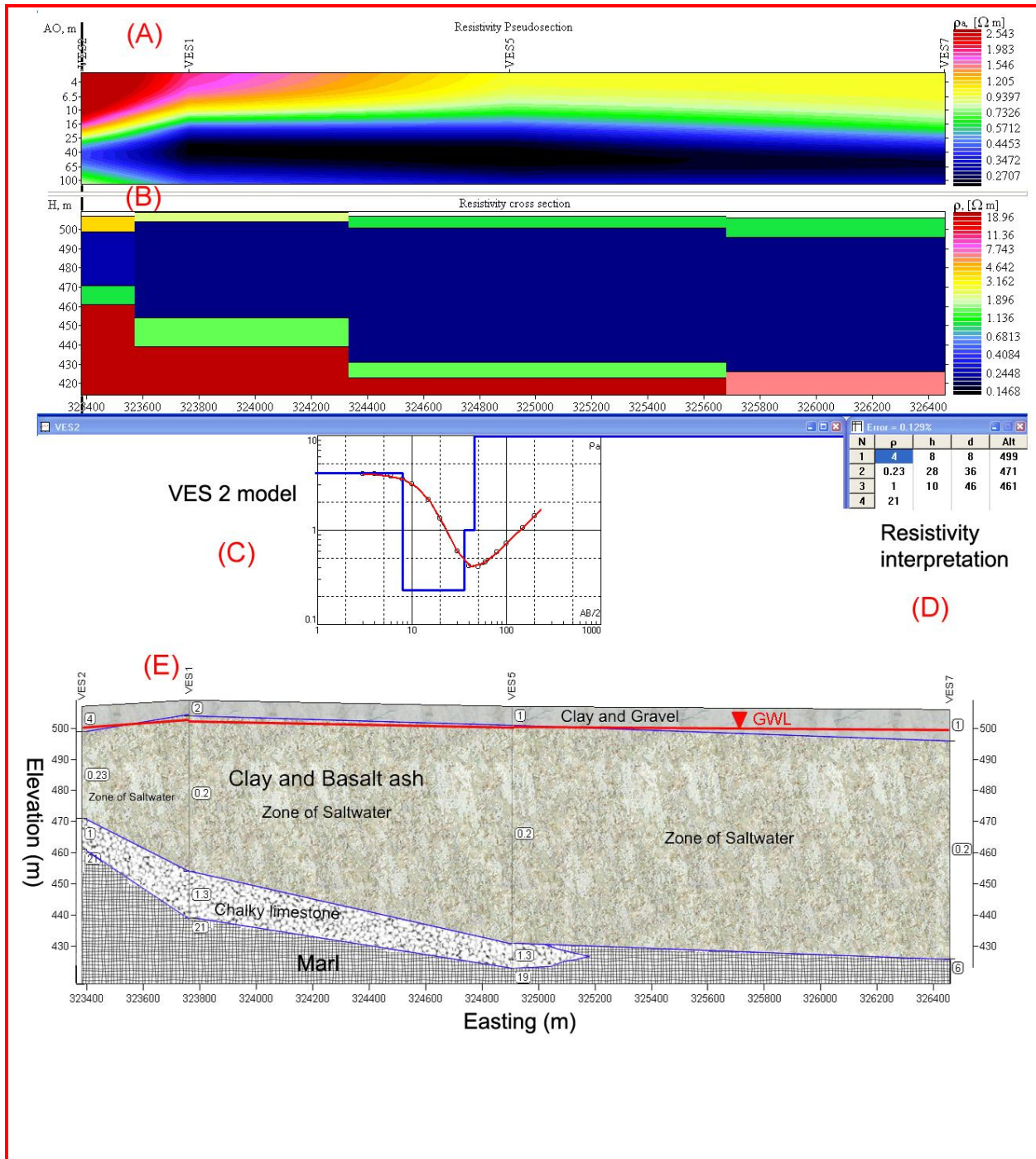


Figure (4.12): Interpreted VES profile along VES's 2,1,5 and 7; A) Apparent resistivity pseudosection , B) Inverted resistivity cross section, C) VES2 model curve, D) Resistivity interpretation into true resistivities and their corresponding thicknesses, E) Geoelectrical cross section model showing geological layers and their true resistivity.

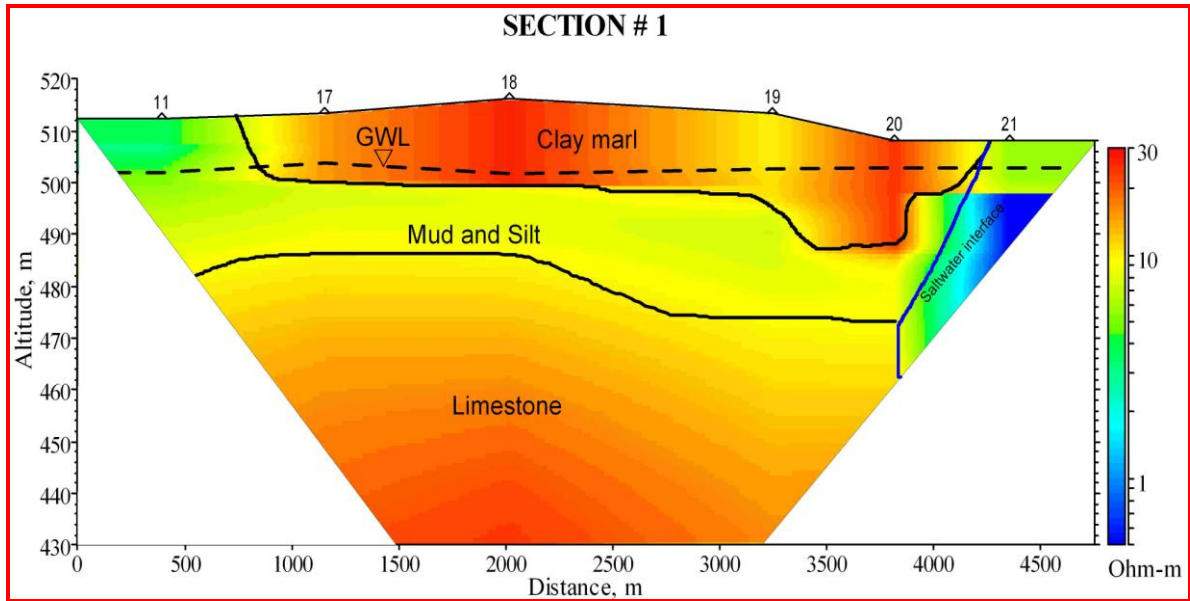


Figure (4.13): Two-dimensional representation of the TDEM resistivity distribution of section 1 with geological and hydrogeological design.

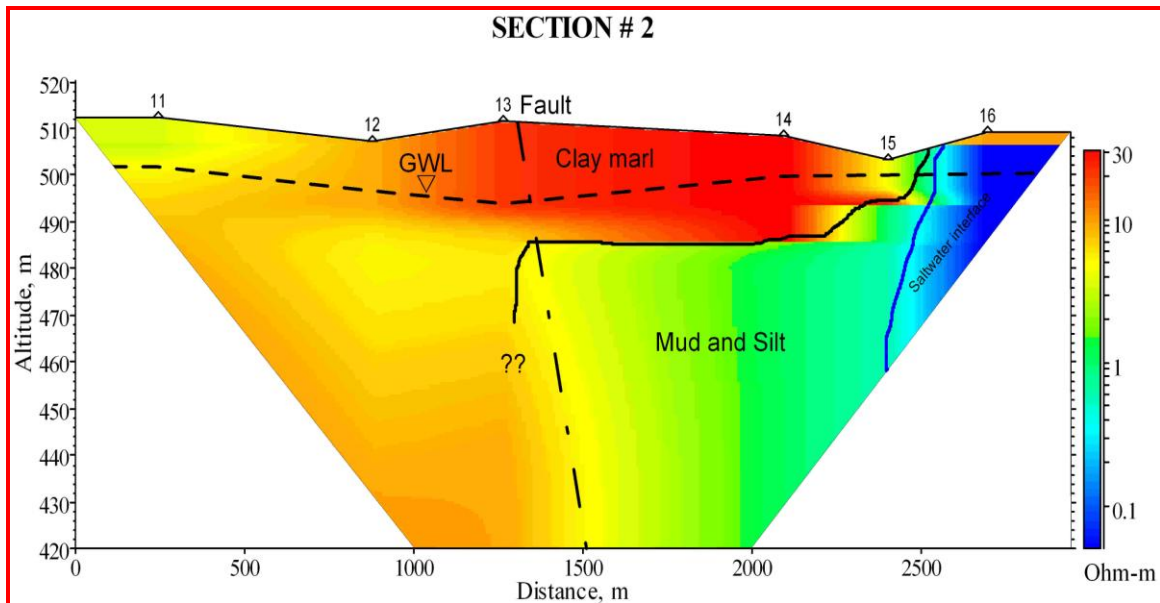


Figure (4.14): Two-dimensional representation of the TDEM resistivity distribution of section 2 with geological and hydrogeological design.

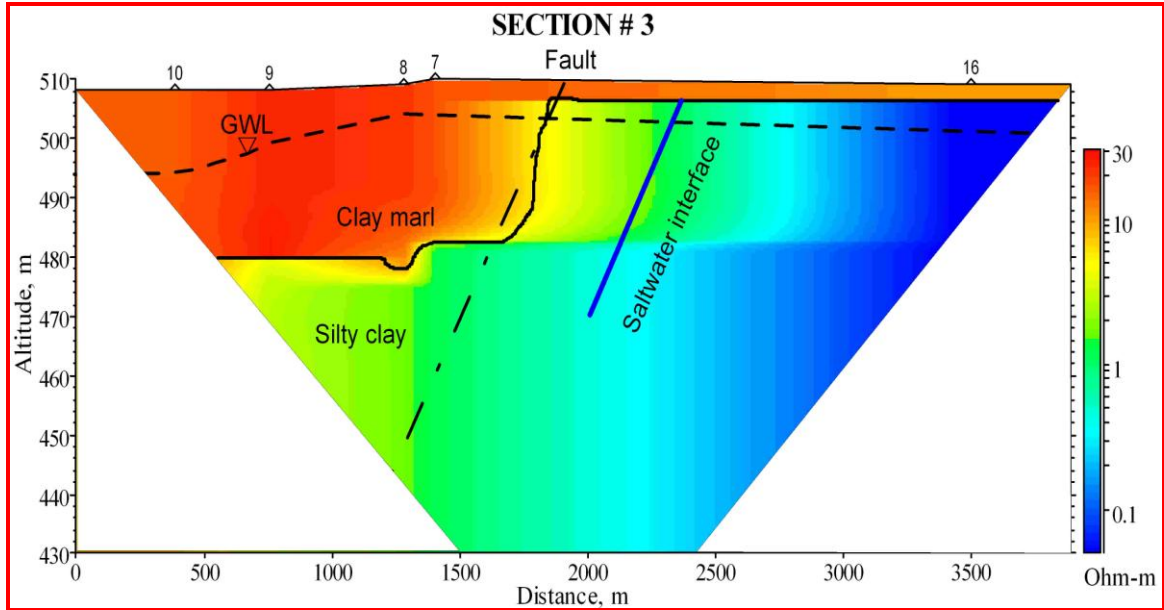


Figure (4.15): Two-dimensional representation of the TDEM resistivity distribution of of section 3 with geological and hydrogeological design.

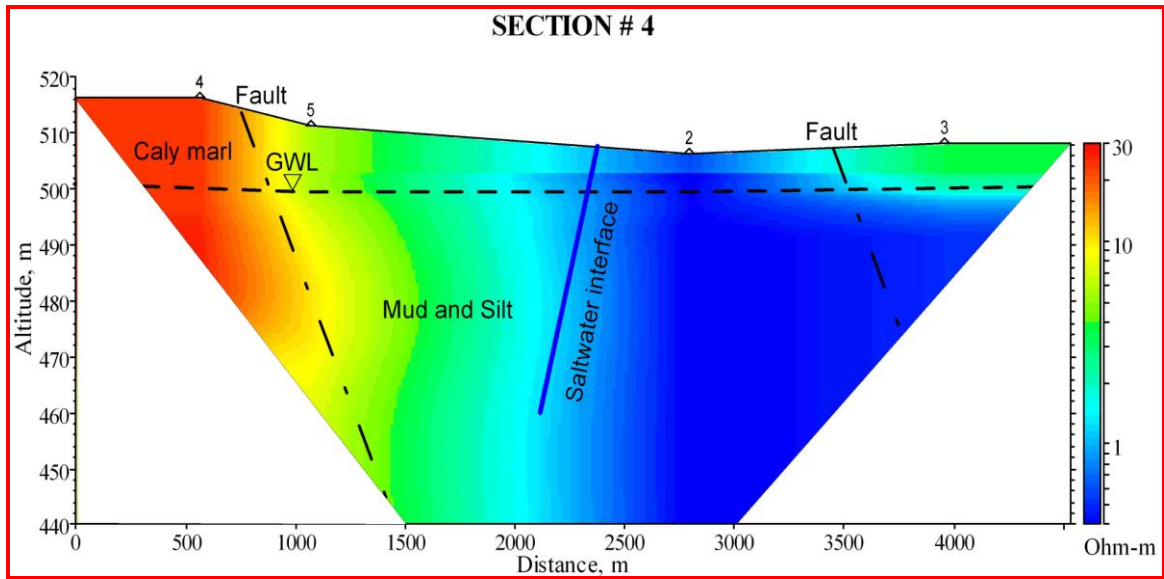


Fig.(4.16):Two-dimensional representation of TDEM resistivity distribution of section 4 with geological and hydrogeological design.

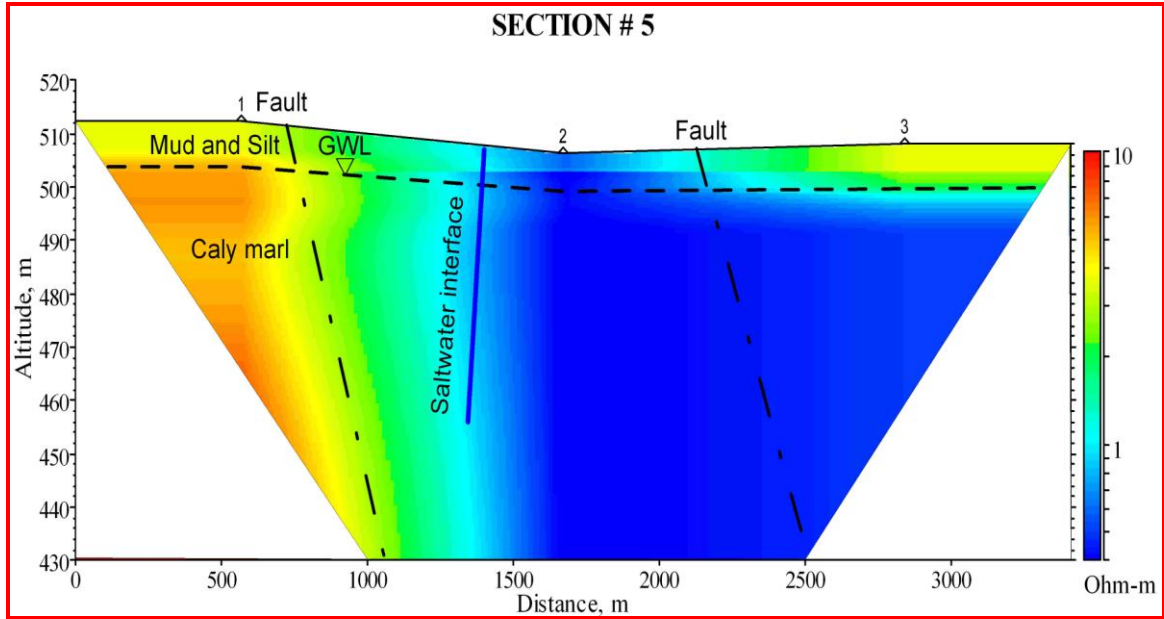


Figure (4.17): Two-dimensional representation of TDEM resistivity distribution of section 5 with geological and hydrogeological design.

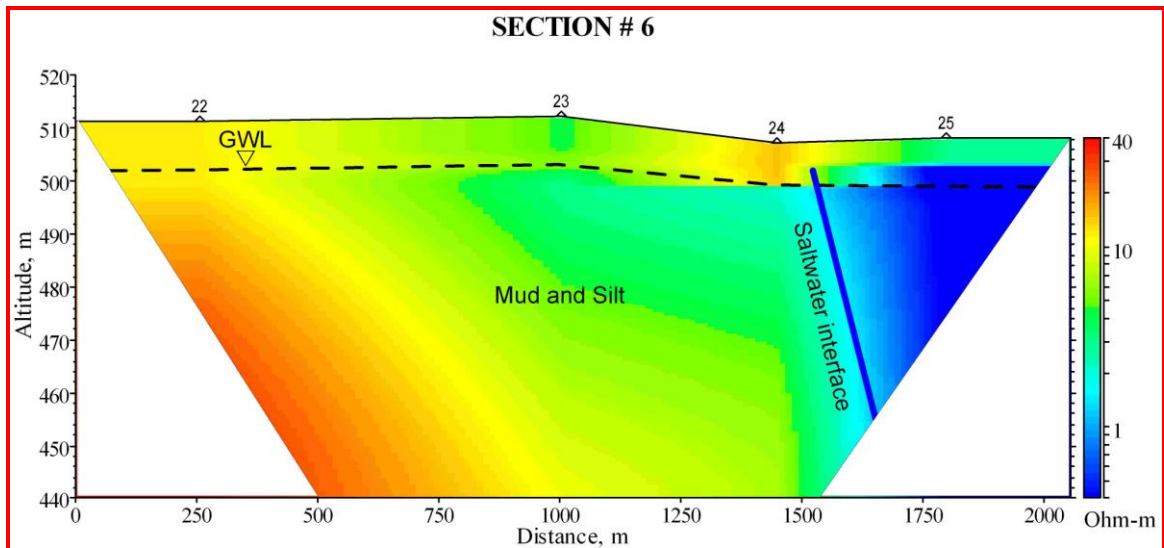


Figure (4.18): Two-dimensional representation of TDEM resistivity distribution of section 6 with geological and hydrogeological design.

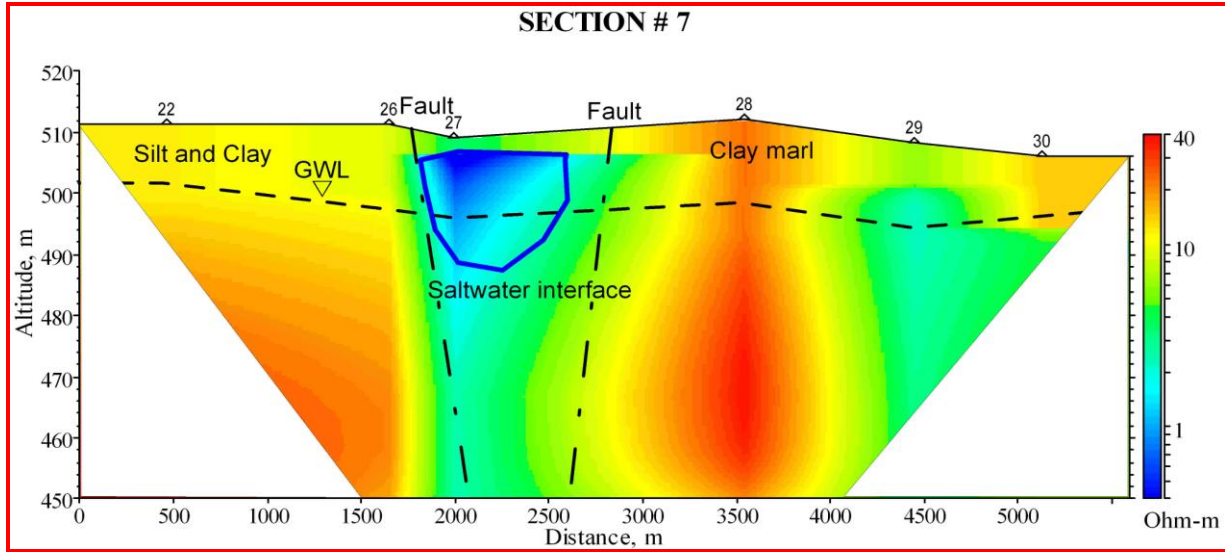


Figure (4.19): Two-dimensional representation of TDEM resistivity distribution of section 7 with geological and hydrogeological design.

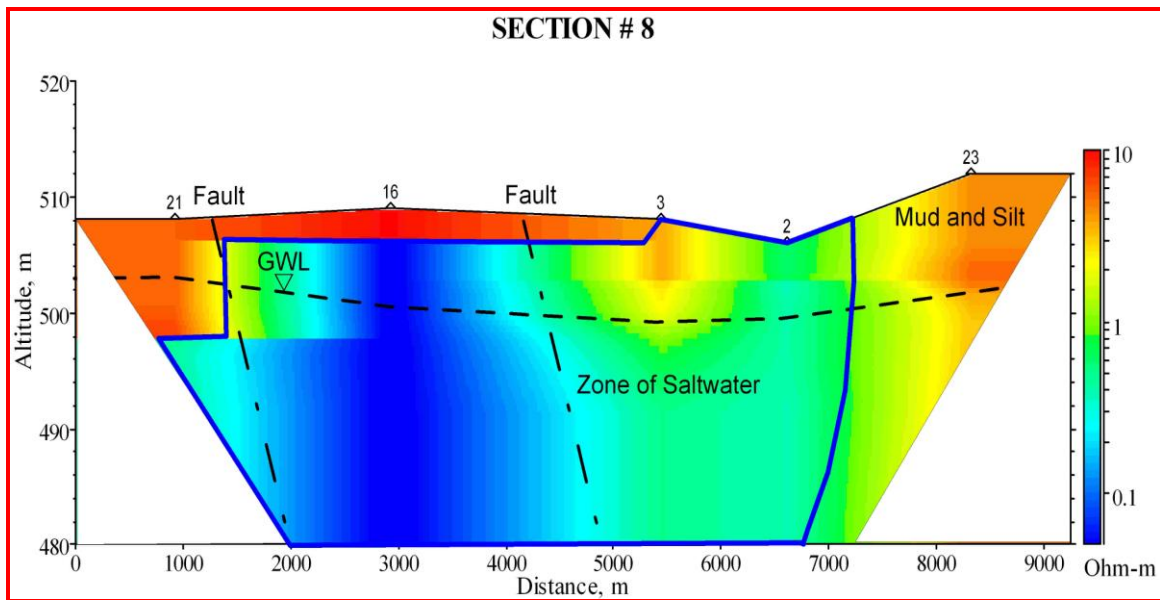


Figure (4.20): Two-dimensional representation of TDEM resistivity distribution of section 8 with geological and hydrogeological design.

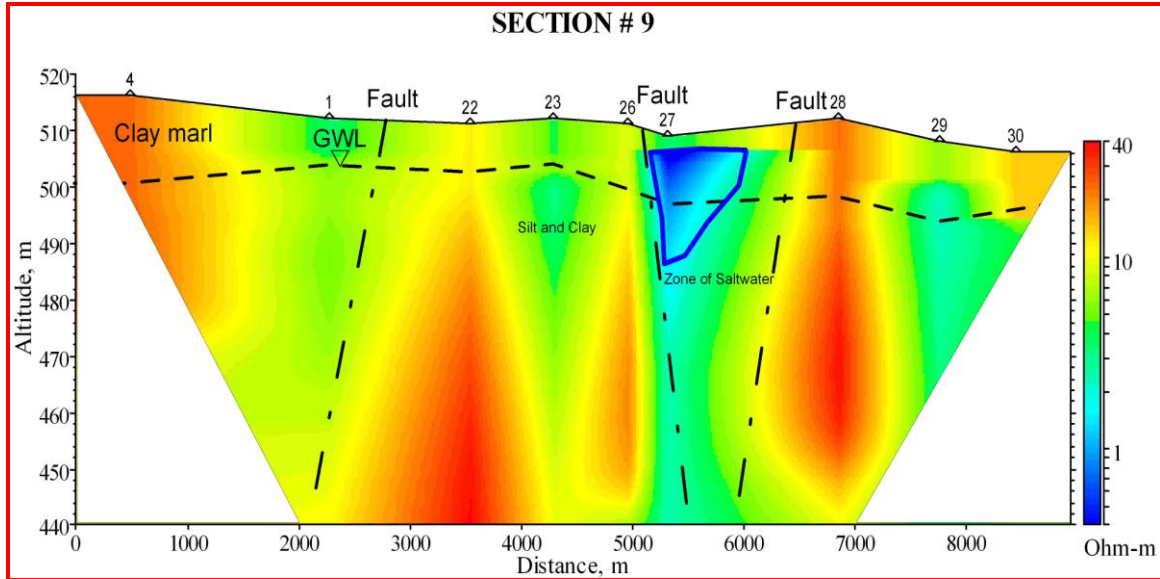


Figure (4.21):Two-dimensional representation of TDEM resistivity distribution of section 9 with geological and hydrogeological design.

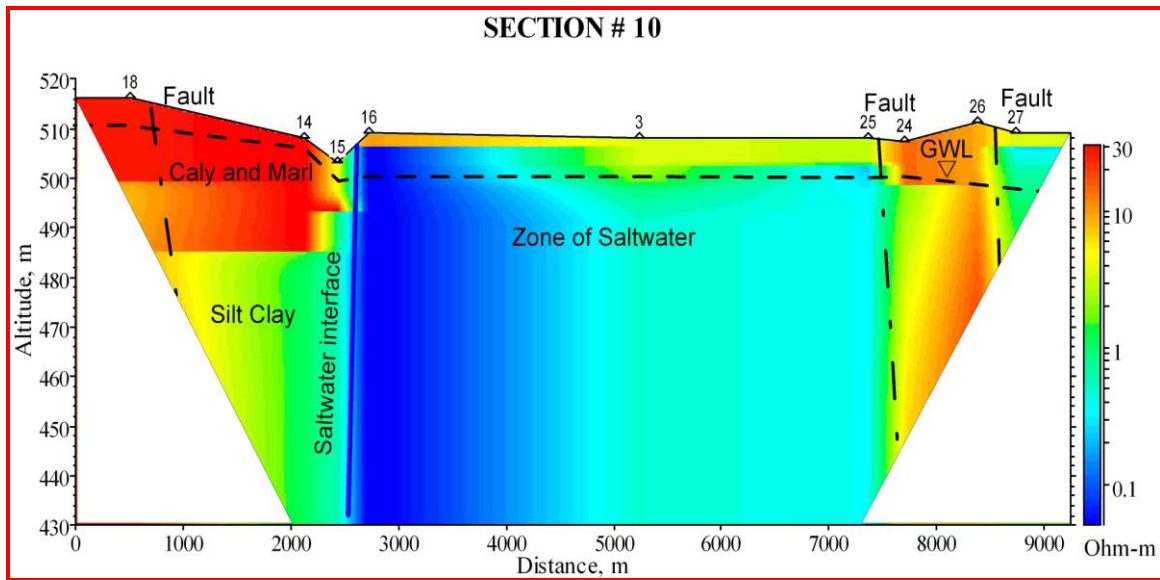


Figure (4.22):Two-dimensional representation of TDEM resistivity distribution of section 10 with geological and hydrogeological design.

4.9 3D Image: Saltwater interface at Depth Slice (5m-40m)

The final 1D inverted models from all the available (good quality, free of noise) VES and TEM data were topographically corrected (taking into account the real elevation of each measurement) and merged to form slices differentiated according to depth. The roof and the bottom of target zone of saltwater is recognized from 1D & 2D class interpretation and the

depth ranges from 5m to 40m is considered as the zone where the interface might be developed. Incorporating geological, tectonic and hydrogeological data together with final geophysical interpretation have helped to trace the most promising location of the saltwater interface (Figure 4.23).

Beyond the results concerning the main objectives of the study, the presented work has shown that the VES and TEM methods are practically, effective techniques for the hydrogeological delineation of saltwater invasion interface, even if no other adequate geoenvironmental information are available for calibrating the model (such as, borehole logs). Consequently, we propose to install the 5 underground sensors at specified depths to monitor the salt water invasion toward the fresh water aquifer and the locations of these sensors are summarized in Table (4.1) and shown in Figure (4.23).

Table (4.1): Promising Coordinated sites to install underground saltwater sensors.

Sensor No.	PG(Easting, m)	PG (Northing, m)	Depth to target (m)	Rank (priority)
1	327323	142864	8	1
2	326280	143346	8	1
3	323470	142101	10	1
4	323109	140657	15	2
5	322376	139583	16	2

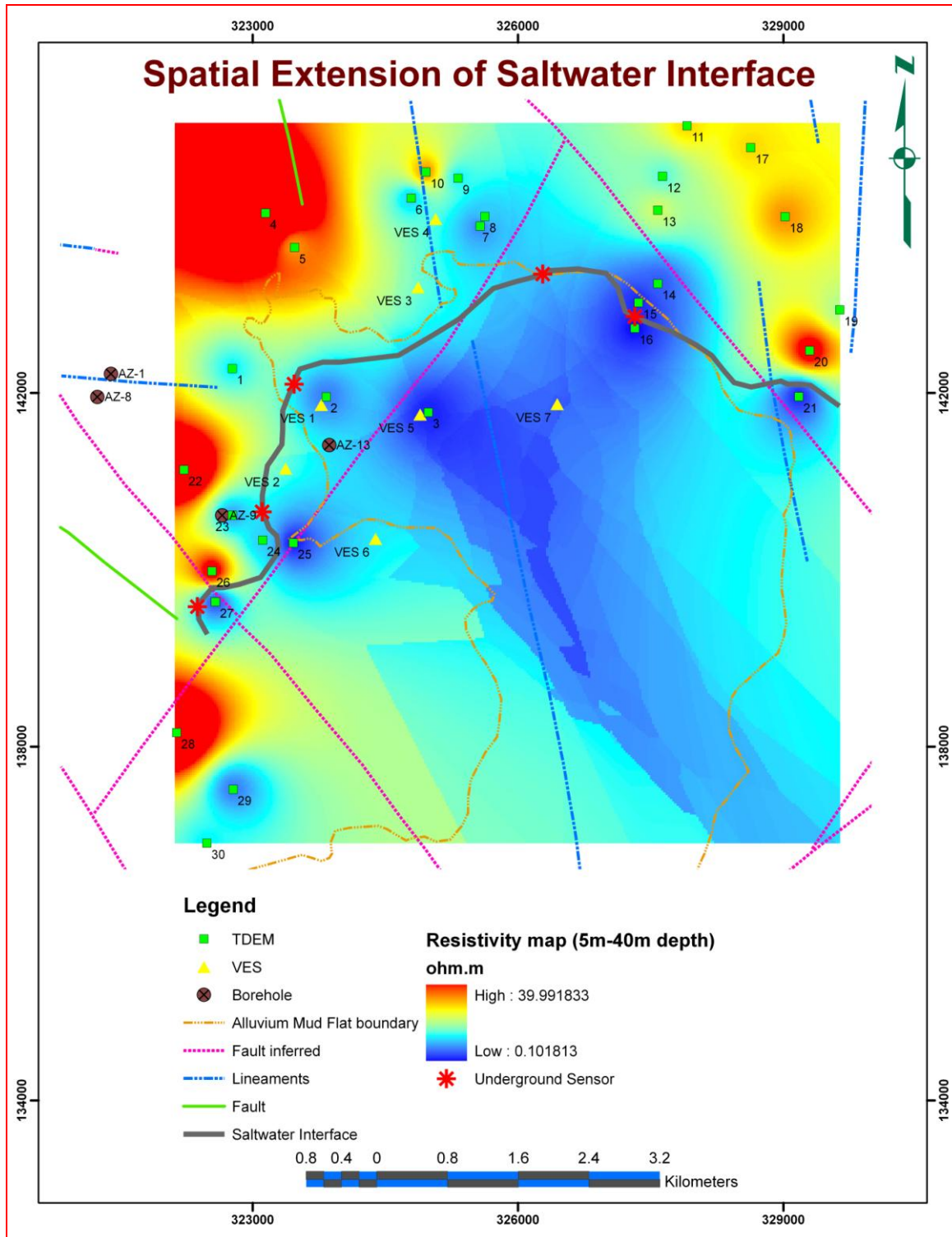


Figure (4.23): Spatial extension of saltwater interface produced by combined interpretation of the collected TEM and VES data with the acquired hydrogeology and geology themes at depth slice from 5m to 40 m.

CHAPTER 5 HYDROCHEMISTRY AND WATER QUALITY OF UPPER AQUIFER

5.1 Background

The waters of the Azraq basin and the Azraq oasis in northeastern Jordan have been overexploited for more than 20 years, resulting in a drop of the water table as well as lower water quality. This has resulted in the decimation of the oasis and the ecosystem which it supported. Efforts to achieve sustainable development in the area and reverse the damage which has already occurred requires a full understanding of the hydrological system.

The geo-electric studies in Azraq depression confirm the division of Quaternary sediments into three parts. These studies show that the salt water body has a thickness of 50-80 m. Below it there is fresh water body. This clear separation of dense salt water at the top of the formation and fresh water in the deeper parts can be explained only by a thick clay layer between the two water bodies

5.2 Sampling and Analysis

Samples were taken from operating wells covering the entire area (Table 5.1). Two-liter samples were taken from each well, and the temperature, conductivity and pH were measured in the field. Bicarbonate was measured by titration to the methyl orange indicator end point. Chloride was determined by titration and precipitation of AgCl until silver chromate appeared. Sulfate was determined by precipitation of BaSO₄ and thereafter by measuring absorbency with a spectrophotometer. Cations were determined using atomic absorption spectrophotometry.

Sixteen (16) water samples were collected from the farm wells to determine their chemical constituents. Figure (5.1) shows the water sampling from a farm well in the study area. The electrical conductivity of most shallow farm wells is subject to seasonal variation between 1500-5000 $\mu\text{S}/\text{cm}$ with some exceptional values as in Fawzi Sweilem well which reaches 31300 $\mu\text{S}/\text{cm}$. The list of farm wells where the water samples have been collected is shown in Table (5.1).

Table (5.1) : List of Farm wells used in this study in Qa Azraq area

Well_Code	Name	PGE	PGN	Conductivity (μS/cm)	SWL (m)	Elevation (m)	Aquifer	GWL (m)	Sample No.
F 3436	Fawzi Sweilem	326800.0	144108.0	31300	3	507		504	3
F 3733	Nail Najdawi	325757.0	143932.0		4	508		504	
F 3901	Mansour Bassar	322316.0	144079.0	4000	18	520		502	2
F 4121	Naji Ghanem	322359.0	139736.0	2600	13	508		495	15
F 3161	Murad Shawqi	323148.0	140630.0	2700	10	508		498	12
F 4177	Ali Abu Malouh	323571.0	140137.0	2800	10	508		498	13
F 3808	Izz Eddein Abu Baker	323771.0	140827.0		5	512		507	
F 4061	Mohammad Ibrahim	322546.0	137145.0	4600	15	508		493	
F 0000	Ziad Shebli al shoumary	322832.0	142233.0	4500	5	509		504	1
F 3441	Abdel kareem Mustafa	324728.0	144591.0	1640	15	507		492	4
F 3622	Daoud Abdel Hafeez	327747.0	144834.0	923	10	512		502	5
F 3970	Muneer odeh akeel	328015.0	144503.0	1156	18	509		491	6
F 3388	Mustafa Mohd attalah	327160.0	144070.0	7100	20	509		489	7
F 0001	Salt mine1	326955.0	142782.0	177000	5	506		501	8
F 3269	Waddee al afeer	328229.0	144777.0	1031	5	516		511	9
F 3960	Yehya al omari	329005.0	142570.0	7000	6	508		502	10
F 3620	Frehat al akrabawi	329136.0	142461.0	2100	6	510		504	11
F 3159	Rafat al remawi (fromer, Adham)	323088.0	140495.0	4400	10	509		499	14
F 4116	Al awawdeh	322536.0	136984.0	2100	10	509		499	16
F 1022	Azraq observation well No.11	320376.0	141300.0		22	520	B4/B5	498	
F 1284	AWSA-7 observation well	324387.0	143229.0		6	507	BAS	501	
F 1042	AWSA15	321182.0	146909.0		30	524	BAS	494	
F 1280	AWSA-2 observation well	323783.0	147863.0		15	514	BAS+B4	499	
F 1043	AZ 12 PP 195	322395.0	149404.0		21	517	BAS+B4/B5	496	
F 1002	Agr. Station 1 Shomary	316420.0	130033.0		10	523	AI	513	
F 1056	AZ 5 PP 410	342225.0	144670.0		64	576	B4/B5	512	
F 1162	Azraq Co-operation Association	318300.0	141700.0		40	551	B4	511	



Figure (5.1): water sampling from a farm well in Azraq area

5.3 Results and Discussion

Chemical and isotopic data are presented in Table (5.2). The following discussion will illustrate the significance of these results in the context of water types, recharge, movement, and evolution in the area.

5.4 Water Types

The water types in the area are plotted on a trilinear piper diagram (Figure 5.2). This diagram shows the water types in the shallow aquifer in Azraq area. Water in the Qa Azraq area is characterized by the dominance of chloride, sulfate, and sodium. One sample from the salt mine is of interest because of it is characterized by very high salinity reaching 271000 mg/l. Water in the northwestern basalt area has higher proportions of sodium, bicarbonate, and sulfate. Chloride concentrations illustrate the major types of water in the area. The lowest chloride water is in the northwest basalt aquifer, the highest is in the deep Um Rijam aquifer. Furthermore, the chemical analyses of the water samples were plotted on Extended Durov diagram to depict the type of water as well as the geochemical processes that take place between water and rock matrix during water rock interaction as shown in Figure (5.3). Figure (5.4) shows the Expanded Durov Diagram, for water from various environments. It can be seen that the water of the shallow aquifer is sodium chloride water type of typical natural saline water or can be formed by the return flow from irrigation or natural deterioration of the groundwater quality by ion exchange within the aquifer. The chemical analyses show a higher salt content with large amounts of highly soluble sulphates and halite as a result of dissolution processes between water and the superficial deposits outcropping on the surface

The concentration of the dissolved matter depends mainly on the depth of water withdrawal. Water from the deeper wells in the farming area northeast of Azraq Druze has a lower electrical conductivity than the dug wells in that area. The same situation was observed east of Qa'a Azraq. Layers of low permeability formations separate the aquifers, thus causing a difference in the salinities of the water in the aquifers. Two circulation patterns are observed, a shallow circulation influenced by wadi floods with high conductivity and a deeper circulation with low conductivity. The electrical conductivity of most shallow farm wells is subject to seasonal variation between 1000 to 3000 $\mu\text{S}/\text{cm}$.

Table (5.2) Chemical analyses of selected farm wells

Well No.	Well Owner	Bicarbonate	Calcium	Chloride	Electrical Conductivity	Hardness	Magnesium	Nitrate	Potassium	Sodium	Sulfate	pH
		mg/L	mg/L	mg/L	Us/cm	mg/L As CaCO ₃	mg/L	mg/L	mg/L	mg/L	mg/L	unit
F 0000	Ziad Shebli al shoumary	337.33	153.31	1249.25	5040	689	74.66	5.09	38.71	796.49	455.04	7.29
F 3901	Mansour Bassar	198.86	104.61	1345.45	5020	554	71.38	11.06	32.06	807.07	358.56	8.11
F 3436	Fawzi Sweilem	192.76	319.64	11532.18	35500	2037	301.45	<.2	174.78	7619.44	1750.08	7.41
F 3441	Abdel kareem Mustafa	157.99	71.74	838.87	3130	356	42.92	0.89	18.38	473.8	146.4	7.84
F 3622	Daoud Abdel Hafeez	143.35	31.46	220.1	1140	149	17.27	4.47	7.43	154.33	79.68	7.91
F 3970	Muneer odeh akeel	156.77	44.09	290.39	1415	207	23.71	4.15	9.38	187.91	93.6	7.81
F 3388	Mustafa Mohd attalah	527.65	122.24	1631.94	6720	632	79.53	6.05	37.54	1191.17	519.36	7.27
F 0001	Salt mine1	164.09	790.58	107564.3	270400	6858	1188.03	<.2	1441.62	65503.8	13050.7	7.04
F 3269	Waddee al afeer	157.99	31.06	242.47	1264	144	16.05	5.04	8.21	189.06	87.36	8.12
F 3960	Yehya al omari	196.42		2487.84	8120	1386	167.2	14.05	37.15	1075.02	290.88	7.48
F 3620	Frehat al akwabawi	124.44	117.43	592.5	2530	570	67.49	0.77	13.29	259.21	144.48	7.52
F 3161	Murad Shawqi	218.99	74.15	794.49	3660	368	44.63	2.18	25.81	584.43	304.8	7.81
F 4177	Ali Abu Malouh	236.68	68.34	809.76	3650	361	46.45	2	30.89	583.28	276.48	7.78
F 3159	Rafat al remawi (fromer, Adham)	235.46	52.1	1504.14	5630	307	43.05	3.33	45.75	1041.44	319.2	7.81
F 4121	Naji Ghanem	254.98	72.34	743.02	3340	362	44.26	6.73	25.42	531.99	319.2	7.67
F 4116	Al awawdeh	212.89	98.8	610.96	2650	464	53.02	3.33	15.25	335.34	218.88	7.14

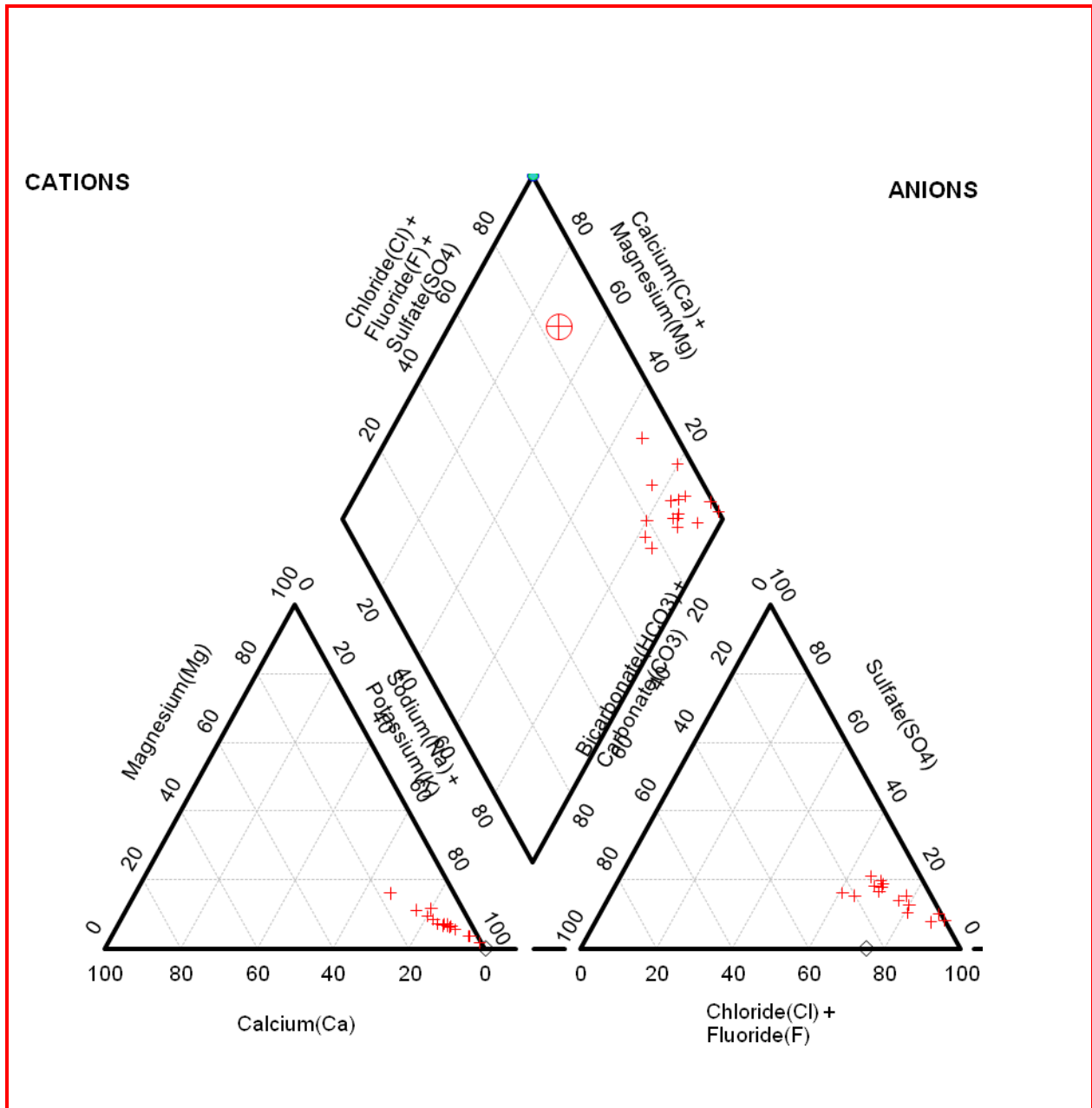


Figure (5.2): Water type of selected farm wells

The groundwater contour map in the study area is shown in Figure (5.5), where the groundwater level ranges from 489 m to 513 m above the sea level. The lowest groundwater level is encountered on the central part of Azraq basin in the vicinity of Qa' area. The generated groundwater conductivity map of the sampled groundwater wells, shows a well defined scheme of highly contrast in groundwater salinity. Besides, the spatial extension of it is mostly affected by two geological lineaments; they have the control factor in saltwater invasion toward the north direction of the study area (Figure 5.6).

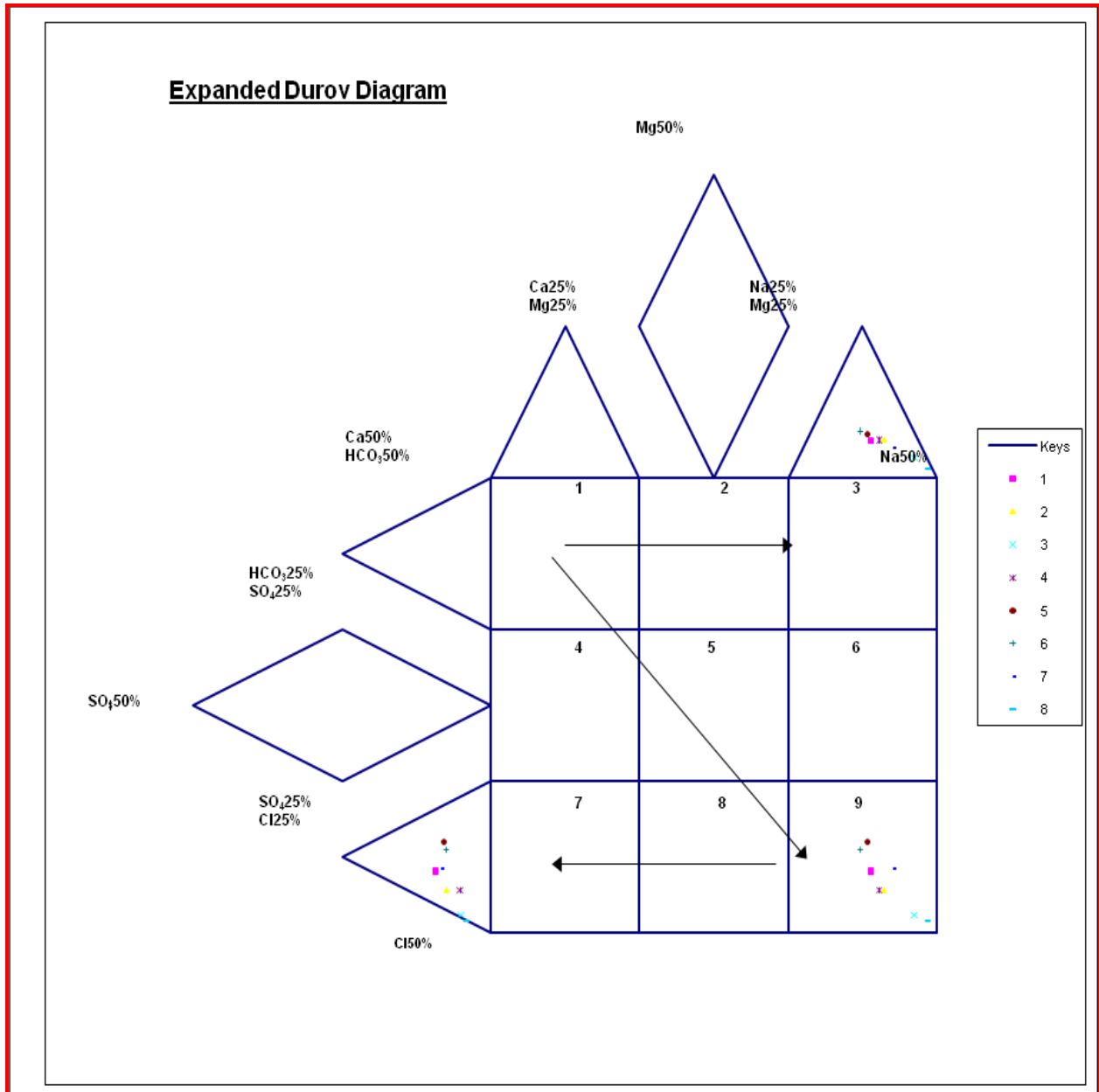


Figure (5.3): Plotting of Water samples on expanded Durov diagram

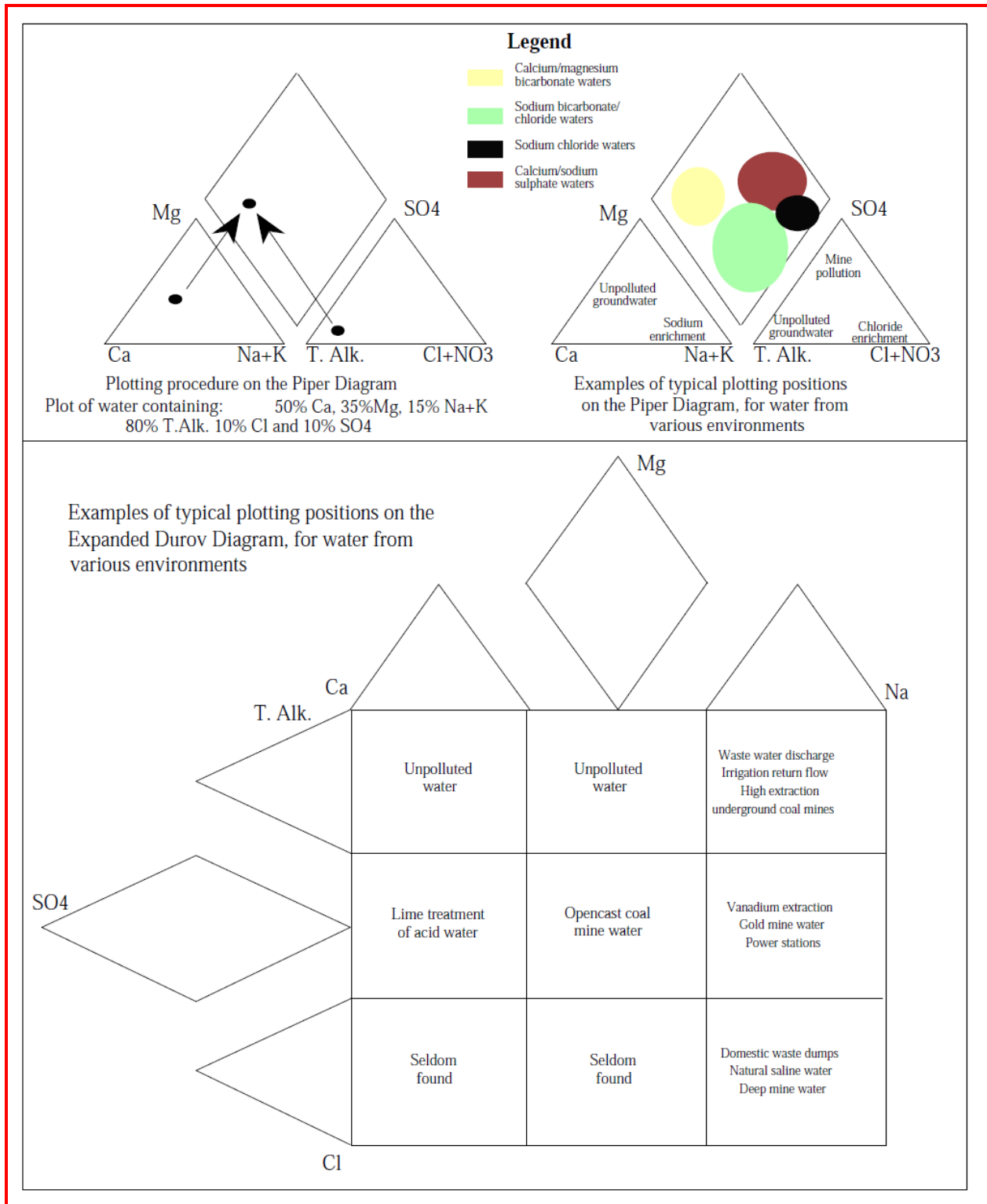


Figure (5.4): Expanded Durov Diagram, for water from various environments

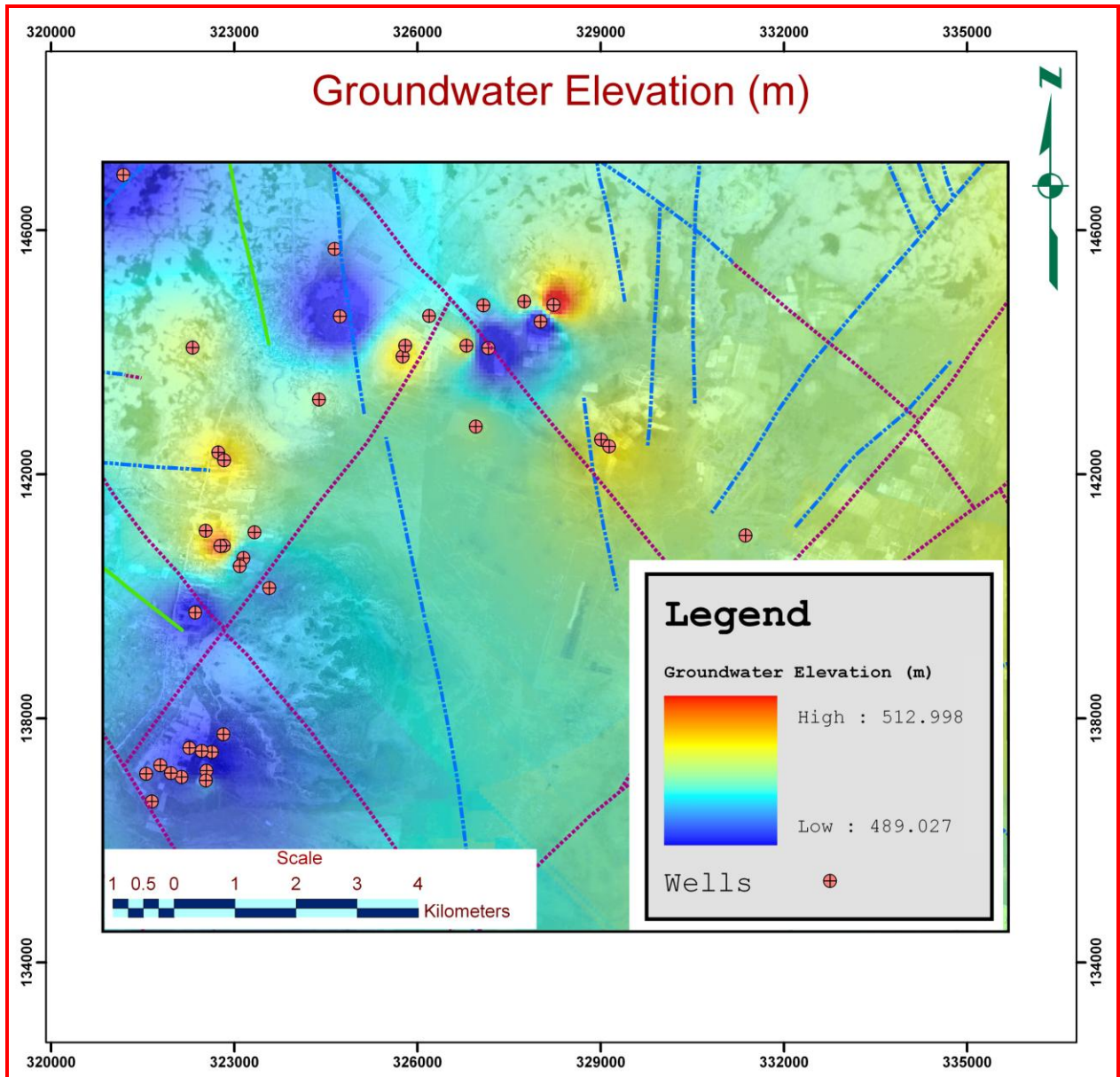


Figure (5.5): Groundwater contour map of the shallow aquifer in the study area

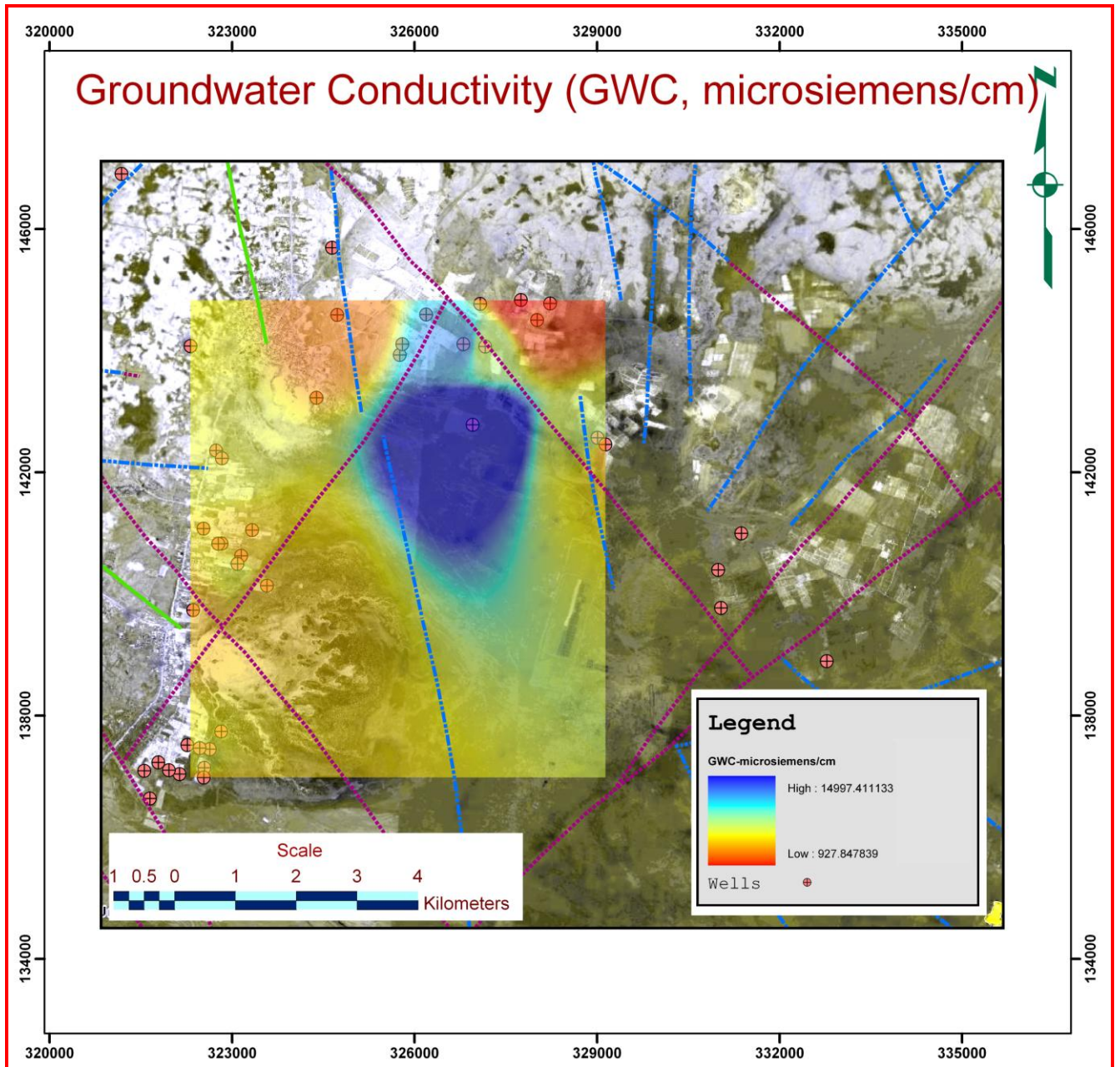


Figure (5.6): Groundwater conductivity map in microsiemens/cm for sampled wells.

Suzan et al. (2003) studied the chemistry of the unsaturated zone in the Azraq area. They collected four cores from the unsaturated zone for the estimation of the rates of recharge that the upper aquifer receives. The first three boreholes were located in the vicinity of existing water wells in which the water level was measured, below the existing ground surface.

The water samples were analyzed for SO₄, Cl, NO₃, and humidity determination (Figure 5.7). It is clear that the farm well chemistry showed anhydrite, gypsum and dolomite dissolution processes especially in the upper parts of the formation as indicated by the profiles of core drilled in the vicinity of Azraq farms. It is very obvious that the Cl (and consequently Na) and SO₄ are extremely high in Azraq Sabkha.

As mentioned earlier one of the scenarios is the threat of reverse flow from Sabkha to AWSA well field resulting from low hydraulic gradient of the aquifer water table and increased drawdown in the AWSA well field (Suzan et al. (2003). However, the current hydrodynamic systems shows that groundwater flow is still in the direction of Azraq depression. Another evidence is the depleted isotopic content in AWSA well field especially in those of them that were subject to salinity and their isotopic content stability over time. This means that the isotopically enriched Sabkha water did not mix with AWSA well field water.

On the other hand excessive abstraction by farmers and the private well owners might invite the groundwater in Sabkha area towards the farm area increasing the salinity in the farm wells. The movement of the fresh-salt water interface depends on the distance as well as on the amount of withdrawal and on the hydrogeological situation in the area.

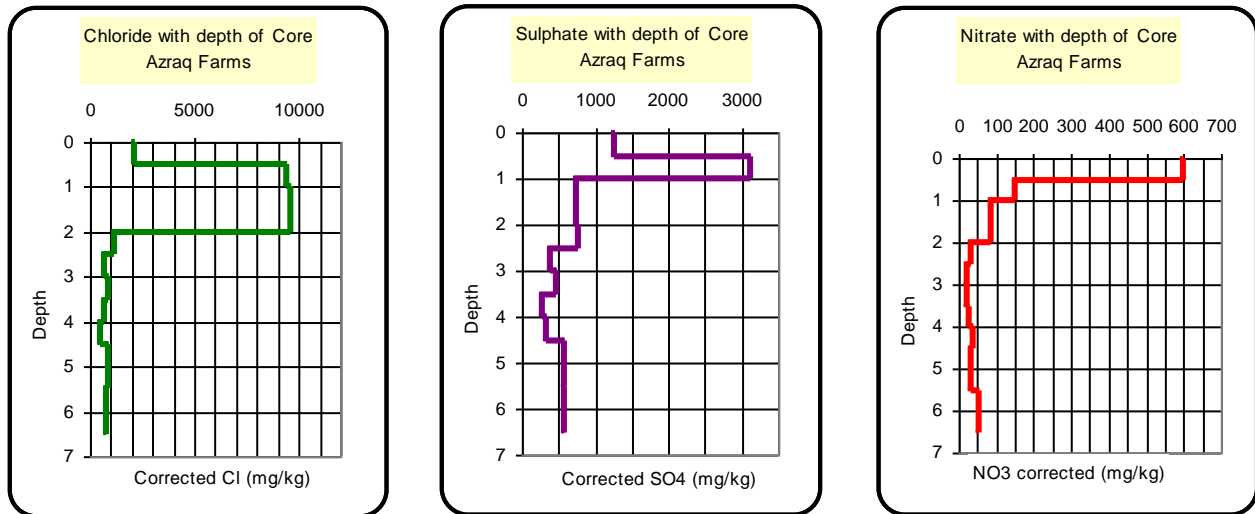


Figure (5.7) : Variation of Chemistry with depth of unsaturated zone in Azraq farms

CHAPTER 6 CONCLUSIONS AND RECOMMENDATIONS

6.1 Conclusions

A detailed Geophysical (geoelectromagnetic) survey was carried out acquiring 37 TEM and VES soundings to reconstruct the 2D and 3D subsurface resistivity distribution. The detailed geoelectromagnetic survey in combination with the geological, tectonic and hydrogeological study of the area is a useful tool for providing information on the geometrical extension of saltwater interface in the shallow aquifer.

The saltwater in the center of the basin (Qa-Azraq) started to move in the direction of the AWSA well-field. In this study a combination of geophysical and hydrogeochemical models were used to construct and to analyze the size and behavior of the saltwater intrusion in the upper aquifer. The water quality deterioration is related to the intrusion of brine groundwater from the middle aquifer into the shallow aquifer, prompted by over-pumping disturbances. The study showed that the saltwater was initially confined to the top Quaternary sediments in Qa-Azraq as it is bounded by horizontal and vertical barriers (i.e. faults). The interface between freshwater/saltwater is transitional forming a mixing zone. The induced movement caused the saltwater to move horizontally in the beginning until it passed the vertical boundary fault and then tended to move vertically under the influence of its density. The saltwater completely extended vertically and tends at present time to flow horizontally in the direction of the well-field. The wells that are adjacent to the Qa-Azraq are showing a continuous increase in salinity. The model results indicate that if present abstraction rates continue (2010: 65 MCM/yr), the saltwater will continue moving. Expected arrival time to the AWSA well-field ranges between 500 - 2000 year. Pessimistic prediction scenarios showed that any increase in abstraction from the AWSA well-field or in the area north of the well-field, will cause severe drawdown and dryness of several wells in the springs area to the east and Azraq center. Optimistic scenarios showed that an abstraction quantity of 16-18 MCM/yr, is the appropriate safe yield of the Upper Aquifers System.

6.2 Recommendations

Based on the VES and TEM information, the salt fresh water interface was delineated as shown in Figure (4.23). In order to monitor the movement of this interface, it is proposed to install the underground monitoring sensors to monitor the groundwater level fluctuation as well as the concentration of ions that contributed to the salinity such as chloride and sodium.

In future assignment and by using the resistivity distribution in depth, we can estimate some hydraulic characteristics of the aquifer, such as hydraulic conductivity and transmissivity. These data can be later used for simulating the groundwater flow that controlling the interface of fresh/saline groundwater.

once saltwater intrusion has occurred, it is almost impossible to reverse, making this a significant threat to freshwater resources. Mitigation strategies that are designed to slow or halt the rate of saltwater intrusion can be expensive but are necessary to protect the water resources from more damage.

Finally we recommend that the Ministry of Water and Irrigation takes an action plan to help the local people of Azraq to extract the high saline waters to produce salts and to reduce the pumping from the governmental wells to enhance and to present the salt water intrusion towards the AWSA wellfield in the near future.

Acknowledgements

I would like to thank the IUCN Office at Amman for funding this research project and for their generous support during the execution of the project. Also I would like to express my sincere thanks to Mrs. Fidda Hadad from the IUCN and Dr. Khair Al Hadidi and Eng. Ali Subuh from the Ministry of Water and Irrigation for their continuous encouragement and support. Also I would like to thank my colleagues with special thanks to Mr. Jafar Abu Rajab who help me a lot in this work.

References

[AEMR, 1996] AEMR (1996). TEM-FAST ProSystem Manual. Applied Electromagnetic Research, Holland.

[AEMR, 1999] AEMR (1999). TEM-RESEARCHER. Applied Electro-Magnetic Research, the Netherlands.

Albouy Y, Andrieux P, Rakotondrasoa G, Ritz M, Descloitres M, Join JL, Rasolomanana E (2001) Mapping coastal aquifers by joint inversion of DC and TEM soundings—three case histories. *Ground Water* 39:87–97

Al-Hadidi, K and Subuh, A. (2001): Jordan Badia Research and Development Program: Integrated Studies of Azraq Basin for Optimum Utilization of the Natural Resources, Water Group. Vol. 4, The Higher Council of Science and Technology, Amman, Jordan.

Al-Momani, M.; Kilani, S. El-Naqa, A. and Amro, H. (2003): Isotope Response to Hydrological Systems for Long – Term Exploitation Case of Azraq Basin, Jordan, IAEA, Ministry of Water and Irrigation, Vienna, 2003, 125 pp.

AUKEN E.(1995). 1D Time Domain Electromagnetic Interpretation over 2D/3D structures. Proceedings of the Symposium on the application of geophysics Engineering and Environmental problems, Orlando, April 1995 : 329-338.

Bajjali, Isotopic and Hydrochemical Characteristics of Precipitation in Jordan, M.Sc. Thesis, Jordan University, Amman-Jordan, 1990, pp. 99.

Bajjali, W and Hadidi, K. (2005): Hydrochemical Evaluation of Groundwater in Azraq Basin, Jordan Using Environmental Isotopes and GIS Techniques, Proc. of the 25th Annual ESRI International User Conference, San Diego, California, July 25 – 29, 2005.

BARBIERI G., BARROCU G., RANIERI G.(1986). Hydrogeological and geophysical investigations for the evaluation of salt intrusion phenomena in Sardinia. Proceedings of the 9th SWIM, Delft, may: Selected Paper.

Barsukov PO, Fainberg EB, Khabensky EO (2007) Shallow investigation by TEM-FAST technique: methodology and case histories. In: Spichak VV (ed) Methods of geochemistry and geophysics. Elsevier, pp 55–77

BEAR, J., CHENG, A.H.-D., SOREK, S., OUAZAR, D., HERRERA, I. (1999) . Seawater Intrusion in Coastal Aquifers- Concepts, Methods Practices. Kluwer Academic Publishers, Dordrecht/ Boston/ London, 625 p.

Bender, F. Geology of Jordan, Gebrüder Bornträger, Berlin 1974, pp.196.

Bundesanstalt für Geowissenschaften und Rohstoffe (BGR) and Water Authority of Jordan (WAJ), Groundwater Resources of Northern Jordan, Vol. 3, Structural Features of the Main Hydrogeological Units in Northern Jordan. Unpubl. Rep. Water Authority of Jordan (WAJ),

Chalikakis K, Nielsen MR, Legchenko A (2008) MRS applicability for a study of glacial sedimentary aquifers in Central Jutland, Denmark. J Appl Geophys 66:176–187

CHRISTENSEN N.B. (1997). Twodimensional imaging of transient electromagnetic soundings. SAGEEP 1997 :397-406.

CHRISTENSEN N.B.& AUKEN E. (1992). Simultaneous Electromagnetic Layered Model Analysis: Proceedings of the Interdisciplinary Workshop 1, Aarhus 1992. Geoskrifter 41: 49-56.

CHRISTENSEN N.B.& SORENSEN K.I. (1994). Integrated use of electromagnetic methods for Hydrogeological investigation. Proceedings of the Symposium on the application of geophysics Engineering and Environmental problems . Boston, March 1994 : 163-176.

Christensen NB (1995) 1D imaging of central loop transient electromagnetic soundings. J Environ Eng Geophys, pp 53–66

Christensen NB, Sørensen KI (1998) Surface and borehole electric and electromagnetic methods for hydrogeophysical investigations. Eur J Environ Eng Geophys 3(1):75–90

Clark, D. and Fritz, P. (1997): Environmental Isotopes in Hydrogeology, CRC Press, Boca Raton, FL, 1997, pp. 352.

Custodio. E. & Bruggeman, G.A. (1987). Groundwater problems in coastal areas. Studies and Reports in Hydrology, 45: 1-576 . UNESCO, Paris, France.

Danielsen JE, Auken E, Jørgensen F, Søndergaard VH, Sørensen KI (2003) The application of the transient electromagnetic method in hydrogeophysical surveys. J Appl Geophys 53:181–198
de Mayo 1999: 365-370.

DEIDDA G.P. , RANIERI G.(2000) : On vertical and lateral resolution in TDEM soundings. In press.
DEIDDA G.P., URAS G., RANIERI G., COSENTINO P.L., MARTORANA R.(2000). Seismic reflection and TDEM imaging of a complex aquifer system. XXV EGS General Assembly. Nice 24-30 April.
Duque C, Calvache ML, Pedrera A, Martín-Rosales VM, López-Chicano M (2008) Combined time domain electromagnetic soundings and gravimetry to determine marine intrusion in a detrital coastal aquifer (Southern Spain). J Hydrol 349:536–547

El-Naqa, A. Al-Momani, M.; Kilani,S. , A. and Hammour, N. (2007): Groundwater Deterioration of Shallow Groundwater Aquifers Due to Overexploitation in Northeast Jordan. Clean, Vol. 35 (2), 156 – 166.

Fitterman DV, Labson VF (2005) Electromagnetic methods for environmental problems. In: Butler DK (ed) Near-surface geophysics. SEG Tulsa, Oklahoma, pp 295–349

FITTERMANN D.V. AND STEWART M.T,1995. Transient electromagnetic sounding for groundwater. Geophysics, vol 51, n.4 April : 995-1005.

Giovanni BARROCU & Gaetano RANIERI (2004): TDEM: A useful tool for identifying and monitoring the fresh-saltwater interface.

GODIO A., SAMBUELLI L., BARROCU G., RANIERI G.(1999). Applicació del metodo TDEM para la delimitacion de la intrusion salina en el acuífero costero de Capoterra (Cerdena sud-occidental). Jornadas sobre Actualidad de las Tecnicas geofisicas aplicadas en Hidrogeologia. Granada 10-12

GOLDMAN M., et al.(1996). Application of the marine time domain electromagnetic method Higher Council for Science and Technology (HCST), Integrated Studies of Azraq Basin for Optimum Utilization of the Natural Resources, Internal Report, HCST, Amman, Jordan 1999.

HOEKSTRA P., HARTHILL N., BLOHM M., PHILLIPS D.R. (1996) : Definition of a critical confining zone using surface geophysical methods. SAGEEP 1996 P.387-391. in lakes : the sea of Galilee, Israel. European journal of Environmental and Engineering Geophysics, 1: 125-138.

Howard Humphreys Ltd., Azraq Wellfield Evaluation, Water Authority
K. Ibrahim, Al Azraq Sheet 33531 Geological Map Series, NRA, Amman 1993.

- Kafri U, Goldman M (2005) The use of the time domain electromagnetic method to delineate saline groundwater in granular and carbonate aquifers and to evaluate their porosity. *J Appl Geophys* 57:167–178
- Kemna A, Nguyen F, Antonsson A, Engesgaard P, Tsourlos P (2006) Characterization of saltwater intrusion using electrical imaging: a numerical simulation study. In: Proceedings of 1st international joint salt water intrusion conference (SWIM-SWICA), Calgiari, Italy, 24–29 Sep 2006
- Kharabsheh, A (1991): Hydrological and hydrochemical study of the Upper Aquifer system in Azraq Basin (Jordan), M.Sc. Thesis, Yarmouk University, Jordan 1991.
- MC NEILL J.D. (1996). Principles and applications of time domain electromagnetic techniques for resistivity sounding. Technical note TN-27 . Geonics Limited.
- MEJU M.A.(1994). Assessing the role of infield resistivity image processing in shallow subsurface investigation. *SAGEEP 1994*, 19-40.
- MEJU M.A.(1994). Geophysical data analysis: understanding inverse problem theory and practice: Society of Exploration Geophysicist. Course notes series, vol. 6, Society of Exploration Geophysicist. Publishers, Tulsa, Oklahoma.296p.
- MEJU M.A.(1995).Simple resistivity-depth transformation for infield or real-time data processing. *Computers & Geosciences* 21, 985-992.
- MEJU M.A.(1996). Joint inversion of TDEM and distorted MT data: simple effective practical consideration: *Geophysics* 61: 55-62
- Meju MA (1996) Joint inversion of TEM and distorted MT soundings: some effective practical considerations. *Geophysics* 61:56–65
- Meju MA (1998) A simple method of transient electromagnetic data analysis. *Geophysics* 63:405–410
- Momani, M. (1991) Isotope field application for groundwater studies in the Middle East, IAEA-TECDOC-890, IAEA, Vienna 1991.
- Nabighian M. N. (Ed), *Electromagnetic methods in Applied Geophysics*, Vol. 2A. Tulsa: Society of
- NABIGHIAN M.N., MACNAE J.C.(1991). Time domain electromagnetic prospecting methods.
- Nielsen L, Jorgensen NO, Gelting P (2007) Mapping of the freshwater lens in a coastal aquifer on the Keta Barrier (Ghana) by transient electromagnetic soundings. *J Appl Geophys* 62:1–15
- North Jordan Water Resources Investigation Project (NJWRIP), Azraq Basin Water Resources Study, Draft Final Report, Water Resources Department, Water Authority, Jordan 1989.

of Jordan (WAT), Jordan 1982, p. 37.

RICHARDS R.T., TROESTER J.W., MARTINEZ M.I. (1995). A comparison of electrical techniques used in reconnaissance of the groundwater resources under the coastal plain of the Isla de Mona, Puerto Rico. SAGEEP 1995: 251-260.

Rimawi, O. (1985): Hydrogeochemistry and Isotope Hydrology of the Ground-and Surface Water in North Jordan (North-Northeast of Mafrq, Dhuleil-Hallabat, Azraq-Basin, PhD Thesis, TU M_nchen, Germany, 1985.

Rimawi, O. and Udluft, P. (1985): Natural Water Groups and Origin of the Shallow Aquifer Complex in the Azraq-Depression, Jordan, Geol. Jahrb., Reihe C38, Hannover 1985, C38m, 17 – 38.

Sahawneh, J. (1996): Geology of Al Azraq Basin, Geology Directorate, Subsurface Geology Division, Groundwater Basin Project, Internal Report No. 2, Natural Resources Authority, Amman, Jordan 1996.

SORENSEN K.I. (1996). Detailed Regional Hydrogeophysical Investigations –The Solbjerg Case. SAGEEP 96 :343-351.

SORENSEN K.I. (1998). Continuous transient electromagnetic sounding. SAGEEP 1998:173-177. Water Authority of Jordan (WAJ), Azraq Basin Water Resources Study, Internal Report of WAJ, Amman, Jordan 1989, 250 pp.

Wolfgang, W. and Geyh, M. (1999): Application of environmental isotope methods for groundwater studies in the ESCWA region, Economic And Social Commission for Western Asia, United Nation, 1999, pp. 129.

YUHR L.&BENSON R.C. (1995). Saltwater intrusion: concepts for measurements and a regional characterisation for Broward County, Florida. SAGEEP1995: 231-242

Zuppi, G. (1986): Environmental isotope study of groundwater systems in the Azraq area, Technical report, IAEA ,Vienna 1986.